2006-11-06

M_1 Muscarinic Modulation of N-Type Calcium Channels: A Dissertation

John F. Heneghan
University of Massachusetts Medical School

A Dissertation Presented

By

John Heneghan

Submitted to the Faculty of the

University of Massachusetts Graduate School of Biomedical Sciences, Worcester

in partial fulfillment of the requirements for the degree of

DOCTOR OF PHILOSOPHY

(November, 6, 2006)

Program in Neuroscience

M1 muscarinic modulation of N-type Calcium Channels

A Dissertation Presented

By

John Heneghan

Approved as to style and content by:

_____
Lawrence J. Hayward, M.D., PhD., Chair of Committee

_____
John Marshall PhD

_____
Jose R. Lemos, PhD.

_____
Steve Treistman, PhD.

_____
Anthony Carruthers, Ph.D.,

_____
Anthony Carruthers, Ph.D.,
Dean of the Graduate School of Biomedical Sciences

Ph.D. Program in Neuroscience

DEDICATION

This is dedicated to my mother, Anne Riedman Heneghan, to whom, as she lay dying, I promised I would complete a graduate degree. Ironically, I'm not sure she would agree with the premise of this thesis. Here I present the results of research on small physical events, the movement of ions, with the assumption that this ebb and flow of tiny bits of salt is what underlies the workings of we call the human mind, self or soul. I'm sure she'd believe the human soul is part of something much larger that controls the movement of ions.

November 17, 2006

ACKNOWLEDGMENTS

Many persons deserve my gratitude for what they have given me during this process. First, thank you to Ann Rittenhouse, for encouraging me to learn not only about electrophysiology but all aspects of neuroscience. I can't say enough about the other members of Ann's lab with whom I've had the pleasure to work since Prosper N'Gouemo, Pam Gonzalez, and Curtis Barrett were in the lab. I owe a debt of gratitude to Tora Mitra-Ganguli, Mandy Roberts-Crowley, Lee Stanish, Maggie Lee and especially Liwang Liu. I have the deepest appreciation to my committee: Larry Hayward, José Lemos, Steve Treistman and Tony Carruthers, each of whom, individually, has been a support during difficult times.

More than anyone I have to thank Eve, my wife, who has been incredibly patient and supportive over these years.

ABSTRACT

The influx of calcium through N-type calcium channels (N-current) affects a myriad of neuronal functions. These include the triggering of synaptic release of neurotransmitter, adjustment of membrane potential and changes in gene transcription. N-channels are highly modulated proteins, so that N-current is attenuated or potentiated in response to environmental changes. In turn, the modulation of N-current has a direct effect on the downstream events, making the N-channel a focal point in neural signaling, and its modulation a mechanism for short term plasticity.

The modulation of N-current by M_1 muscarinic receptors (M_1Rs) is of particular interest for several reasons. The M_1R is instrumental in both cognition and memory formation as indicated by studies using either pharmacological agents aimed at M_1Rs or knockout animals lacking M_1Rs. Clinically, the M_1R is an important target in the treatment of Alzheimer's disease. Thus, like the N-channel, the M_1R is an important element of neural signaling. Moreover, the stimulation of M_1Rs affects N-current by through signaling pathways which despite being studied for decades, are not completely understood.

For my dissertation I have investigated of M_1R signaling on N-current using electrophysiological recordings of N-current from freshly dissociated neurons and from HEK cells expressing N-channels and M_1Rs. Asking how one receptor affects one type of calcium channel would seem to be a simple question. However, the answer has many facets. Since M_1Rs have multiple downstream effects and N-channels are highly modulated proteins, stimulation of M_1Rs initiates several different pathways which modulate N-current. This thesis aims to unravel some of the complexities of the interactions of two vital components of neuronal signaling. Here

I present the results of studies elucidating three different actions of M_1 signaling of N-current modulation.

The first study I present here examines the effect of N-channel subunit composition on modulation of N-current. The stimulation of M_1Rs in superior cervical ganglion (SCG) neurons elicits a distinct pattern of modulation; inhibiting N-current elicited by strong depolarizations and enhancing current elicited by lesser depolarizations. Thus M_1Rs cause two simultaneous modulatory effects on N-current; increasing voltage sensitivity and decreasing overall conductance. I found the expression of the N-channel's β subunit ($Ca_V\beta$) determines the observed effect. Specifically when the isoform $Ca_V\beta2a$ is expressed M_1 stimulation elicits enhancement without inhibition. Conversely, when $Ca_V\beta1b$, $Ca_V\beta3$, or $Ca_V\beta4$ are expressed M_1 stimulation elicits inhibition with out enhancement. These results fit a model in which both the enhancing and inhibiting effects of M_1 stimulation occur in all channels, but typically inhibition dominates. $Ca_V\beta2a$ blocks inhibition unmasking latent enhancement. Moreover, using mutants and chimeras I found palmitoylation of $Ca_V\beta2a$ at the N-terminus plays a key role in blocking inhibition. My findings predict the expression and localization of different $Ca_V\beta$ isoforms would dramatically alter modulation of N-current and thus may represent a previously unrecognized form of plasticity.

The inhibition of N-current by M_1Rs is controversial. It has been proposed recently that inhibition is directly attributable to the depletion of phosphatidylinositol-4,5-bisphosphate [PtdIns(4,5)P_2] during M_1 stimulation. However, in our lab, we have found arachidonic acid (AA) release, which occurs subsequent to PtdIns(4,5)P_2 hydrolysis, is both necessary and sufficient to elicit inhibition. Therefore, in a second study, I tested the effect of $Ca_V\beta$ expression on N-current during exogenous AA application and found a pattern of modulation identical to

M_1R stimulation. Furthermore, I took part in a collaborative project identifying the AA producing enzyme, diacylglycerol lipase (DAGL), to be a necessary component of the inhibitory pathway elicited by M_1Rs. These findings provide increased evidence for AA release being a key factor in the M_1R stimulated pathway of inhibition. Moreover, these discoveries identify the expression of $Ca_V\beta2a$ and use of specific DAGL inhibitors as a molecular and pharmacological strategy to block inhibition of N-current, respectively. These tools allow the dissection of downstream effects of M_1R stimulation, so that other modulatory effects may be observed.

The phosphorylation of N-channels by protein kinase C (PKC) blocks inhibition of current brought on by G-protein β and γ subunits (Gβγ) binding directly to the channel. Relief of Gβγ inhibition by other means has been identified as a mechanism of short term plasticity. M_1Rs are known to simulate PKC, but a connection between M_1Rs and PKC phosphorylation of N-channels had not been demonstrated. I hypothesized that PKC stimulation may be occluded by other downstream effects of M_1Rs. Therefore in a third study, I used a pharmacological approach on SCG neurons to dissect the PKC activating pathway from the other downstream effects of M_1 stimulation. I observed modulation of N-current indicating a loss of Gβγ inhibition, thus consistent with PKC phosphorylation of channels. This conclusion reveals another aspect of M_1 modulation, which can function as a means of short term plasticity.

TABLE OF CONTENTS

LIST OF FIGURES

LIST OF FIGURES (continued)

* These figures courtesy of Liwang Liu, UMass Medical School, Worcester, MA.
† This figure courtesy of Lee F. Stanish, UMass Medical School, Worcester, MA.
‡ This figure courtesy of Greg Michael, Queen's University, London, UK.

LIST OF ABBREVIATIONS

ACh	acetylcholine
AID	alpha interaction domain
AA	arachidonic acid
BAPTA	bis(*O*-aminophenoxy)ethane-*N*,*N*,*N*',*N*'-tetraacetic acid
BID	beta interaction domain
BLM	bisindolylmaleimide
BSA	bovine serum albumin (in this thesis refers to fatty acid free form)
cAMP	cyclic adenosine mono-phosphate
cGMP	cyclic guanosine mono-phosphate
$Ca_V\beta$	voltage gated calcium channel β subunit
ω-CTX	ω-conotoxin GVIA
DAG	diacylglycerol
DAGL	diacylglycerol lipase
DHP	dihydropyridine
DMEM	Dulbecco's modified Eagle's medium
DMSO	dimethyl sulfoxide
DRG	dorsal root ganglion
FPL	FPL 64176 (2,5-dimethyl-4-[2-(phenylmethyl)benzoyl]-1H-pyrrole-3-carboxylic acid methylester)
Gβγ	G-protein β and γ subunits
GFP	green fluorescent protein
GK	guanylate kinase

LIST OF ABBREVI ATIONS (continued)

GPCRs	G-protein coupled receptors
GqPCRs	Gq-coupled receptors
HEK	human embryonic kidney (cell line)
HEK-M1	HEK cell with a stably transfected M_1R
HVA	high voltage activated
Ins(1,4,5)P_3	Inositol(1,4,5)trisphosphate
I-V plots	graphs current vs. voltage for whole-cell recordings
LVA	low voltage activated
MAGUK	membrane-associated guanylate kinase
M-current	a voltage-gated potassium current sensitive to muscarinic stimulation
M_1R	M_1 muscarinic receptor M_2R (also M_2R: muscarinic receptor, etc)
MDCK	Madin Darby canine kidney (cells)
METH	methoctramine (M_2R preferring antagonist)
MT-7	Mamba toxin 7
N-channels	N-type calcium channels
N-current	charge influx through N-type calcium channels
NE	norepinephrine -(+)-bitartrate
NT	neurotransmitter
OPC	oleyloxyethyl phosphocholine
Oxo-M	oxotremorine methiodone
PA	phosphatidic acid
PH	pleckstin-homology

LIST OF ABBREVI ATIONS (continued)

PI	phosphoinositide
PI4K	phosphoinositide-4 kinase
PKC	protein kinase C
PKCε-TIP	PKCε translocating inhibiting peptide
PLC	phospholipase C
PMA	phorbol 12-myristate 13-acetate
PtdIns(4,5)P_2	phosphatidylinositol-4,5-bisphosphate
PTX	pertussis toxin
RHC	RHC 80267 [1,6-di(O-(carbamoyl)cyclohexanone oxime)hexane]
SCG	superior cervical ganglion
tsA 201	HEK cell line transformed with temperature sensitive antigen
TTX	Tetrodatoxin (Sodium Channel Blocker)
VGCC	voltage-gated calcium channel

CHAPTER I

BACKGROUND

A. Introduction

In his book *Astonishing Hypothesis: The Scientific Search for the Soul,* Francis Crick contends the human self with all its emotion, memory, consciousness and free will is no more than the summed activities of a vast array of nerve cells. As Dr. Crick puts it, Lewis Carroll's Alice might say, "You're nothing but a pack of neurons." (Crick, 1994). This proposition is the fundamental working hypothesis of modern neuroscience, expanded by Eric Kandel in his book, *In Search of Memory: The Emergence of a New Science of Mind*. Amongst neuroscientists it is understood that the human psyche is the apparent manifestation of physical interactions within the human brain. Therefore, the mysteries of what is called self, soul, or mind, may be unraveled as the modern tools of science elucidate the various molecular mechanisms of neuronal function (Kandel 2006).

The molecular mechanisms may be studied as any of a number of neuronal transformations; such as changes in gene expression or cell morphology. However, antecedent to any lasting plastic changes occurring in neurons are biochemical events elicited by surface receptor activation and electrical events conducted by the movement of ions. My thesis describes the how one receptor affects one subtype of voltage-gated calcium channel (VGCC); specifically how the activity of N-type calcium channels (N-channels) is modulated by the activation of M_1 muscarinic receptors. Since VGCCs are implicated in a variety of neuronal signaling pathways, their modulation can be considered a mechanism of short term plasticity (Brody and Yue 2000).

B. Voltage-Gated Calcium Channels

The physiological basis for electric signaling was described over a half a century ago when Hodgkin and Huxley (1952) determined that action potentials, the fundamental unit of electric signaling, are due to reversible alterations in the ion permeability across the plasma membrane. Their work established the concept of ion selective pores in the membrane, and that changes ion flux through sodium and potassium channels conduct action potentials. Soon after, Fatt and Katz (1953) found a current independent of sodium or potassium flux and hypothesized the possibility of calcium selective permeability.

We now know VGCCs exist and serve numerous functions within neurons. For example, N-type calcium channels are deemed important for triggering neurotransmitter release at synaptic terminals (Hirning et al., 1988; Takahashi and Momiyama, 1993; Turner et al., 1993), biochemical changes including: enzyme activation (Rittenhouse and Zigmond, 1999) and gene transcription (Brosenitsch and Katz, 2001; West et al., 2002). N-current also affects calcium activated potassium channels altering the membrane potential itself (Wisgirda and Dryer, 1994).

Calcium's importance as a signaling molecule starts early in the development of life itself. Since calcium readily forms complexes with anionic species, evolutionary pressure mandated intracellular calcium levels kept low, otherwise calcium and phosphate would precipitate out leaving deposits of hard bone-like solid within cells (Jaiswal, 2001; Carafoli, 2002). Cells developed exquisite mechanisms buffering calcium to extremely low levels (< 100 nM) making calcium an ideal signaling molecule. In fact, calcium influences a huge diversity of functions; everything from the initiation of life at

the moment of fertilization to the termination cell life by inducing apoptosis. (for review see Berridge, 1998 or Carafoli, 2002).

VGCCs are multimeric proteins comprising subunits α_1, β, $\alpha_2\delta$ and γ (**Fig. 1-1 a)**. The α_1 subunit forms the calcium pore and contains the voltage sensor which allows the channel to gate during changes in membrane potential. (**Fig. 1-1 b**; Catterall, 2000; Hille, 2001). The α_1 is surrounded by and modulated by the other ancillary subunits. VGCCs can be broken down into two large groups high voltage activated (HVA) and low voltage activated (LVA). LVA channels respond to relatively low depolarization and comprise the T-type channels. HVA channels are further classified based on biophysical properties and sensitivity to pharmacological agents. These are the N-, L- and P/Q- and R- types of channels. L-channels are all sensitive to dihydropyridines (DHP), a class of chemical compounds which comprises both L-channel agonists and antagonists. P/Q-channels are blocked by the toxin ω-Aga IVA isolated from spider venom, and N-channels are blocked by ω-conotoxin GVIA (ω-CTX) (McCleskey et al., 1987; Tsien et al., 1988). R-current was originally used to describe the HVA calcium current that is remaining after pharmacological block by DHPs and the two aforementioned toxins. Now R-current more commonly refers to a current through a specific channel type closely related to P/Q- and N- channels.

A new nomenclature has been established for VGCCs (**Fig 1-2**; Ertel et al., 2000). The new taxonomy groups channels according to homology. The Ca_V1 comprises the different L-channels, while the closely related P/Q, N and R- type channels make up the Ca_V2 family. Finally the Ca_V3 family consists of the known T-type channels. This nomenclature was established by a committee of eminent channel scientists studying

VGCCs and was meant to supplant the traditional terms which were becoming confusing as the list of known α_1 subunits expanded. In his text *Ion Channels of Excitable Membranes*, Bertil Hille has outlined how the conventions are still used. A "phenomenological" nomenclature (i.e. HVA vs. LVA or L vs. N) still applies to descriptions of currents from cells expressing unknown mixtures of VGCC gene products such as dissociated excitable cells. A "clone" nomenclature (i.e. $Ca_V2.2e$) is required for to describe experiments using particular gene products or splice variants (Hille 2001).

The primary structure of VGCC α_1 subunit was first determined by Tanabe and colleagues in 1987. The analysis of hydrophobic and hydrophilic residues suggested the calcium channel had twenty-four membrane spanning a-helices arranged in four repeating domains (I-IV) of six alpha helices (S1-S6) (Noda et al 1984). The four repeating domains are often called pseudo-subunits as they are homologous in structure and function to the subunits of tetrameric voltage-gated potassium channels. In each pseudo-subunit contains at the S4 position is an alpha helix rich in cationic residues. The S4 is known to be important in voltage sensing (Liman et al 1992). At rest the inside of the cell membrane is negatively charged with respect to the extracellular surface, and the positive charges of the S4 alpha helices are attracted toward the inside of the cell. During depolarization the charge distribution across the membrane reverses and the positively charged portions of the channel are pushed towards the extracellular surface (Durell and Guy, 1992). Between the fifth and sixth helix is a short peptide sequence, the P-loop. When the channel is properly folded the P-loops converge to form the pore at the center of the channel (MacKinnon and Yellen, 1990) (**Fig 1-1 a,b**).

The pseudo-subunits of the α_1 are connected by intracellular loops. These loops together with the amino and carboxy termini of the α_1 subunit provide sites for modulation by intracellular events. Although many different proteins can interact with α_1 subunits, only three proteins are considered ancillary or auxiliary subunits of the channel. These proteins meet the following recommended criteria (from Arikkath and Campbell, 2003): An ancillary subunit 1) exists in purified channel complexes, 2) directly interacts with the α_1 subunit, 3) modulates trafficking or biophysical properties of the channel, and 4) is stably associated with the α_1 subunit. The ancillary subunits β and $\alpha_2\delta$ are particularly important for channel conductivity and expression at the cell surface (Catterall, 2000).

The VGCC β subunit (now commonly referred to as $Ca_V\beta$) is encoded by four distinct genes $Ca_V\beta$ ($Ca_V\beta$1-4), each gene giving rise to numerous splice variants (Dolphin 2003; Birbaumer 1998). All four genes are expressed in the brain. Each $Ca_V\beta$ is made up of five domains (D1-D5). Domains D1, D3, and D5 are highly variable regions. While the other two are highly conserved domains, D2 and D4 forming an SH3 domain and a guanylate kinase (GK) domain respectively (**Fig. 1-1 b**). The two conserved domains place $Ca_V\beta$ as a member of the membrane-associated guanylate kinase (MAGUK) family (for review see Dolphin, 2003). All $Ca_V\beta$ subunits bind α_1 subunits at a highly conserved sequence at the I-II linker termed the alpha interaction domain (AID; Pragnell et al., 1994; **Fig.1-1 b**). The binding of $Ca_V\beta$ increases surface expression of VGCCs by masking an ER retention sequence on the α_1 subunit (Bichet et al., 2000). The AID corresponding site of the $Ca_V\beta$ subunit was previously identified as the beta interaction domain (BID) through mutation and analysis. However, recently, three

different labs have obtained crystal structures of $Ca_V\beta$ subunits bound to AID peptides. This work published almost simultaneously all show the AID binds $Ca_V\beta$ at a site distinct from the BID (Opatowsky et al., 2004; Van Petegem et al., 2004; Chen et al., 2004). Since $Ca_V\beta$ subunits contain no transmembrane segments they typically exist completely in the cytoplasm. Some forms can associate with the plasma membrane independent of the α_1 subunit, most notably the splice variant $Ca_V\beta$2a which is palmitoylated at two cysteine residues near the amino terminus (Chien et al., 1998).

$Ca_V\beta$ subunits have numerous effects on channel localization and function. In Madin Darby Canine Kidney (MDCK) cells, a polarized epithelial cell line, coexpression of Cav2.1 with $Ca_V\beta$1b and $Ca_V\beta$4 resulted in transport to the apical membrane, while $Ca_V\beta$2a resulted in transport to the basolateral membrane (Brice and Dolphin, 1999). $Ca_V\beta$ subunits have been reported to influence modulation by the fast pathway (Roche et al., 1995, Roche and Treistman, 1998). The findings I will present in the third chapter of this thesis describe the influence of $Ca_V\beta$ subunits on N-current modulation via the slow pathway.

Like $Ca_V\beta$, four known genes exist for $\alpha_2\delta$ each with multiple splice variants. The $\alpha_2\delta$ complex associated with a given channel is the product of a single gene which is cleaved post-translationally and linked with disulfide bridges. The δ portion of the complex is a transmembrane α-helix which anchors the highly glycosylated α_2 portion of the complex (Klugbauer et al., 2003). The α_2 seems to be essential for increasing current amplitude by a mechanism which is unknown (Caterall, 2000; Arikkath and Campbell, 2003). A fourth subunit γ is known to associate with some VGCCs although unlike $Ca_V\beta$

and $\alpha_2\delta$, γ subunits do not affect localization of channels to the cell surface (Caterall, 2000; Arikkath and Campbell, 2003).

C. N-Channels

N-currents were first described by members of the Tsien lab using chick dorsal root ganglion neurons (Nowycky et al., 1985). Using whole-cell and single-channel recordings they identified previously unknown voltage-gated calcium currents. The current discovered by Nowycky and colleagues was given the distinction "N" for neither L- nor T-type current; the two previously described VGCCs. These conclusions were based on the N-current's biophysical properties and resistance to DHP (Nowycky et al., 1985; Fox et al. 1987). As research in the field continued several types of currents similar to N-current which are insensitive to DHP emerged. The discovery of ω-conotoxin GVIA isolated from snail venom (ω-CTX) presented a pharmacological tool to distinguish N-channels (McCleskey et al 1987, Tsien et al 1988, Plummer et al., 1989, Boland et al., 1994). In 1992 an ω-CTX-sensitive VGCC α_1 subunit was cloned first from rat (Dubel et al., 1992) and then human cells (Williams et al., 1992). The two constructs were 92.8% identical, and had the same architecture for VGCCs described by Tanabe and colleagues in 1987 (see **Fig 1-1**). It was noted at the time of their discovery the expression of N-channels requires the β and $\alpha_2\delta$ subunits in addition to the α_1 (Williams et al., 1992).

It was first thought that N-channels expression is restricted to neurons. N–channels are almost exclusively expressed in neuronal cells although they have been

found in cells outside the nervous system including chromaffin cells (Jan et al., 1990) and pancreatic beta cells (Sher et al., 1992).

Recently N-channels have become notable as a therapeutic target for pain (Snutch, 2005). ω-CTX and other N-channel specific inhibitors are the basis of pharmacological agents being developed to target chronic pain. The N-channel is also the target of a class of compounds referred to as nootropics which can enhance cognition in patients with dementia. It is thought that potentiating N-current enhances release of neurotransmitters thus improving neural function (Keren et al 1997, 1999). Specifically, N-current enhancing nootropics are thought to increase synaptic release of neurotransmitters (Gouliaev et al. 1994; Chorvat et al 1998; Yoshii et al 2000, 2004).

The N-channel is a highly modulated protein. Biochemical changes within a neuron activate signaling pathways altering N-channel activity. In particular, upon release, neurotransmitters bind G-protein coupled receptors (GPCRs) and initiate signaling pathways, modulating the N-channel's response to changing membrane potential (Elmslie 2003; Hille 1994). The signaling pathways which modulate N-current have been studied intensely for decades. Some signaling pathways remain mysterious, despite the concerted efforts of many labs. However, other pathways are well described so that now both the necessary components for signaling and the sites on the channel which are involved in signaling are known.

D. Muscarinic Receptors

Muscarinic receptors are seven transmembrane G-protein coupled receptors, comprising a family of proteins named encoded by five different genes (M_1-M_5). M_1 and

M_2 receptors were determined by members of the Numa lab (Kubo et al, 1986a; 1986b), followed by the discovery of sequences for M_3, M_4, and M_5 (Bonner et al.,1987, 1988; Peralta et al., 1987). All five are expressed in the CNS (Levey et al., 1991; Wei et al., 1994). In vivo muscarinic receptors are activated by acetylcholine (ACh) (Feldberg and Gaddum, 1934). ACh is known as the major ganglionic transmitter in the sympathetic nervous system, whereas in the central nervous system (CNS), ACh is crucial for cognition, learning and memory (Woolf 1996). Activation of the M_1 muscarinic receptor (M_1R) is of particular interest, as it is the most prevalent subtype expressed in hippocampus and cortex regions of the brain associated with learning and memory (Levey et al., 1991; Wei et al., 1994). Severe memory deficits occur in knockout mice lacking M_1Rs (Anagnostaras et al. 2003). Clinically, the M_1R is a therapeutic target for Alzheimer's disease (AD). In fact, at the present time the majority of drugs approved to treat AD act by increasing ACh at M_1Rs (Ibach & Haen 2004).

Muscarinic stimulation affects numerous neural functions including the modulation of voltage gated ion channels. In the early 1980s, M-current, a low threshold potassium current inhibited by muscarinic stimulation was identified in frog sympathetic neurons (Brown and Adams 1980) and rat superior cervical ganglion (SCG) neurons (Constanti and Brown 1981). These findings led to a putative model for how muscarinic receptors enhance the excitability of neurons (Brown 1983). The inhibition of M-current was shown to be require stimulation of M_1Rs (Marrion et al. 1989; Bernheim et al. 1992) acting through Gαq subunits of heterotrimeric GTP binding proteins (Haley et al. 1998).

After the discovery of M-current, muscarinic stimulation was found to inhibit N-channels by two distinct pathways a rapid process (less than 1 second) and a slower

process (greater than 4 seconds; Bernheim et al., 1991). The fast-pathway is elicited by M_2 and M_4 receptors and the slow pathway is induced mainly by M_1 receptors (Shapiro et al 1999). These two pathways are discussed in greater detail in the next sections.

E. The Fast Pathway

The study of fast pathway inhibition began 28 years ago when Dunlap and Fischbach (1978) reported exogenously applied norepinephrine (NE) reduces voltage-gated calcium current in chick dorsal root ganglion (DRG) neurons. Subsequently Holz and colleagues (1986) implicated G-proteins in the pathway of inhibition when they showed inhibition is blocked by pretreating cells with pertussis toxin (PTX) or dialyzing cells with GDP-βS. Soon afterward, Wanke and colleagues (1987) showed muscarnic stimulation also inhibits N-current by a PTX-sensitive pathway in rat sympathetic neurons. The importance of G-proteins was corroborated by experiments in which dialysis of GTP-γS mimicked the effect of neurotransmitter of calcium currents in DRG neurons; first in rat (Dolphin and Scott, 1987) then in chick (Marchetti and Robello, 1989). Moreover, inhibition of calcium currents in rat sympathetic neurons by either ACh or NE becomes irreversible when cells are dialyzed with GTP-γS (Song et al., 1989).

Originally it was thought that neurotransmitters inhibit current by somehow reducing the number of functional channels in the cell (Dunlap and Fischbach, 1978). An alternative model was proposed by Bruce Bean (1989) in which transmitters inhibit N-current by changing the voltage-dependence of channels. Bean noticed that neurotransmitters do not inhibit N-current equally across all test potentials. At low to moderate test potentials (-40 mV to +30 mV) neurotransmitters reduce the probability

that channels will open upon depolarization. At higher test potentials the neurotransmitters elicit little effect. Bean proposed channels exist in either a "willing" or "reluctant" state, and the activation of certain GPCRs pushes the bulk of channels from the willing to reluctant state. At low to moderate test potentials, the current elicited from channels in the reluctant state increases over a prolonged (100 msec) depolarization. Bean reasoned that slowly activating currents during prolonged depolarizations were due to channels moving from the reluctant to willing state.

Bean's model fit well with a previously proposed hypothesis that GPCR elicited inhibition might be relieved by a series of depolarizations (Marchetti et al 1986). The voltage-dependent model was advanced when Keith Elmslie and colleagues, using frog sympathetic neurons, found that a large transient depolarization reverses the inhibition elicited by a neurotransmitter or internally dialyzed GTP-γS (Elmslie et al., 1990). Elmslie's prepulse experiments confirmed the notion that the two states willing and reluctant could be separated rapidly and easily by voltage. Moreover, Elmslie's protocol established an elegant method to observe the proportion of channels in the willing or reluctant state under specific conditions of modulation. The relief of inhibition was termed facilitation and eventually, it was shown that repetitive physiological depolarizations transiently relieve inhibition in a similar manner (Brody et al., 1997; Artim and Meriney 2000).

Having identified a role for specific G-proteins and a biophysical mechanism for inhibition the next challenge for the field was to work out other steps in the pathway. Lopez and Brown (1991) discovered the re-inhibition of N-currents after prepulse facilitation is dependent on the concentration of activated G protein and hypothesized that

inhibition results from G-proteins bound directly to channels. Their hypothesis was supported by the co-precipitation of both Gα and Gβγ subunits bound directly to N-channels (McEnery et al 1994).

To determine whether Gα, Gβγ or both subunits were necessary for modulation of Ca_V2 channels, N- currents were recorded from SCG neurons injected with mRNAs for G-protein subunits (Ikeda, 1996) and P/Q- currents were recorded from tsA cells overexpressing G-protein subunits (Herlitze et al., 1996). In both cases overexpression of Gβγ mimicked the voltage-dependent inhibition normally elicited by neurotransmitters or internally dialyzed GTP-γS. Conversely, neither transfection of a constitutively active Gα subunit in SCG neurons, nor a range of Gα subunit concentrations in tsA cells elicits inhibition of Ca_V2 channels (Ikeda, 1996; Herlitze et al., 1996). These data indicated the reluctant state of Ca_V2 reflects the direct binding of Gβγ subunits to Ca_V2 subunits. Moreover, they strongly suggested prepulse facilitation works by dislodging Gβγ subunits from Ca_V2.

Having established the mechanism for current inhibition, many labs tried to pinpoint the site of Gβγ binding on Ca_V2 subunits. The site of Gβγ was sought using mutated Ca_V2 subunits and chimerae of Ca_V2 and Ca_V1 sequences since L-channels are G-protein insensitive. Three regions of Ca_V2 emerged as important for Gβγ interaction; the intracellular loop between pseudo-subunits I and II (I-II linker; DeWaard et al., 1997; Zamponi et al 1997), the carboxy tail (Qin et al 1997), and the amino terminus (Zhang et al., 1996; Page et al., 1998; Canti et al., 1999). The most recent intensive work in this area on N-channels indicated that inhibition arises from an interaction between the Ca_V2

amino terminus and the I-II loop (Agler et al., 2005), however the specifics of this interaction are not well described.

F. Block of Gβγ Modulation by Protein Kinase C

At the same time the mechanism for inhibition of calcium currents by GPCRs was being worked out, it was shown that phorbol esters enhance calcium currents in sympathetic neurons (Yang and Tsien, 1993; Swartz et al 1993, Zhu and Ikeda 1994). The two observations intersected when it was shown that pretreatment of neurons with phorbol esters blocked inhibition by neurotransmitters (Swartz et al., 1993; Swartz, 1993). These data implicated protein kinase C (PKC) as an agent for control of the fast pathway. Since phorbol esters can activate enzymes other than PKC, the experiments were repeated using intracellular dialysis of a PKC inhibiting peptide. The blocking peptide, but not the "scrambled" peptide control, attenuates the block of inhibition by phorbol esters (Swartz, 1993). Moreover the actions of phorbol esters were equivalent to prepulse facilitation (**Fig 1-4 a, b**). Using phorbol esters, GTP-γS, and Elmslie's voltage protocol, Barrett and Rittenhouse (2000) set up an array of experiments which extended the model still further; showing that as phosphorylation blocks G-protein binding, G-protein binding interferes with phosphorylation. They expanded Bean's designations of channels to include "willing and available" to describe those channels which were neither inhibited by Gβγ binding nor phosphorylated by PKC (**Fig 1-5 b**).

The work by Swartz suggested a direct antagonism between PKC activity and G-protein binding. In 1997 Gerard Zamponi and colleagues identified what they termed a center of "crosstalk" at the I-II linker, the intracellular loop of Ca_V2 connecting pseudo-

subunits I and II. The I-II linker of $Ca_V2.2$ has several consensus sites for phosphorylation by PKC (Dubel et al 1992), and, as noted above, the I-II linker of $Ca_V2.2$ was implicated as an important site for Gβγ binding. The I-II linker was shown to bind Gβγ subunits *in vivo* experiments (De Waard et al., 1997, Zamponi et al, 1997) and in a yeast-two hybrid assay (Garcia et al., 1998). Peptides consisting of residues from this region prevented inhibition when dialyzed into cells, presumably by competitively binding, thus effectively sequestering Gβγ subunits (Herlitze et al., 1997; Zamponi et al., 1997). However, when I-II linker peptides were phosphorylated *in vitro* they lost the capacity to block inhibition (Zamponi et al., 1997). These data led to the conclusion that phosphorylation of the I-II linker prevents the direct binding of Gβγ subunits thus blocking transition to the "reluctant" state.

To ascertain the specific site of phosphorylation that is important for cross-talk a series of $Ca_V2.2$ subunit mutations were produced, expressed in HEK cells, and examined for resistance to modulation (Hamid et al., 1999). There are four possible PKC phosphorylation sites on the I-II linker (**Fig 1-4 a**). A series of experiments in which the possible PKC sites were mutated to alanine (to show loss of phosphorylation) or glutamate (to approximate constitutive phosphorylation) proved Thr^{422} is the most essential phosphorylation site to block inhibition by Gβγ subunits (Hamid et al., 1999).

Although the cross-talk between PKC and G-protein inhibition provides a reasonable and attractive model for modulation of $Ca_V2.2$, the *in vitro* activators of PKC to block fast pathway inhibition have proven to be elusive. PKC is typically activated by diacylglycerol (DAG) which is released by activation of phospholipase. A number of GPCRs are known to activate phospholipses, among them the M_1Rs activation of

phospholipase C-β (PLC-β). In the fifth chapter of this thesis I will describe experiments I've conducted to examine a role for M_1Rs in crosstalk with the fast pathway. The observation of PKC activation by M_1Rs may be normally occluded by other signaling pathways which occur downstream of M_1R stimulation, most notably the so-called slow pathway which is described in the next section.

G. The slow pathway

In addition to the previously described fast pathway, muscarinic stimulation inhibits whole cell calcium currents in sympathetic neurons through M_1Rs by a pathway known as the slow pathway. The two pathways can be differentiated by several features (**Fig 1-3**). Unlike the fast pathway, the slow pathway is both PTX-insensitive and voltage insensitive (Wanke et al., 1987; Beech et al., 1992) Also, the slow pathway is disrupted by high concentrations (20 mM) of the calcium chelator bis(*O*-aminophenoxy)ethane-*N*,*N*,*N*',*N*'-tetraacetic acid (BAPTA; Beech et al., 1991; Mathie et al., 1992). Finally, in single-channel recordings, channels isolated by the patch pipette are still affected by the agonist indicating there is at least one diffusible second messenger in the pathway (Bernheim et al 1991; for review see Hille 1994).

The discovery of M_1R mediated inhibition of N-current followed the discovery of M_1R mediated inhibition of a voltage-gated potassium current (M-current; Brown and Adams, 1980). The two types of inhibition share several common characteristics including the concentration of muscarinic agonist required to induce inhibition and the time frame in which inhibition occurs. Therefore, it was postulated that the two types of inhibition may be caused by a similar mechanism. That is, hypothetically, one diffusible second messenger or set of second messengers released during M_1 stimulation might be

responsible for both types of inhibition (Hille 1994; Delmas et al 2005; Delmas and Brown, 2005). Of course, a similarity in function does not prove a conservation of mechanism, and the fact that the same concentration of agonists elicits both effects may have more to do with the agonist's affinity for the receptor than a parallel response of downstream effects. Still, the resemblance of modulation by two voltage-gated channels by stimulation the one receptor merits constant comparison between the two fields of research.

Even though inhibition of both N- and M- current by muscarinic agonists has been the subject of study for many labs the identification of the diffusible second messenger(s) has been elusive. Early experiments ruled out a role for cAMP, cGMP, nitric oxide and protein kinases in the slow pathway (reviewed by Hille, 1994). The predominant effect of M_1R stimulation is the activation of phospholipase C. The necessity for PLC activation in both M- and N-current modulation has been well documented (reviewed in Suh and Hille 2005; Delmas and Brown 2005). Amongst the different downstream effects of M_1Rs through PLC two have emerged as possible key mechanisms for N-current inhibition. They are: 1) the breakdown of phosphatidylinositol-4,5-bisphosphate [PtdIns(4,5)P_2] and its consequent dissociation from Ca_V2 subunits (Wu et al Gamper et al 2002; Delmas et al 2005), and 2) the release of arachidonic acid (AA) which occurs subsequent to PtdIns(4,5)P_2 hydrolysis and inhibits N-current either directly or indirectly (**Fig. 1-6;** Liu et al 2006; Liu and Rittenhouse 2003).

H. Modulation of N-current by PtdIns(4,5)P_2

PtdIns(4,5)P_2 constitutes less than 1% of the membrane phospholipids yet it is the component of a vast array of signaling paradigms (Czech 2000). PtdIns(4,5)P_2 is known classically for the effects of its breakdown products PKC activation by DAG and internal calcium release from IP_3 receptors activated by Ins(1,4,5)P_3. However, there is a new field of PtdIns(4,5)P_2 study which focuses on direct binding of PtdIns(4,5)P_2 and subsequent activation of proteins The low concentration of PtdIns(4,5)P_2 allows for its rapid depletion when PLC is stimulated. In neuroblastoma cells muscarinic stimulation reduces PtdIns(4,5)P_2 by 75% within 60 seconds (Willars et al 1998). The study of PtdIns(4,5)P_2 mediated effects received a lift from advent of green fluorescent protein (GFP)-PLCδ-pleckstin-homology (PH) domain binds PtdIns(4,5)P_2 at cell surfaces and thus allows the real time comparison of PtdIns(4,5)P_2 breakdown with downstream effects (Czech 2000).

The implication of PtdIns(4,5)P_2 as the signaling molecule for Ca_V2 coincides with work connecting PtdIns(4,5)P_2 with inhibition M-current and follows seminal work indicating PtdIns(4,5)P_2 directly modulates ATP sensitive potassium channels (Hilgemann and Ball, 1996). For M-current the time course of inhibition and recovery mirrors the breakdown and resynthesis of PtdIns(4,5)P_2. In whole-cell recordings and excised patches PtdIns(4,5)P_2 activates channels and attenuates rundown of current (Zhang et al., 2003; Ford et al., 2004).

The evidence for PtdIns(4,5)P_2 having a role in Ca_V2 modulation comes mainly from two studies. First, dual opposing modulatory effects of PtdIns(4,5)P_2 were reported for $Ca_V2.1$ (Wu et al 2002). In large excised patches from frog oocytes channel activity

ran down Channel activity was restored by puffing PtdIns(4,5)P_2 Channel activity was decreased by sequestering PtdIns(4,5)P_2 with cationic peptides or antibodies specific for PtdIns(4,5)P_2. Wu and colleagues postulated PtdIns(4,5)P_2 binds to the "S" (for stabilization) domain of the channel thus stabilizing current. Surprisingly the authors found PtdIns(4,5)P_2 also caused a shift in activation potential. The authors compared the shift in voltage sensitivity to Bruce Bean's willing and reluctant model. They postulated a second binding site for PtdIns(4,5)P_2 on the channel, the "R" (for reluctant) domain. PtdIns(4,5)P_2 binding to the R domain hypothetically shifts the channel to the reluctant mode, requiring stronger depolarizations.

The second study was done on native N-channels in SCG neurons (Gamper et al 2004). The authors of this study also found PtdIns(4,5)P_2 attenuates rundown. PtdIns(4,5)P_2 dialyzed into cells during whole-cell recordings reduces inhibition elicited by the muscarinic agonist oxotremorine methiodone (oxo-M). Also, inhibition by oxo-M becomes irreversible when resynthesis of PtdIns(4,5)P_2 is blocked by wortmannin.

These data taken together have been declared clear evidence that Ca_V2 channels require PtdIns(4,5)P_2 for activation (Suh and Hille, 2005; Delmas and Brown, 2005).

I. Modulation of N-current by AA

The requirement for PtdIns(4,5)P_2 hydrolysis in the slow pathway is clear. However, previously Liwang Liu in Ann Rittenhouse's lab determined modulation of N-current by M_1Rs requires events downstream of PtdIns(4,5)P_2 hydrolysis (Liu et al 2004). In superior cervical ganglion (SCG) neurons M_1R stimulation and arachidonic acid (AA) elicit the same distinct pattern of modulation (Liu et al. 2001; Liu et al. 2003); inhibiting

whole-cell N-current at positive test potentials and enhancing N-current at negative test potentials (**Fig 1-7**). A similar pattern of modulation emerges when AA or its corresponding amide anandamide is applied to VGCCs. For example, whole-cell currents from adult rat SCG neurons are enhanced at negative potentials and inhibited at positive potentials by anandamide (Guo and Ikeda 2004). Although enhancement was not observed in T-type channels, AA also simultaneously shifts activation towards negative potentials and increases steady state inactivation (Talavera et al 2004).

M_1R stimulation releases AA (Tence et al 1994; Strosznajder & Samochocki 1992) suggesting a role in the slow pathway. Consistent with this hypothesis, reduction of AA levels either by the PLA_2 antagonist oleyloxyethyl phosphocholine (OPC) or by absorption of AA with a fatty acid free bovine serum albumin (BSA) minimizes both enhancement and inhibition of N-current (Liu & Rittenhouse 2003; Liu et al. 2004). More recently Liwang Liu has examined the role of AA production in inhibition of L-current. He has found the slow pathway is attenuated by PLA_2 specific antibodies dialyzed internally and in recordings from neurons harvested from $PLA_2^{-/-}$ knockout mice (Liu et al., 2006).

In the fourth chapter of this thesis I will describe a collaborative project between Liwang and myself demonstrating the necessity of another AA producing enzyme, DAG lipase, in slow pathway inhibition.

J. A controversy for PtdIns(4,5)P_2 and AA

The assumption that PtdIns(4,5)P_2 binds directly to Ca_V2 channels, thus stabilizing its current has been proposed and acknowledged by several labs (Delmas et al

2005, Suh and Hille 2005). Still, at present, no binding site for PtdIns(4,5)P_2 on any VGCC has been determined. However, there is increasing evidence that M-current and Ca_V currents are modulated by divergent pathways. For example it was recently reported that palmitoylated cationic peptides designed to sequester PtdIns(4,5)P_2 blocked inhibition of M- but not N- current (Robbins et al 2006). These data would agree with our finding that AA production is necessary for inhibition of N- and L- but not M-current (Liu et al 2006; Chapter IV of this thesis).

It is possible the PtdIns(4,5)P_2 model and AA model can co-exist. A model in which PtdIns(4,5)P_2 and AA act in opposition on the same pathway has been reported in potassium channels (Oliver et al 2004). Fast inactivation of certain Kv channels is blocked by PtdIns(4,5)P_2 but enhanced by AA. The authors of this study reported a PtdIns(4,5)P_2 binding site at the N-terminus of the Kv channel and postulated AA acts through an allosteric modification of the channel.

Here, I have described two modulatory effects of PtdIns(4,5)P_2 on Ca_V2 and two modulatory effects of AA on Ca_V2. In both types of modulations PtdIns(4,5)P_2 and AA act in opposite directions. PtdIns(4,5)P_2 sustains Ca_V2 currents while AA inhibits currents. PtdIns(4,5)P_2 causes an activation shift to positive potentials while AA causes an activation shift to negative potentials. Thus, as for the Kv channel PtdIns(4,5)P_2 and AA may act on the same pathways but in opposite directions. Our data indicate the block of AA production completely eliminates inhibition, also exogenous AA elicits inhibition, so AA is necessary and sufficient to cause inhibition. It is possible under normal physiological conditions as PtdIns(4,5)P_2 depletion and AA formation occur simultaneously, VGCCs are sensitive to both consequences of M_1R stimulation.

Moreover, it is possible under experimental conditions application of either PtdIns(4,5)P_2 or AA could seem to function independently if either was used at high enough concentrations.

In summary, the modulation of N-current by M_1Rs is highly complex. M_1Rs initiate multiple signaling cascades several of which may converge on the N-channel. The remainder of this thesis will be descriptions of how those signaling cascades may be teased apart for a better understanding of how M_1Rs affect N-current.

Figure 1-1. Voltage-gated Calcium Channels (VGCC). (**a**) Voltage gated calcium channels are multimeric complexes made up of a large (170- 250 kDa) α_1 subunit, which is surrounded by and modulated by the ancillary subunits β and $\alpha_2\delta$. A fourth subunit γ which may be associated with VGCCs is not shown. VGCCs span the plasma membrane and allow the permeation of calcium into the cell during periods of depolarization. (**b**) Shown here is the secondary structure of VGCC subunits. The α_1 subunit 24 membrane spanning α-helices are grouped into four homologous pseudo-subunits (I-IV), each containing six membrane-spanning α-helices. Of note is the fourth α-helix of each pseudo-subunit (S4) which contains a concentration of cationic residues which are crucial for sensing changes in membrane potential. Also of note are the fifth and sixth α-helices (S5 and S6) and the short loop of peptide between the two (the P-loop). The P-loop forms the structure of the pore and thus determines the selection of ion by the channel. Between the pseudo-subunits are large intracellular loops. These loops in conjunction with the amino and carboxy termini provide sites for biochemical interactions with intracellular proteins. β subunits are completely cytoplasmic and bind the α_1 subunit at a sequence termed the AID located within the I-II linker. β subunits each have a SH3 domain and a guanylate kinase (GK) domain. The AID is bound at the GK of the β subunit. The $\alpha_2\delta$ subunit is the result of one gene which is spliced post-translationally and secured with disulfide bridges. The δ portion of the subunit forms a single membrane spanning α-helix, anchoring the $\alpha_2\delta$ subunit in the membrane. The α_2 portion of the subunit is highly glycosylated and completely extracellular. The figures shown were created from a compilation reports cited in the text.

a

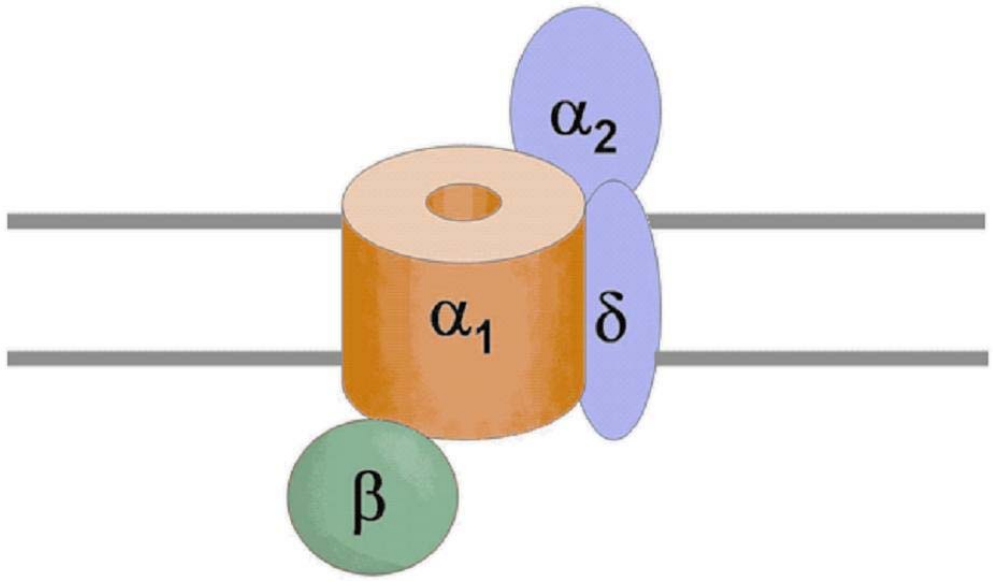

b

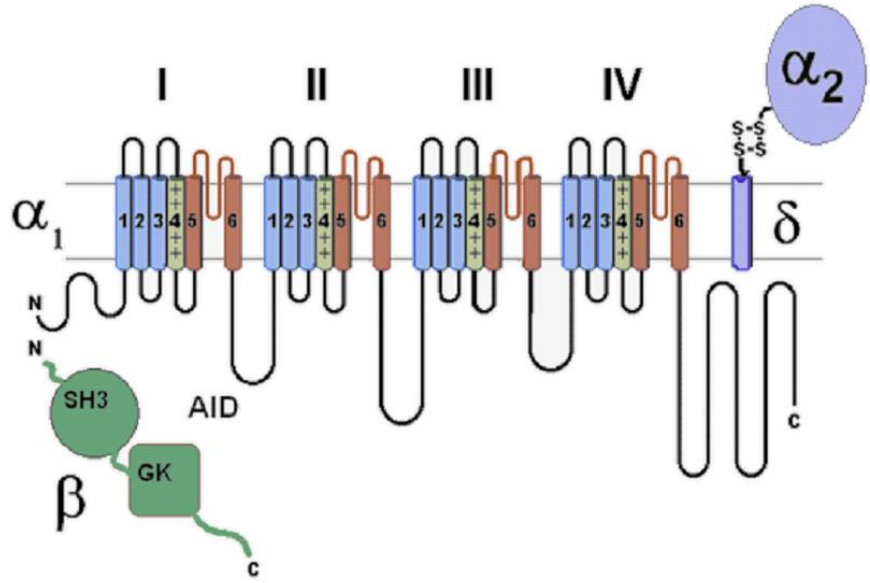

Figure 1-2. Subfamilies of Voltage-Gated Calcium Channels (VGCCs). Presented is a dendogram depicting taxonomy of voltage-gated calcium channels as determined by sequence homology. Modern nomenclature categorizes VGCC genes in three large subfamilies; Ca_V1, Ca_V2, and Ca_V3. The high voltage activated channels (HVA) comprises Ca_V1 and Ca_V2, which encompass the L-, P/Q, N- and "R"- type channels as labeled on the horizontal connectors of the dendogram. These were first differentiated by biophysical properties, and later by pharmacology: L-channels being sensitive to dihydropyridines, P/Q-channels sensitive to the toxin ω-Aga IVA isolated from spider venom, and N-channels sensitive to ω-conotoxin GVIA isolated from snail venom. "R"-channels were named for the HVA channels not sensitive to the aforementioned pharmacological agents, however more recently the designation "R" has come to be used more specifically and correspond to the $Ca_V2.3$ channel as shown. The low voltage activated channels (LVA) comprise the T-type channels. The matching percentage of amino acid sequences was determined by comparing the homologous regions of the different channel sequences (the transmembrane segments and P-loops; see Fig 1-2), about 350 amino, acids using the CLUSTAL algorithm (see Ertel et al 2000). Shown at far right, in parentheses, are the previously used conventional designations for VGCC genes. The classification was superseded by the classification shown in the dendogram which reflects homology between channel types (see Ertel et al 2000; also Hille 2001)

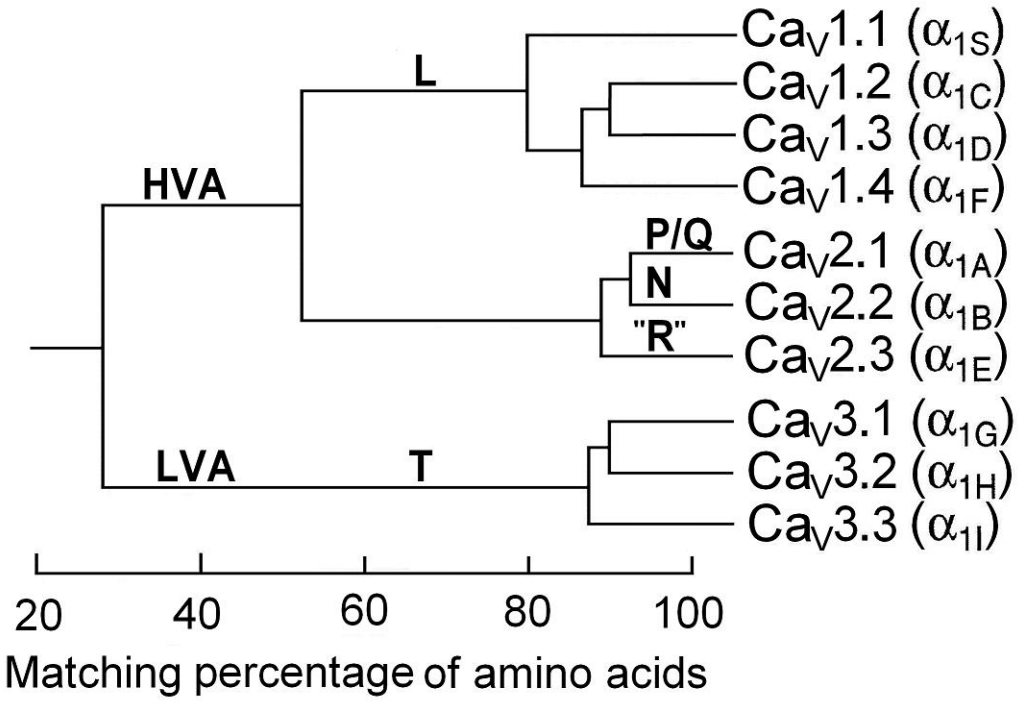
$Ca_V1.1$ (α_{1S})
$Ca_V1.2$ (α_{1C})
$Ca_V1.3$ (α_{1D})
$Ca_V1.4$ (α_{1F})
$Ca_V2.1$ (α_{1A})
$Ca_V2.2$ (α_{1B})
$Ca_V2.3$ (α_{1E})
$Ca_V3.1$ (α_{1G})
$Ca_V3.2$ (α_{1H})
$Ca_V3.3$ (α_{1I})
L
HVA
P/Q
N
"R"
LVA
T
20
40
60
80
100
Matching percentage of amino acids

Figure 1-3. Pathways of Muscarinic inhibition of N-type Calcium Channels. Muscarinic stimulation of SCG neurons elicits modulation of N-channels through two distinct pathways as shown. The fast pathway illustrated at left was formerly called the membrane delimited pathway since channels isolated by a patch pipette are not affected by ligands for receptors outside the pipette. The muscarinic receptors which elicit fast pathway inhibition are the M_2 and M_4 receptors. It is known now known that fast pathway inhibition results from direct binding of Gβγ subunits to $Ca_V2.2$. See text for details. The slow pathway illustrated at right is elicited by M1 muscarinic receptors in SCG neurons. M_1 simulation will affect channels isolated from muscarinic agonists by the patch pipette and thus the slow pathway is known to involve at least one diffusible second messenger. Slow pathway inhibition requires PtdIns(4,5)P_2 breakdown by the enzyme phospholipase C. However, whether or not events subsequent to PtdIns(4,5)P_2 hydrolysis are essential for N-current modulation remains controversial. Each of the two pathways may be induced by ligands other than muscarinic agonists. As listed at the bottom of the figure, the two pathways are distinguished by several characteristics including sensitivity to voltage protocols, the Ca^{2+} chelator BAPTA, and PTX toxin.

Muscarinic Modulation of N-Current in SCG Neurons

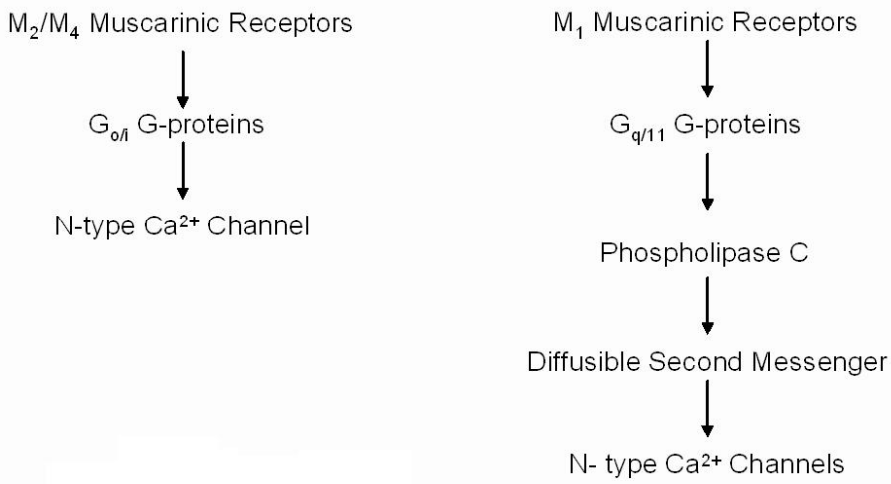

Properties

Voltage-Dependent
PTX-sensitive
[BAPTA]-insensitive
Time for inhibition <1 sec

Properties

Voltage-Independent
PTX-insensitive
[BAPTA]-sensitive
Time for inhibition > 4 sec

Figure 1-4. Crosstalk for Gβγ and PKC. (a) Stimulation of GCPRs actvates G-proteins direct binding of Gβγ to $Ca_V2.2$, inhibiting N-current. Activation of PKC blocks inhibition. (b) Intracellular loops provide sites of interaction with intracellular mechanisms. Gβγ binds $Ca_V2.2$ at several sites including N-terminus, I-II linker and C-terminus. Mutational analysis of PKC consensus sites at the I-II linker has demonstrated phosphorylation of the I–II linker blocks Gβγ binding. Note: The site of crosstalk for PKC and Gβγ and the binding site for calcium channel β-subunit ($Ca_V\beta$) are on the I-II linker of the $\alpha_1$subunit (Zamponi et al., 1997; Pragnell et al., 1994; Hamid et al., 1999).

a

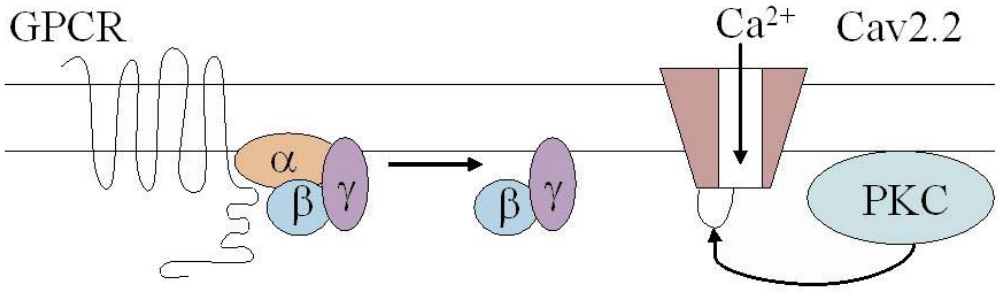
GPCR
Ca2+
Cav2.2
α
β
γ
β
γ
PKC

b

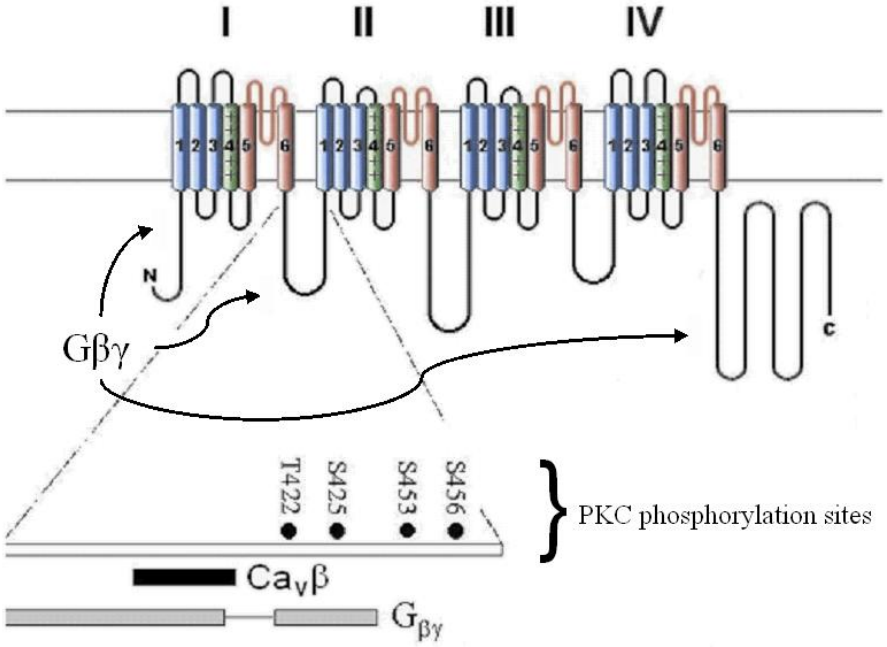
I
II
III
IV
1 2 3 4 5 6
N
C
Gβγ
T422
S425
S453
S456
PKC phosphorylation sites
CaVβ
Gβγ

Figure 1-5. Willing, Reluctant and Available Modes of Channel Activity (a) voltage protocol established by Keith Elmslie (Elmslie et al 1990) relieves tonic inhibition of N-current. A strong prepulse to +80 mV drives channel from "reluctant" to "willing" state evidently by dislodging Gβγ from $Ca_V2.2$. Prepulse increases amplitude of current and changes kinetics (b) whole cell recordings from cells exposed to PMA activates PKC and results in loss of prepulse facilitation (c) Model proposed by Barrett and Rittenhouse (2000) in which channels phosphorylated and dephosphorylated channels both behave as "willing". Only dephosphorylated channels are available for G-protein modulation. Moreover G-protein binding limits availability of PKC site.

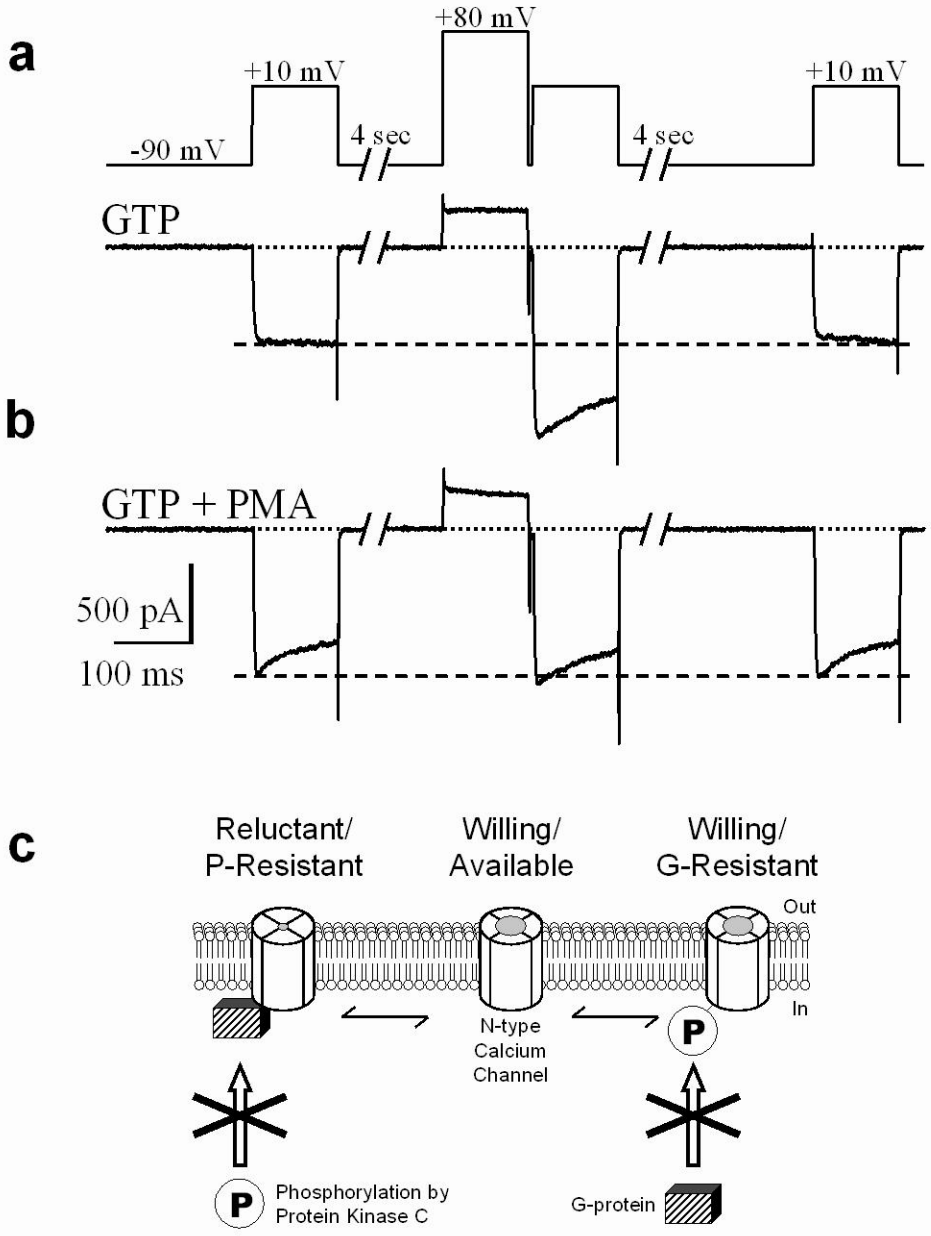
a
+80 mV
+10 mV
+10 mV
-90 mV
4 sec
4 sec
GTP
b
GTP + PMA
500 pA
100 ms
c
Reluctant/
P-Resistant
Willing/
Available
Willing/
G-Resistant
Out
In
N-type
Calcium
Channel
P
P
Phosphorylation by
Protein Kinase C
G-protein

Figure 1-6. The PtdIns(4,5)P_2 cycle. Phosphorylation of phosphoinositide (PI) at the 3,4, and 5 positions on the inositol ring generates mono-, bis-, and trisphosphate derivatives with different signaling possibilities. This figure depicts signaling pathways affected by PtdIns(4,5)P_2 which may directly or indirectly modulate N-current. The consecutive activity of phosphoinositide-4 kinase (PI4K) and phosphoinositide 5-kinase (PIP5K) produces phosphatidylinositol-4-phosphate [PtdIns(4)P] and phosphatidylinositol-4,5-bisphosphate [PtdIns(4,5)P_2], respectively. PtdIns(4,5)P2 may be dephosphorylated by 5-phosphatase (PIP2 5-Pase) to PtdIns(4)P, which in turn can be dephosphorylated to PI. Stimulation of certain G-protein-coupled receptors (GPCRs) activates phospholipase C (PLC). In turn, PLC cleaves PtdIns(4,5)P_2, producing the second messengers inositol (1,4,5)-trisphosphate [Ins(1,4,5)P_3] and diacylglycerol (DAG). Ins(1,4,5)P_3 releases Ca^{2+} from intracellular stores through activation of the Ins(1,4,5)P_3 receptor (IP_3R). Free Ins(1,4,5)P_3 is quickly dephosphorylated by specialized phosphatases that remove specific phosphates to generate inositol. DAG can activate protein kinase C (PKC) either by itself or in conjunction with Ca^{2+}. Alternatively, DAG may be recycled into phosphoinositide through DAG kinase mediated phosphorylation to phosphatidic acid (PA). After which PA combines with inositol to reform PI. Finally, DAG can be hydrolyzed by DAG lipases to release arachidonic acid (AA).

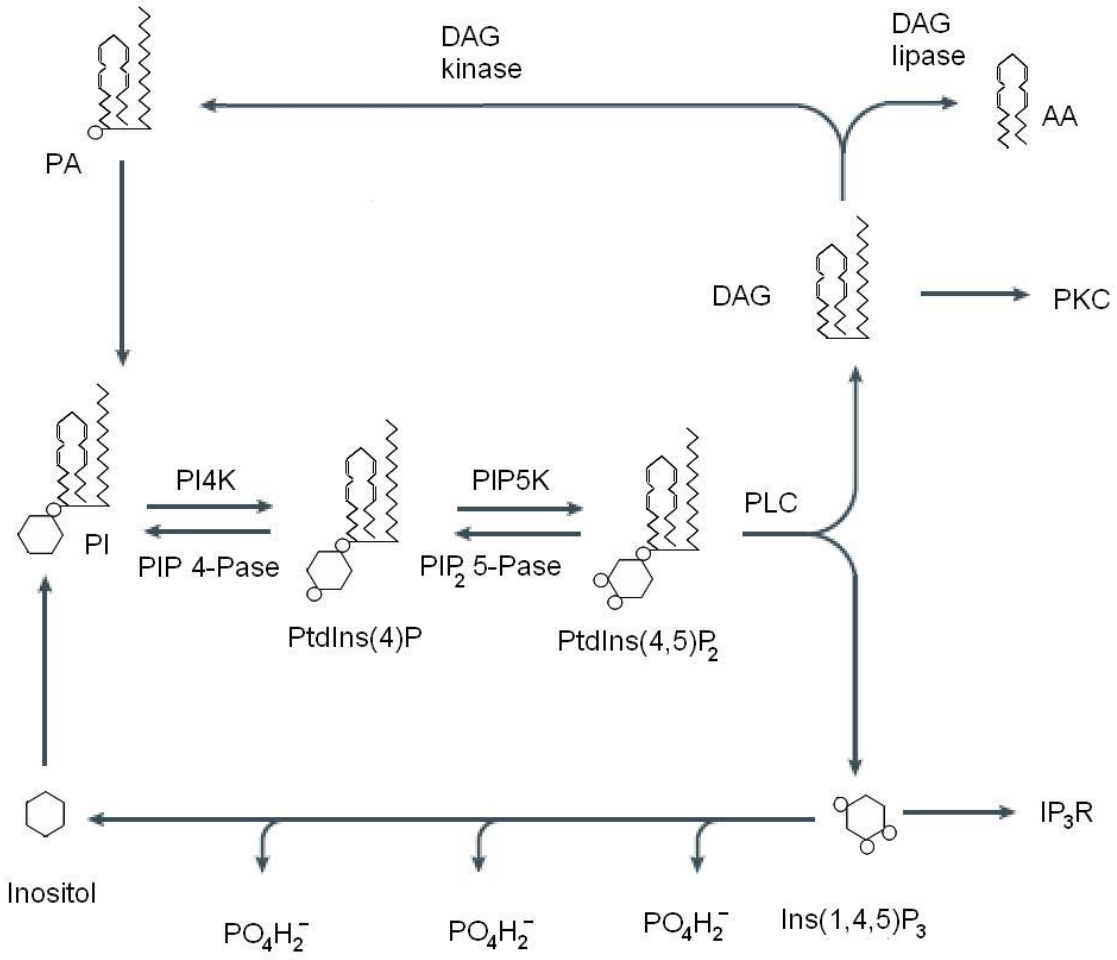
DAG
kinase
DAG
lipase
AA
PA
DAG
PKC
PI4K
PIP5K
PLC
PI
PIP 4-Pase
PIP2 5-Pase
PtdIns(4)P
PtdIns(4,5)P2
IP3R
Inositol
PO4H2-
PO4H2-
PO4H2-
Ins(1,4,5)P3

Figure 1-7. AA and Oxo-M Elicit Eame Distinct Pattern of Current Modulation. Here are shown current relations voltage (I-V plots) for averaged whole-cell recordings from SCG neurons as shown for either oxo-M or AA whole-cell current is enhanced at negative potentials but inhibited at positive potentials (a) averaged paired recordings in absence an presence of 5 μM AA. (b) averaged paired recordings in absence an presence of 10 μM oxo-M. (from Liu and Rittenhouse 2003)

a

Arachidonic Acid

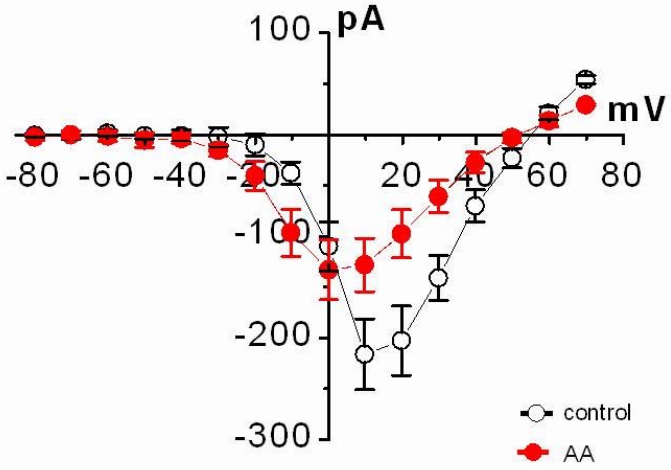

b

Oxo-M

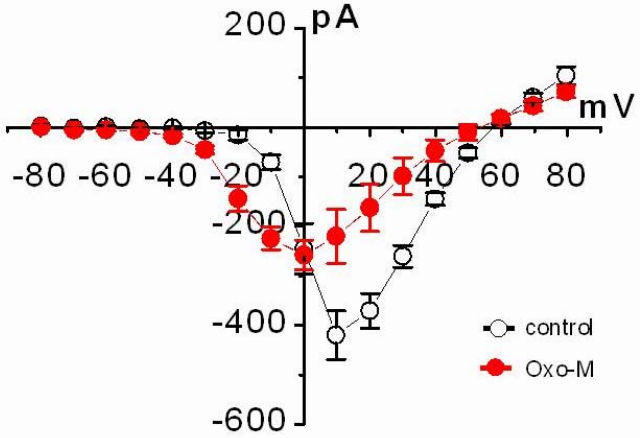

CHAPTER II

MATERIALS AND METHODS

A.Transfection of HEK M1 cells

Human embryonic kidney (HEK) cells with a stably transfected M_1R [HEK-M1, a generous gift of Emily Liman (University of Southern California, Pasadena, CA), originally transfected by Peralta et al., (see Peralta et al., 1988)] were transferred into 12-well plates for transfection. Recombinant cells at 50-80% confluence were transfected for 1 hour with $Ca_V2.2e$, $\alpha_2\delta$-1, and various $Ca_V\beta$s at a 1:1:1 molar ratio along with enhanced green fluorescent protein (eGFP) at ~10% of the total DNA, using Lipofectamine and PLUS reagent [Invitrogen (Carlsbad, CA)] per the manufacturer's instructions. 500-1000ng total DNA were transfected per well. 24-48 hours post-transfection cells were replated on poly-L-lysine coated coverslips and allowed to settle for at least 1-1.5 hours prior to recording. tsA 201 cells stably transfected with $Ca_V2.2e$, $\alpha_2\delta$-1, and $Ca_V\beta3$ were generously provided by Diane Lipscombe (Brown University, Providence, RI). Cells were transfected with 500-1000 ng per well of the M_1R (#J04192; generous gift of Neil Nathanson) along with along with eGFP at 10% of the total DNA and processed for whole cell current recording as above.

The β subunits used were $Ca_V\beta_{1b}$ (GenBank #X61394), $Ca_V\beta2a$(#M80545) and $Ca_V\beta4$ (#L02315) were provided by Edward Perez-Reyes (University of Virginia, Charlottesville, VA); $Ca_V2.2e$ (# AF055477), $\alpha_2\delta$-1 (#AF286488), and $Ca_V\beta_3$ (#M88751) provided by Diane Lipscombe (Brown University, Providence, RI); the $Ca_V\beta2a$(C3,4S) mutant generously provided by Anne Cahill (University of Chicago, Chicago, IL), $Ca_V\beta2a\beta3$ chimera and $Ca_V\beta2a\beta1b$ chimera generously provided by Robert Ten Eick (Northwestern University, Chicago, IL) were generated by Marlene Hosey's lab (see Chien et al 1998). Recordings from untransfected cells yielded whole cell currents of 9.0

+/- 1.3 pA in 20 mM Ba (data provided by Mandy Roberts-Crowley). To avoid spurious results from endogenous currents, any transfected cells cells having less than 150 pA were discarded.

B. Preparation and culture of SCG neurons

Following decapitation, the superior cervical ganglia (SCG) were removed from 1- to 4-day-old Sprague-Dawley rats (Charles River Laboratories, Wilmington, MA), and neurons were dissociated by trituration through a 22-gauge, 1.5-in. needle. Following dissociation, cells were plated on poly-L-lysine-coated glass coverslips in 35-mm culture dishes and incubated at least 2 hours before recording. Cells were maintained in 5% CO_2 at 37°C, in Dulbecco's Modified Eagle's Medium (DMEM) supplemented with 7.5% fetal bovine serum, 7.5% calf serum, 100 IU/ml penicillin, 0.1 mg/ml streptomycin, 4 mM L-glutamine and 0.2 μg/ml nerve growth factor (Bioproducts for Science, Indianapolis IL). Cells were used within 14 h of preparation.

C. Electrophysiology

All currents were recorded at room temperature (20-24°C) using the whole-cell configuration of a Dagan 3900a patch-clamp amplifier (Dagan Instruments Inc., Minneapolis, MN). Currents were filtered at 5 kHz using the amplifier's four-pole low-pass Bessel filter, then digitized at 20 kHz with a CED micro1401 interface (Cambridge Electronic Design, Cambridge, U.K.). Data were collected using the CED Patch software suite, version 6.3 (Cambridge Electronic Design) and stored on a personal computer.

Ba^{2+} currents were obtained using standard whole-cell techniques. Cells were placed in a glass-bottomed dish holding approximately 0.75 ml of bath solution. Patch electrodes were filled with the internal solution containing (in mM): 135 Cs-Asp, 10 HEPES, 0.1 1,2-bis(O-aminophenoxy)ethane-N,N,N',N'-tetraacetic acid (BAPTA), 5 $MgCl_2$, 4 ATP, 0.4 GTP, adjusted to pH 7.5 with CsOH and brought into contact with cells selected for roundness. Cells were patched in Tyrode's solution containing (in mM) 145 NaCl, 5.4 KCl, 10 HEPES, pH adjusted to 7.5 with NaOH. After rupturing the cell membrane, the bath solution was exchanged by a gravity fed perfusion system flowing at approximately 8 ml/min. The external solution contained (in mM): 125 NMG-Aspartate, 10 HEPES, 0.005 Tetrodatoxin (TTX) 20 Barium Acetate, pH adjusted to 7.5 with CsOH. For measurements in which concentration was lowered from 20 to 5 mM the external solution as diluted with a solution containing (in mM) 135 NMG –Aspartate, and 10 HEPES. TTX was not used when measuring currents from recombinant cells. For all Ba^{2+} recordings cells were held at -90 mV and given a 100 msec depolarization to the test potential indicated in the results section of each chapter. For prepulse experiments a 100 ms depolarization to +80 mV was applied, cells returned to -90 mV holding potential briefly (5 msec) and then given a 100 msec depolarization to +10 mV (protocol based on Emslie et al, 1990; see **Fig 1-5 a**) Prior to analysis, capacitive and leak currents were subtracted using a scaled-up current elicited with a test pulse to -100 mV. Pipette resistance ranged from 2.5 to 5 MΩ.

M-currents were also measured using standard whole-cell techniques. The internal solution contained (in mM): 175 KCl, 5 $MgCl_2$, 5 HEPES, 0.1 BAPTA 4 ATP, 0.4 GTP, adjusted to pH 7.5 with KOH. The external solution contained (in mM): 160 NaCl, 2.5

KCl, 2 $CaCl_2 \cdot 6H_2O$, 1 $MgCl_2$, 11 HEPES, 8 glucose, 0.005 TTX. pH adjusted to 7.5 with NaOH. Cells were patched and membranes were ruptured in external solution. For measurement of M-current cells were held at -20 mV and hyperpolarized to -60 mV for 500 msec, then repolarized to -20 mV. For time courses current was measured 400 msec after repolarization. M-current traces were not leak subtracted. Pipette resistance ranged from 2.5 to 5 MΩ

D. Pharmacology

Oxotremorine methiodide, [oxo-M; Tocris Biosciences Inc (Bristol, UK)], norepiepherne –(+)-bitartrate [NE; Calbiochem La Jolla, CA), bovine serum albumin fraction V, heat shock, fatty acid ultra-free [BSA; Roche Dagnostics (Indianapolis IN)] methoctramine (METH), bisindolylmaleimide HCl (BLM; Calbiochem), or protein kinase Cε translocator inhibitor peptide (PKCε-TIP) were prepared as stock solutions in double-distilled water and then diluted 1,000 times with bath solution. Arachidonic acid (AA; Nu Chek Prep, Elysian, MN) FPL 64176 (2,5-dimethyl-4-[2-(phenylmethyl)benzoyl]-1H-pyrrole-3-carboxylic acid methylester) [FPL; Research Biomedicals (Natick, MA)], nimodipine [NMN; Miles (New Haven, CT)], RHC 80267 [1,6-di(O-(carbamoyl)cyclohexanone oxime)hexane] (RHC, Biomol (Plymouth Meeting, PA)] or oleyloxyethyl-phosphorylcholine (OPC; Calbiochem), were prepared as stock solutions made up in 100% ethanol and diluted 1,000 times with bath solution. Aliquots of AA were seal in vials under nitrogen and stored at -80°C. Phorbol 12-myristate 13-acetate (PMA, Calbiochem) was prepared as a stock solution in dimethyl sulfoxide (DMSO) and diluted 1,000 times with bath solution. Pertussis toxin [PTX; List Biological

Laboratories Inc (Campbell, CA)] was prepared as a stock solution in double-distilled water and then diluted 1,000 times in incubation medium five hours before patching cells. All chemicals obtained from Sigma-Aldrich Inc. (St. Louis, MO) except where noted.

E. Data Analysis

The Patch 6.4 and Signal 2.15 software packages (Cambridge Electronic Design, Cambridge, U.K.) were used to measure peak inward current of whole-cell traces. The trough seeking function of Patch 6.4 was used to determine peak current where indicated. Data were further analyzed using EXCEL (Microsoft, Seattle, WA), and ORIGIN (Microcal Software, Northampton, MA). Percent inhibition was calculated as

$$= ((I-I')/I)*100$$

where I is the control current determined by an average of five whole-cell current measurements prior to application of a particular agent and I' is the average of five current measurements at the time specified for the determination. Percent facilitation was calculated as

$$= ((I_f-I_u)/I_u)*100$$

where I_f is the facilitated current recorded after a +80 mV depolarization (see description above) and I_u is the unfacilitated current. Time to peak was determined using the trough seeking function of Patch 6.4 across each sweep of a recording. Conductance was calculated from a modified Ohm's Law equation:

$$G = I/(V_m - V_{rev})$$

where I is the peak current at each test potential, Vm is the test potential, and V_{rev} is the apparent reversal potential. Relative conductance (G/G_{max})-voltage (V_m) curves were

plotted for whole-cell recordings before and after AA application. Data were curve fit using the Boltzmann Equation function in the Origin 7.0 software package yielding a curve fitting the equation:

$$G/G_{max} = G_{max} + (G_{min}-G_{max})/(1 + \exp((V_m-V_m½)/k))$$

where G_{max} is the maximal conductance, G_{min} is the minimal conductance, V_m is the test potential, $V_m½$ is the voltage at half maximal conductance and k is the slope factor.

F. Statistical analyses

All data are summaries presented as mean ± s.e.m. (standard error of the mean) for the designated number of experiments. For multiple comparisons statistical significance was determined (Origin 7.0) by a one-way analysis of variance (ANOVA) followed by a Tukey multiple-comparison post-hoc test. For comparisons of two groups, data were analyzed by unpaired two-sided Student's t-test for two means; respective p values are reported for each comparison. Statistical significance was set at $p \leq 0.05$.

G. *In situ* Hybridization

Fresh frozen SCG sections were fixed by perfusion with 4% paraformaldehyde in 0.1 M phosphate buffer, pH 7.4, postfixed for 2 hours in the same fixative and cryoprotected overnight in 20% sucrose in 0.1 M phosphate buffer, pH 7.4 before blocking and cutting using a cryostat in 8 micron sections for *in situ* hybridization using radioactively end labeled oligonucleotides as described in Bridges, et al. (2003). Antisense oligonucleotide sequences were synthesized (Sigma Genosys) to be complimentary to nucleotides 599-632 and 760-793 of the rat DAGL alpha sequence

(GenBank accession number XM_219575). Oligonucleotides were end-labelled using terminal transferase (Promega) and 33P-dATP (Perkin Elmer). Antisense probes were used together in hybridisation in order to increase signal intensity. A competition control for the specificity of the signal consisted of addition of a 250 fold excess of unlabelled oligonucleotides to the reaction mixture during hybridization. Following appropriate high stringency washes and air drying, slides were dipped in autoradiographic emulsion (Amersham). After 5 weeks they were developed, sections counterstained with toluidine blue and coverslipped with DPX mountant. Silver grains were visualised with polarized epifluorescence microscopy and toluidine blue with brightfield microscopy.

H. Immunohistochemistry

Rabbit antibodies raised and affinity purified against the GASPTKQDDLVISAR epitope in diacylglycerol lipase α (DAGLα) as previously described (Bisogno et al 2003) were a generous gift of Prof. Pat Doherty of Kings College. SCG from adult rats were prepared by perfusion fixation with 4% paraformaldehyde in 0.1 M phosphate buffer, pH 7.4, postfixed for 2 hours in the same fixative and cryoprotected overnight in 20% sucrose in 0.1 M phosphate buffer, pH 7.4 before blocking and freezing. Eight micron sections were cut using a cryostat. Immunohistochemistry was performed using indirect tyramide signal amplification (Perkin Elmer) visualized with Avidin FITC as previously described (Michael et al 1999).

CHAPTER III

The Ca^{2+} Channel β-Subunit Determines Whether Stimulation of M_1 Muscarinic Receptor Enhances or Inhibits N-Current

Abstract

In dissociated neurons, stimulation of M_1 muscarinic receptors (M_1Rs) produces a distinct pattern of modulation on N-type calcium (N-) channels, enhancing currents at negative test potentials and inhibiting currents elicited with positive test potentials. Exogenously applied arachidonic acid (AA) reproduces the same profile of modulation; suggesting AA functions as a downstream effector of M_1Rs. In addition, techniques which limit AA concentration minimize N-current modulation by M_1R stimulation. Still, a role for AA in a pathway of modulation remains controversial. Here we used an expression system to examine the physiological mechanisms regulating modulation. In the course of the investigation we found the N-channel's β-subunit ($Ca_V\beta$) acts as a molecular switch regulating whether modulation results in enhancement or inhibition. In HEK-293 cells, M_1R stimulation inhibited activity of N-channels containing $Ca_V\beta$1b, $Ca_V\beta$3, or $Ca_V\beta$4, but enhanced activity of N-channels containing $Ca_V\beta$2a. Exogenously applied AA produced the same pattern of modulation. Our data fit a model in which $Ca_V\beta$2a blocks inhibition, thus unmasking enhancement. Studies with mutated and chimeric $Ca_V\beta$ subunits revealed palmitoylation of $Ca_V\beta$2a as essential for loss of inhibition. These results predict that within neurons, modulation of N-channel activity by M_1Rs will fluctuate between enhancement and inhibition based on the presence of palmitoylated $Ca_V\beta$2a.

Introduction

All neural function results from a series of electrical and chemical signals. The two realms of signaling are often bridged within neurons by voltage-gated calcium channels, such as the N-type calcium (N-) channel (Hille 2001). Changes in voltage across cell membranes open N-channels allowing an influx of calcium (N-current). At postsynaptic sites, N-current triggers biochemical changes including: modulation of certain ion channels (Wisgirda and Dryer, 1992), enzyme activation (Rittenhouse & Zigmond 1999) and gene transcription (Brosenitsch & Katz 2001; West et al., 2002). Neurotransmitters bind to G-protein coupled receptors (GPCRs) stimulating signal transduction cascades that modulate the N-channel's response to changing membrane potential (Elmslie 2003; Hille 1994). Some of these pathways are well described, so that now; both the molecules in the signaling cascades and the sites of modulation on N-channels are known (Suh and Hille 2005). Still, other modulating pathways remain unresolved.

The M_1 muscarinic receptor (M_1R) is one of several Gq-coupled receptors (GqPCRs) that modulates N-channels by an incompletely described pathway referred to as the slow pathway (Mathie et al. 1992; Suh and Hille 2005). Recent reports propose a reduction in levels of phosphatidylinositol-4,5-bisphosphate [PtdIns(4,5)P_2] during GqPCR stimulation suffices to elicit inhibition (Wu et al., 2002; Gamper et al., 2004; Delmas et al., 2005). In this model channels need to have PtdIns(4,5)P_2 bound to function. During M_1R stimulation PtdIns(4,5)P_2 is depleted from the membrane creating a concentration gradient which results in PtdIns(4,5)P_2 dissociating and diffusing away

from the channel. A similar model of PtdIns(4,5)P_2 depletion and dissociation has been established as the mechanism that modulates M-current, a voltage-gated potassium current sensitive to M_1R stimulation.

However, previously our lab determined modulation of N-current by M_1Rs requires events downstream of PtdIns(4,5)P_2 hydrolysis (Liu et al 2004). In superior cervical ganglion (SCG) neurons, the muscarinic agonist oxotremorine-M (oxo-M) and arachidonic acid (AA) elicit the same distinct pattern of modulation (Liu et al. 2001; Liu et al. 2003); inhibiting N-current at positive test potentials and enhancing N-current at negative test potentials. M_1R stimulation releases AA (Tence et al 1994; Strosznajder & Samochocki 1992) suggesting a role in the slow pathway. Consistent with hypothesis, modulation of N-current is minimized when AA levels are reduced by molecular techniques (Liu & Rittenhouse 2003; Liu et al. 2004) or pharmacological block (Liu & Rittenhouse 2003; Liu et al. 2004; cf Gamper et al 2004). At present no binding site for PtdIns(4,5)P_2 or AA on voltage-gated calcium channels has been determined, but we have shown the enhancement and inhibition of N-current by AA are discrete molecular events with different sites of action (Barrett et al 2001; Liu et al 2001).

Whether both AA-sensitive sites reside in the same channels or whether two distinct channel populations are required to observe enhancement and inhibition remains untested. The expression of channels in a recombinant system allows the examination of a homogeneous population of channels. Therefore, we attempted to recapitulate enhancement and inhibition of N-current in HEK-293 cells expressing M_1Rs and N-channels. N-channels are multimeric complexes defined by a large pore-forming subunit ($Ca_V2.2$), which is modified by ancillary subunits $\alpha_2\delta$ and $Ca_V\beta$ (Catterall 2000). We

intended to use the power of mutagenesis to study enhancement and inhibition independently. In doing so, we made the serendipitous discovery that enhancement and inhibition separate without mutagenesis, but simply by varying the composition of wild type $Ca_V\beta$. In particular, the N-currents obtained from channels comprising the $Ca_V\beta 2a$ subunit were uniquely enhanced by either M_1R stimulation or application of AA.

Results

M_1R elicited inhibition of N-current is blocked by OPC

In SCG neurons M_1R stimulation inhibits N-current via the release of (an) unknown diffusible second messenger(s). Previously we found this inhibition is minimized by the PLA_2 antagonist oleyloxyethyl phosphocholine (OPC; Liu & Rittenhouse 2003; Liu et al 2004). We first tested whether in recombinant cells, N-currents were inhibited by M_1R stimulation and if the inhibition was sensitive to OPC. An HEK-293 cell line stably transfected with M_1Rs (HEK-M1; Peralta et al 1988) was transiently transfected with these N-channel subunits: $Ca_V2.2e$ the N-channel variant found in SCG neurons (Lin et al 1997); $Ca_V\beta3$, which most commonly associates with $Ca_V2.2$ (Witcher et al. 1993; Dolphin 2003); and $\alpha_2\delta$-1 which is expressed in SCG (Comm D Lipscombe). In whole cell recordings, a sixty-second exposure to the muscarinic agonist oxotremorine-M (oxo-M; 10 μM) inhibited N-current by 61± 9 % (n = 16; **Figs. 3-1 a,b,g**). In a parallel experiment tsA cells stably transfected with $Ca_V2.2e$, $\alpha_2\delta$-1 and $Ca_V\beta3$ and transiently transfected with the M_1R, oxo-M inhibited current by 70 ± 17 % (n = 5; **Figs. 3-1 c,d,g**), ruling out a system-specific effect. In contrast, OPC reduced current inhibition by oxo-M to 2 ± 6 % (n = 7; **Figs. 3-1 e,f,g**), indicating that in the recombinant system, as with SCG neurons, (Liu & Rittenhouse 2003a; Liu et al 2004), PLA_2 participates in N-current inhibition by M_1Rs (**Fig. 3-1 h**).

$Ca_V\beta$ subunit controls responses of modulation by M_1Rs

We next sought to examine the dependence of N-current enhancement on M_1R stimulation and AA release. Since modulation of N-current in dissociated SCG neurons is voltage-sensitive (Liu et al., 2003a), we compared current-voltage (I-V) plots measured before and after 90 seconds of oxo-M exposure. Based on previous work with dissociated neurons we expected to observe currents enhanced at negative test potentials. However, oxo-M inhibited current at virtually all voltages (**Fig**. **3-2 i**).

In addition to incomplete recapitulation of M_1R modulation, the recombinant N-current exhibited robust, fast inactivation (**Figs. 3-1 b,d** and **3-2 h**) as previously observed with N-current (Olcese et al 1994). In contrast, native N-currents in SCG neurons exhibit kinetics with little inactivation (Plummer et al., 1989) which may be indicative of $Ca_V\beta2a$ expression (Cahill et al 2000). Since $Ca_V\beta2a$ transcripts are present in SCG neurons (Lin et al 1997), we hypothesized $Ca_V\beta2a$-containing channels could form the major portion of N-current in SCG neurons. If so, $Ca_V\beta2a$-containing channels might exhibit both inhibition and enhancement. Application of oxo-M to cells expressing $Ca_V\beta2a$ rapidly inhibited peak inward current within one minute. However, unlike $Ca_V\beta3$, after three minutes the initial inhibition gave way to a steady state enhancement of +21.5 ± 3.8% in 5 of 5 recordings, (**Figs. 3-2 d,e** and **Fig. 3-4 a**). To determine whether enhancement is voltage-sensitive, we compared I-V plots measured before and after application of oxo-M. With $Ca_V\beta2a$ expression, oxo-M no longer inhibited current at any potential, but enhanced current approximately 2-fold at negative test potentials (**Fig. 3-2 f**).

Although we hypothesized expression of $Ca_V\beta2a$ would elicit enhancement at negative potentials, the complete loss of inhibition at all potentials was unanticipated. Likewise, we did not anticipate $Ca_V\beta3$ to yield inhibition exclusively. We next asked if $Ca_V\beta$ subunits other than $Ca_V\beta2a$ exhibit both inhibition and enhancement. Four genes encode the $Ca_V\beta$ isoforms (Birnbaumer et al.1998). Therefore, the above experiments were repeated with two other neuronal $Ca_V\beta$s; $Ca_V\beta1b$ and $Ca_V\beta4$. In each case the application of oxo-M rapidly inhibited peak inward current. We found with the exception of $Ca_V\beta2a$ expressing cells, the initial inhibition receded only slightly within 90 seconds, reaching a stable inhibition which persisted until washout of oxo-M. When $Ca_V\beta1b$ was expressed, currents were stably reduced in 5 of 7 recordings of -41.8 ± 14.4% (**Fig. 3-2 a,b** and **Fig. 3-4a**). When $Ca_V\beta4$ was expressed, currents were stably reduced in 6 of 6 recordings of -56.2 ± 10.8 % (**Fig 3-2 j,k** and **Fig 3-4a**). These data are similar to those obtained from cells expressing $Ca_V\beta3$ in which a three minute exposure to oxo-M elicited inhibition in 8 of 9 recordings with an average change of -54 ± 10% (**Figs. 3-2 g,h** and **Fig. 3-4a**). Also, as with $Ca_V\beta3$, when either $Ca_V\beta1b$ or $Ca_V\beta4$ was expressed, oxo-M inhibited current at all voltages (**Fig. 3-2 c,l**). No significant difference in current modulation occurred among $Ca_V\beta1b$, $Ca_V\beta3$, or $Ca_V\beta4$ ($p > 0.05$, ANOVA). Percent change in current amplitude was highly significant between $Ca_V\beta2a$ and $Ca_V\beta1b$, $Ca_V\beta3$, or $Ca_V\beta4$, ($p \leq 0.005$ ANOVA; **Fig. 3-4a**). These data indicate that channels containing $Ca_V\beta2a$ exhibit unique N-current modulation by M_1Rs.

AA elicits a similar profile of N-current modulation as elicited by the M_1R

In previous studies we found exogenous AA mimics N-current modulation by M_1Rs (Liu et al., 2003). We hypothesized AA also would inhibit or enhance recombinant N-current according to the same restrictions as M_1R stimulation. Therefore, we examined modulation by AA on whole-cell currents from HEK-M1 cells transfected with N-channel subunits comprising one of the four different $Ca_V\beta$ subunits specified earlier. AA (10 μM) initially enhanced currents (**Fig. 3-3 a,d,g,j**). However, enhancement was transient and after a three minute exposure to AA subsequent inhibition dominated the currents of channels containing $Ca_V\beta1b$ (by -58.5 ± 14.4% in 3 of 3 recordings; **Fig. 3-3 a,b** and **3-4 b**), $Ca_V\beta3$ (by -44.2 ± 9.1% in 5 of 5 recordings; **Fig. 3-3 g,h** and **3-4 b**), or $Ca_V\beta4$ (by -26.0 ± 6.7% in 5 of 5 recordings; **Fig. 3-3 j,k** and **3-4 b**). Conversely, when $Ca_V\beta2a$ was expressed, the initial enhancement remained stable at +54 ± 12% in 5 of 5 recordings (**Fig. 3-3 d,e** and **3-4 b**). Percent change in current was highly significant between $Ca_V\beta2a$ and $Ca_V\beta1b$, $Ca_V\beta3$, or $Ca_V\beta4$, ($p \leq 0.005$ ANOVA). No statistical difference occurred among $Ca_V\beta1b$, $Ca_V\beta3$, or $Ca_V\beta4$ ($p > 0.05$, ANOVA) (**Fig. 3-4 b**).

Enhancement of N-current by AA, like oxo-M, is voltage-sensitive in dissociated SCG neurons (Barrett et al 2001; Liu et al., 2001; Liu et al., 2003) therefore we tested the effect of AA on I-V relationships before and after AA application. When $Ca_V\beta2a$ was expressed, AA enhanced current at negative potentials, and did not inhibit current at any potential (**Fig. 3-3 f**). In contrast, AA strongly inhibited current at positive voltages when $Ca_V\beta1b$, $Ca_V\beta3$, or $Ca_V\beta4$ (**Fig. 3-3 c,i,l**) was expressed. There was a slight enhancement of current at negative potentials (**Fig 3-3 i,l**), but it was not statistically significant. Overall, the pattern of modulation elicited by AA, separation of enhancement and

inhibition based on $Ca_V\beta$ expression, matches the pattern of modulation observed with M_1R stimulation (See **Fig 3-4**; Compare Figs. **3-2** and **3-3**).

AA reproduced the modulation elicited by M_1Rs, corroborating the previous assertion that AA is a component of the slow pathway (Liu & Rittenhouse, 2003; Liu et al., 2004). Still, if enhancement and inhibition are attributable to the presence of AA, they should reverse following washout of AA. We found previously in SCG neurons (Liu et al., 2001) that AA's hydrophobic properties made wash out difficult unless the bath solution contained fatty-acid free bovine serum albumin (BSA). As with SCG neurons, washing cells with copious amounts of bath solution slowly reversed inhibition of N-current from $Ca_V\beta3$-containing channels, but did not reverse enhancement of N-current from $Ca_V\beta2a$-containing channels (**Fig. 3-3 d,g**). Enhancement of N-current in cells expressing $Ca_V\beta2a$ by AA readily reversed when washed with 1 mg/ml BSA (**Fig. 3-5 a-d**) as did inhibition of N-current from $Ca_V\beta1b$ and $Ca_V\beta4$-containing channels. (**Figs. 3-3 a,j**). If enhancement is directly attributable to AA it should recur with a second application of AA following wash with BSA. Accordingly we found enhancement reversed rapidly when cells were washed with BSA, and upon reapplication of AA, enhancement recurred within the same cell (**Fig. 3-5 a,c,d**). These data indicate both enhancement and inhibition are reversible effects which can be elicited by AA.

A model for dual modulation effects of N-current

Previous work established enhancement and inhibition as distinct molecular events with distinct sites of action (Liu et al., 2001; Barrett et al., 2001). The separation of enhancement and inhibition by $Ca_V\beta s$ presented a molecular tool to probe the two

sites. We postulated every $Ca_V2.2e$ has a site of enhancement based on the observation that all recombinant currents exhibit an initial enhancement with AA (**Fig. 3-3 a,d,g,j**). Since enhancement of N-current in SCG neurons presents as a leftward shift in voltage sensitivity (Barrett et al., 2001), we constructed normalized conductance-voltage plots to determine whether a leftward shift in voltage sensitivity occurs with N-channels containing $Ca_V\beta$s other than $Ca_V\beta2a$. As shown, both $Ca_V\beta2a$- and $Ca_V\beta3$-containing cells exhibited a negative shift in conductance in response to AA (**Fig. 3-6 a,b**). This treatment of the data indicates AA increases channel voltage sensitivity independently of $Ca_V\beta$ subunit expression. These data indicate the unique effects of $Ca_V\beta2a$ stem from an attenuation of inhibition, rather than a change of enhancement (**Fig 3-6 c**).

Expression of multiple $Ca_V\beta$ isoforms produces heterogeneous currents

The above observations yield a possible explanation for why we previously observed both enhancement and inhibition of whole-cell N-current in SCG neurons (Barrett et al., 2001; Liu & Rittenhouse, 2003; Liu et al., 2004). Diversity in N-channel function has been attributed to a heterogeneous expression of $Ca_V\beta$ in neurons (Scott et al 1996). In recombinant systems the expression of multiple $Ca_V\beta$ subunits results in a mixed population of channels (Jones et al 1998). Therefore individual SCG neurons may exhibit enhancement and inhibition because $Ca_V2.2e$ co-assembles with different $Ca_V\beta$s. To recapitulate the pattern of modulation from SCG, HEK-M1 cells were transfected with both $Ca_V\beta2a$ and $Ca_V\beta$. We found when $Ca_V\beta2a$ was in ten fold excess of $Ca_V\beta3$, the I-V plots recapitulated wild-type I-V plots with enhancement occurring at negative voltages and inhibition at positive voltages (**Fig. 3-7 a-c**). However unlike wild-type

current, the currents rapidly inactivated (**Fig. 3-7 a,b**). SCG neurons express $Ca_V\beta2a$, $Ca_V\beta3$ and $Ca_V\beta4$ mRNA with trace amounts of $Ca_V\beta1b$ (Lin et al., 1996). Therefore, we transfected cells with equal amounts $Ca_V\beta3$ and $Ca_V\beta4$ and a ten-fold excess of $Ca_V\beta2a$, and found these cells closely recapitulated both the I-V relationship and the current kinetics of SCG neurons under control conditions and following M_1R stimulation by oxo-M (**Fig. 3-7 d-f**). These data corroborate previous work indicating within neurons a heterogeneous population of N-channels exhibit unique functional properties based on the expression of $Ca_V\beta$ subtype. Moreover, within a neuron, at specific locations, calcium influx may be enhanced or inhibited during modulation depending on $Ca_V\beta$ expression.

Loss of Palmitoylation Restores Partial Inhibition of Channels by Oxo-M or AA

We next asked what structural feature of $Ca_V\beta2a$ accounts for the attenuation of inhibition. A unique conspicuous feature of $Ca_V\beta2a$ is its palmitoylation near the N-terminus (Chien et al. 1996). Since $Ca_V\beta2a$ interferes with a fatty acid mediated inhibition, it raised the possibility of direct antagonism by palmitic acid at a site of modulation by AA. We therefore tested the importance of palmitoylation by coexpressing in HEK-M1 cells $Ca_V2.2e$, $\alpha2\delta$-1 and a $Ca_V\beta2a$ mutated at the two sites of palmitoylation [$Ca_V\beta2a$(C3,4S); Chien et al 1996]. In these cells oxo-M caused an initial transient inhibition, which subsided leaving the current close to control levels a change in current magnitude of -1.53 ± 7.3% (p = 0.07 vs. wild type $Ca_V\beta2a$). (**Fig. 3-8 a,c** and **Fig. 3-10**). Oxo-M enhanced current in 6 of 12 recordings and inhibited current in the remaining recordings. In these same cells AA (10 μM) initially enhanced current amplitude; however unlike with wild type $Ca_V\beta2a$, subsequent inhibition followed (**Fig.**

3-8 b,d and **Fig. 3-10**). Now rather than enhance current, AA reversibly inhibited current by -16.5 ± 6.9% in 7 of 9 recordings, a significant change from $Ca_V\beta 2a$ ($p = 0.0002$). Still, the magnitude of inhibition was less than observed with wild types $Ca_V\beta$ subunits other than $Ca_V\beta 2a$. These data suggest palmitoylation of $Ca_V\beta 2a$ is necessary to switch modulation from inhibition to enhancement. However, the loss of palmitoylation by itself does not confer complete restoration of full inhibition obtained with non-palmitoylated wild type $Ca_V\beta$ subunits.

To further test whether palmitoylation is both necessary and sufficient to block current inhibition by oxo-M or AA, we tested a chimeric $Ca_V\beta$ in which the initial sixteen amino acids from the N-terminus of $Ca_V\beta 2a$ replaced fifteen amino acids in the corresponding region of $Ca_V\beta 3$ ($Ca_V\beta 2a\beta 3$). This N-terminus substitution adjoins palmitoylation to normally non-palmitoylated $Ca_V\beta$ isoforms (Chien et al 1998). In HEK-M1 cells expressing $Ca_V2.2e$, $\alpha 2\delta$-1 and $Ca_V\beta 2a\beta 3$, oxo-M inhibited peak current in 5 of 6 recordings, -14.5 ± 5.9 % and recovered upon wash out of agonist (**Fig. 3-9 a,b** and **Fig 3-10**) When AA was applied, current was inhibited by -51.9 ± 8.5 % in 7 of 7 recordings, which reversed when cells were washed with 1 mg/ml BSA (**Fig. 3-9 d,e** and **Fig. 3-10**). I-V plots taken before and 90 seconds after application of oxo-M or AA showed inhibition at positive test potentials (**Fig. 3-9 c,f**). These data indicate the addition of palmitoyl side chains did not reproduce the stable enhancement by oxo-M or AA normally observed with wild type $Ca_V\beta 2a$.

The data suggest other structural domains of $Ca_V\beta 2a$ subunit may contribute to the block of inhibition in addition to palmitoylation. $Ca_V\beta$ subunits have two highly conserved regions separating three highly variable regions (for review see Dolphin 2003).

Replacing the N-terminus in the $Ca_V\beta2a\beta3$ chimera substituted the first variable region of $Ca_V\beta3$ leaving the two others intact; a variable region at the center of the peptide and the variable carboxy terminus. To ascertain the effect of other $Ca_V\beta$ variable regions on modulation, we tested a second chimera in which the N-terminus sixteen amino acid residues of $Ca_V\beta2a$ replaced fifty-seven amino acids of the N-terminus of $Ca_V\beta1b$. Since $Ca_V\beta1b$ shares highest sequence homology to $Ca_V\beta2a$ (Birnbaumer et al. 1998), we hypothesized that expression of a $Ca_V\beta2a\beta1b$ chimera would allow less inhibition of N-current than the $Ca_V\beta2a\beta3$ chimera if the protein contributed to the block of inhibition. As expected, oxo-M or AA inhibited currents less with $Ca_V\beta2a\beta1b$ than $Ca_V\beta2a\beta3$. AA still inhibited currents in 7 of 9 recordings, -6.9 ± 8.0 % (**Fig. 3-9 j,k** and **Fig. 3-10**); however inhibition was significantly less than with the $Ca_V\beta2a\beta3$ chimera ($p \leq 0.02$). Oxo-M now no longer inhibited, but enhanced current by +18.8 ± 10.2 % in 4 of 4 recordings (**Fig. 3-9 g,h** and **Fig. 3-10**). This reversal of modulation by oxo-M was significantly different from that observed with the $Ca_V\beta2a\beta3$ chimera ($p \leq 0.04$). Comparisons of I-Vs, measured prior to and 90 seconds after oxo-M or AA both showed enhancement of current at negative test potentials (**Fig. 3-9 i,l**) for cells expressing the $Ca_V\beta2a\beta1b$ chimera. Thus $Ca_V\beta$ subunits with identical palmitoylated N-termini (wild type $Ca_V\beta2a$ and the two aforementioned chimerae) have significantly different effects on the channel's response to modulation by oxo-M or AA. These data indicate that structural features of $Ca_V\beta2a$ in addition to the palmitoylated N-terminus contribute to blocking inhibition and consequently revealing enhancement.

Discussion

Here we used a recombinant system to investigate the enhancement and inhibition of N-current that occurs during M_1R stimulation and AA application. In so doing we made the serendipitous discovery that the N-channel's β subunit directs opposite effects of N-current modulation. Specifically, M_1R stimulation or exogenous AA uniquely enhanced N-currents from whole-cell recordings of cells expressing $Ca_V\beta2a$. This finding allowed us to further examine the modulation of N-current and reach several conclusions. First, the striking recapitulation of M_1R induced modulation by AA, coupled with the loss of modulation when AA is blocked or sequestered is strong evidence that AA is an integral component of the slow pathway. Second, the unique effect of $Ca_V\beta2a$ provided a molecular tool to probe the mechanism by which currents may be enhanced or inhibited. Third, cells expressing multiple forms of $Ca_V\beta$ subunits displayed both inhibition and enhancement of currents during modulation, implying the characteristic pattern of modulation observed in SCG neurons results from a heterogeneous distribution of $Ca_V\beta$ isoforms. Fourth, using mutated and chimeric $Ca_V\beta$ constructs we demonstrated palmitoylation of $Ca_V\beta2a$ is a key feature in its capacity to toggle modulation from inhibition to potentiation.

AA is necessary for slow pathway inhibition

Previously, to demonstrate a role for AA in inhibition, we used pharmacological agents, the AA scavenger BSA, antibodies dialyzed internally, and neurons harvested from $PLA_2^{-/-}$ knockout mice (Liu et al 2004; Liu and Rittenhouse 2003; Liu et al., 2006). The block of inhibition by $Ca_V\beta2a$ provides a highly specific agent to dissect the slow

pathway, while non-palmitoylated wild type $Ca_V\beta$ subunits conveniently act as negative controls. Thus, expression of $Ca_V\beta2a$ can be used as one might use a specific peptide or antibody. The data we have presented here support our previous findings in SCG neurons in which we found AA is necessary for slow pathway inhibition elicited by M_1Rs.

It must be stressed none of the findings reported here minimize the role of PtdIns(4,5)P_2 in N-current modulation, but rather document a requirement for AA in modulation. It is well documented that PtdIns(4,5)P_2 breakdown is necessary for slow pathway inhibition (Suh and Hille 2005; Wu et al 2002; Gamper et al 2004; Delmas et al 2005; Liu et al 2004; Liu and Rittenhouse 2003); whether or not events downstream of PtdIns(4,5)P_2 breakdown are necessary remains controversial (Gamper et al 2004; Delmas et al 2005). Recent reports on calcium channel inhibition have led to the conclusion that depletion of PtdIns(4,5)P_2 is both necessary and sufficient to elicit inhibition of voltage gated channels $Ca_V2.2$ and $Ca_V2.3$ (Gamper et al 2004; Wu et al 2002, reviewed in Suh and Hille 2005). Our data indicate AA production is both necessary and sufficient to elicit inhibition of $Ca_V2.2$ (Liu et al 2004; Liu and Rittenhouse 2003, Liu et al 2006).

A resolution to the paradox would entail a role for both PtdIns(4,5)P_2 acting on the channel and AA either directly or indirectly. A model for PtdIns(4,5)P_2 and AA opposing each other in modulation of potassium channels has been published (Oliver et al., 2004), in which PtdIns(4,5)P_2 and AA act at different sites of the channel. A direct interference is possible since AA is an integral piece of the PtdIns(4,5)P_2 molecule and thus could compete for binding. Indirect actions of PtdIns(4,5)P_2 and AA must be considered as both are bioactive molecules with multiple downstream effects.

A Working Model for the Enhancement and Inhibition

Previously we characterized enhancement and inhibition result as distinct molecular events acting at different sites of the channel through experiments with exogenous AA on isolated N-current in SCG neurons (Barrett et al 2001). Restriction of AA movement across the cell membrane indicated enhancement requires AA on the extracellular side, while inhibition requires AA on the intracellular side (Barrett et al 2001). Since $Ca_V\beta$ subunits are cytoplasmic, we hypothesized that $Ca_V\beta2a$ attenuates inhibition without affecting enhancement. In dissociated neurons, AA induces an initial current enhancement followed by a slower progressing inhibition (Liu et al 2001; Barrett et al 2001). The simplest explanation for these data is that the initial enhancement becomes masked by the subsequent more dominant inhibition. Since previous work indicated enhancement stems from increased voltage sensitivity (Barrett et al 2001) we used normalized G-V curves to show an increase in voltage sensitivity occurs independently of $Ca_V\beta2a$ expression. In contrast, inhibition results from an increase in steady state inactivation (Liu & Rittenhouse 2000). This type of inhibition would essentially reduce the available number of channels providing calcium influx, dominating an enhancement produced by a shift in voltage sensitivity. Thus by blocking a dominant inhibition $Ca_V\beta2a$ unmasks a latent enhancement.

The masking of enhancement offers some explanation for the observation that the majority of studies on N-current modulation have focused on inhibition (Elmslie 2003). Still, the generation of enhancement and inhibition has been reported from experimental systems similar to the one we used here. For example, AA causes both a shift in

activation towards negative potentials and a simultaneous increase steady state inactivation in T-channels (Talavera et al 2004). Also, in SCG neurons, the amide of AA, anandamide, elicited enhancement at negative potentials and inhibition at positive potentials in I-V plots (Guo and Ikeda, 2003). A recent report showed muscarinic enhancement reported R-type channels in hippocampal neurons involved a leftward shift in voltage sensitivity (Tai et al., 2006). It should be noted the hippocampus is one brain region where $Ca_V\beta2a$ is highly expressed (Day et al 1998). Finally, in an earlier report using HEK-293 cells, transiently transfected with recombinant M_1Rs and N-channels containing $Ca_V\beta3$ showed carbachol inhibited calcium current without enhancing. However, the I-V curves presented showed a discernible leftward shift in voltage sensitivity (Melleti et al 2001).

A role for the $Ca_V\beta2a$ N-terminus

We determined the palmitoylation at the N-terminus of $Ca_V\beta2a$ is necessary to invert modulation. However, palmitoylation by itself cannot account for the complete reversal of modulation. Inhibition that was recouped by removal of palmitoylation was substantially less than inhibition observed with wild type non-palmitoylated $Ca_V\beta$ isoforms. Also, addition of the palmitoylated $Ca_V\beta2a$ N-terminus to the $Ca_V\beta2a\beta3$ chimera did not recover enhancement elicited by AA or oxo-M. These data indicate aspects of the $Ca_V\beta2a$ N-terminus other than palmitoylation influence modulation. Several possible models can explain how the $Ca_V\beta2a$ acts as a whole to affect modulation.

One possibility is that the palmitoyl side chains of the $Ca_V\beta2a$ subunit directly interfere with the actions of AA. In this model the $Ca_V\beta2a$ attaches to $Ca_V2.2e$, such that the palmitoyl side chains are positioned to produce steric hindrance to AA binding. In the $Ca_V\beta2a\beta3$ chimera the palmitoyl chains are positioned differently due to the altered structure of the subunit. This would explain why AA inhibition is not blocked by the $Ca_V\beta2a\beta3$ chimera. However, exclusion of palmitoyl chains on the $Ca_V\beta2a$(C3,4S) mutant does not allow inhibition as seen in wild-type non-palmitoylated $Ca_V\beta$ subunits, so other aspects of the N-terminus m contribute to the block of inhibition.

Another possibility is that the N-terminus blocks inhibition by tethering PtdIns(4,5)P_2 to $Ca_V2.2e$. The two palmitoylated cysteines of the N-terminus of $Ca_V\beta2a$ are in close proximity to a concentration of basic residues. The amino acid sequence of the N-terminus is: MQ***CC***GLVH**<u>RRR</u>**V**<u>R</u>**VSY (sites of palmitoylation in bold italics, cationic residues underlined and in bold). Such a concentration of cationic residues is known to bind PtdIns(4,5)P_2 (Oliver et al., 2004; Robbins et al., 2006). In fact a series of different palmitoylated peptide oligomers rich in cationic residues all reduce M-current and block further inhibition by M_1R agonists, presumably by sequestering PtdIns(4,5)P_2 (Robbins et al., 2006). The $Ca_V\beta2a$ N-terminus may act as a PtdIns(4,5)P_2 docking site, tethering a molecule to the channel so that it does not dissociate during depletion of PtdIns(4,5)P_2, nor is it supplanted by high concentrations of AA, thus making the channel immune to inhibition. In this model, removal of palmitoylation would permit greater diffusion of PtdIns(4,5)P_2 from the channel allowing for some inhibition, but the cationic residues would slow the dissociation of PtdIns(4,5)P_2 from the channel, making the inhibition substantially less than obtained with wild-type non-palmitoylated $Ca_V\beta$

isoforms. If the model described above is correct then the PtdIns(4,5)P_2 docking site formed by the $Ca_V\beta$2a N-terminus must be positioned properly in order to function as block of inhibition. Accordingly, the PtdIns(4,5)P_2 sequestering palmitoylated peptides that block M-current inhibition do block N-current modulation elicited by M_1R stimulation (Robbins et al 2006). Since the variable regions of $Ca_V\beta$3 share little homology with those of $Ca_V\beta$2a the PtdIns(4,5)P_2 molecule may be tethered, but not at the correct site of the channel. Accordingly, addition of palmitoylation to the $Ca_V\beta$2aβ1b chimera, a construct more homologous with $Ca_V\beta$2a, allowed significantly less inhibition by AA and recovered enhancement by oxo-M.

A role for Multiple $Ca_V\beta$ Isoforms in Neurons

Here we have shown multiple $Ca_V\beta$ isoforms expressed in a recombinant system can recapitulate the enhancement and inhibition of N-current modulation observed in neurons. Given the diversity of neuronal functions for calcium influx, there must be localized control of a channel's response to modulation. Our findings provide a previously unrecognized role for $Ca_V\beta$ subunits in modulation and represent a means by which either M_1R stimulation or AA release can have diverse effects in a single cell.

Figure 3-1. M_1R Induced Inhibition of Recombinant N-current is Blocked by PLA_2 Antagonist. HEK-M1 cells were transiently transfected with N-channel subunits $Ca_V2.2e$, α_2-δ-1 and $Ca_V\beta3$. Modulation of N-current by M_1R stimulation is demonstrated by (**a**) time courses of peak inward current using 5 mM Ba as charge carrier; before, during and after a 3 min bath application of oxo-M (10 μM), (**b**) representative whole-cell current traces taken from the respective time course prior to (—), 1 min after (—) oxo-M application and, 1 min after wash (—). Cells were held at -90 mV for the recordings in this and all subsequent figures. Currents were elicited every 4 sec by stepping to a test potential of 0 mV for 100 ms unless noted. Vertical portion of black bars in representative sweeps correspond to 0.4 nA, horizontal portion corresponds to 20 msec. (**c, d**) Modulation of N-current from tsA cells with stably transfected N-channel subunits $Ca_V2.2e$, α_2-δ-1 and $Ca_V\beta3$; transiently expressing M_1R is shown in time course and representative sweeps as described above. The charge carrier was increased to 20 mM Ba to improve signal to noise ratio, and accordingly the test potential was adjusted to 10 mV for surface-potential shift. (**e,f**) N-current modulation from cells expressing HEK-M1 cells transfected as for **a** and **b**. Here cells were exposed to PLA_2 antagonist OPC for at least 3 minutes prior to application of Oxo-M (**g**) Summary of inhibition after 1 min of exposure to Oxo-M. (**h**) Data supports working model of slow pathway depicted in schematic in which PLA_2 is necessary component to elicit N-current inhibition.

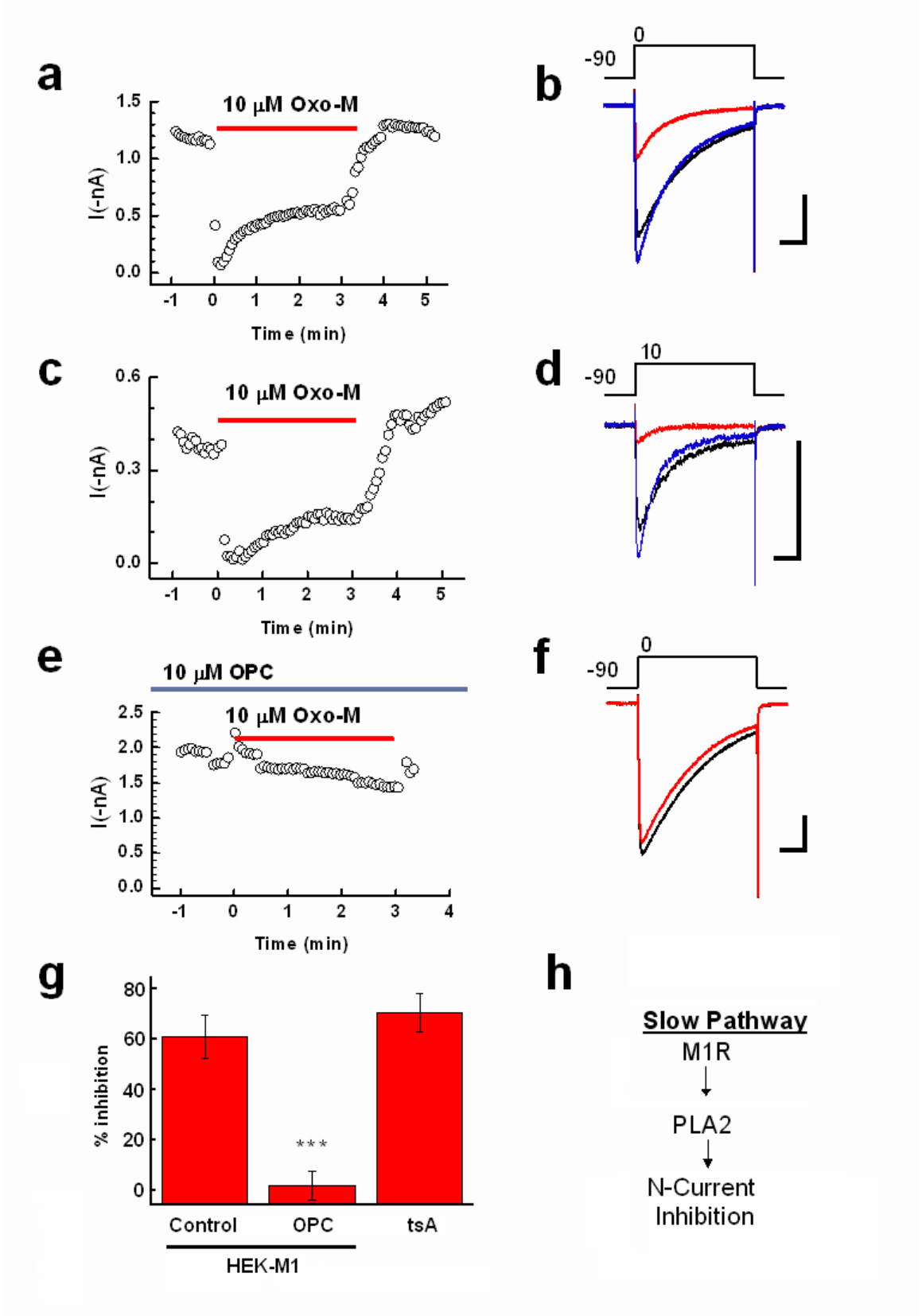
a
10 μM Oxo-M
I(-nA)
Time (min)
b
0
-90
c
10 μM Oxo-M
I(-nA)
Time (min)
d
10
-90
e
10 μM OPC
10 μM Oxo-M
I(-nA)
Time (min)
f
0
-90
g
% inhibition
***
Control
OPC
tsA
HEK-M1
h
Slow Pathway
M1R
PLA2
N-Current
Inhibition

Figure 3-2. $Ca_V\beta$ Subunit Expression Determines N-current Response to Modulation by M_1R Stimulation. HEK-M1 cells were transiently transfected with $Ca_V2.2e$, α_2-δ-1 and various $Ca_V\beta$ subunits. Modulation of N-current in cells expressing $Ca_V\beta1b$ by M_1R stimulation is demonstrated by (**a**) time courses of peak inward current using 5 mM Ba as charge carrier; before, during and after a 3 min bath application of oxo-M (10 μM), (**b**) representative whole-cell current traces taken from the respective time course prior to (**—**) and 3 min after (**—**) oxo-M application and, (**c**) averaged normalized I-V plots before (●) and after (**o**) oxo-M application (n = 6). Currents were elicited every 4 sec by stepping to a test potential of 0 mV for 100 ms unless noted. (**d-e**) Modulation of N-current from cells expressing $Ca_V\beta2a$. The charge carrier was increased to 20 mM Ba to improve signal to noise ratio, and the test potential was adjusted to 10 mV for surface-potential shift. (**f**) Averaged normalized I-V plots for cells expressing $Ca_V\beta2a$ (n = 5). (**g-h**) Time course and representative sweeps of N-current modulation from cells expressing $Ca_V\beta3$ using 20 Ba for charge carrier with test potential of 10 mV (compare to **Fig 2-1 a,b**). (**i**) Averaged normalized I-V plots for cells expressing $Ca_V\beta3$ measured in 5 Ba (n = 3) (**j-l**) Demonstration of N-current modulation from cells expressing $Ca_V\beta4$. Time course, representative sweeps, and averaged normalized I-V plots (n = 3) measured in 5 Ba. A second set of I-V plots measured in 20 Ba showed the same pattern of modulation, inhibition without enhancement (n = 3, data not shown). For current-voltage plots, the test potential was stepped in 10 mV increments from -60mV to +70 mV. Black bars in representative sweeps correspond to 0.4 nA.

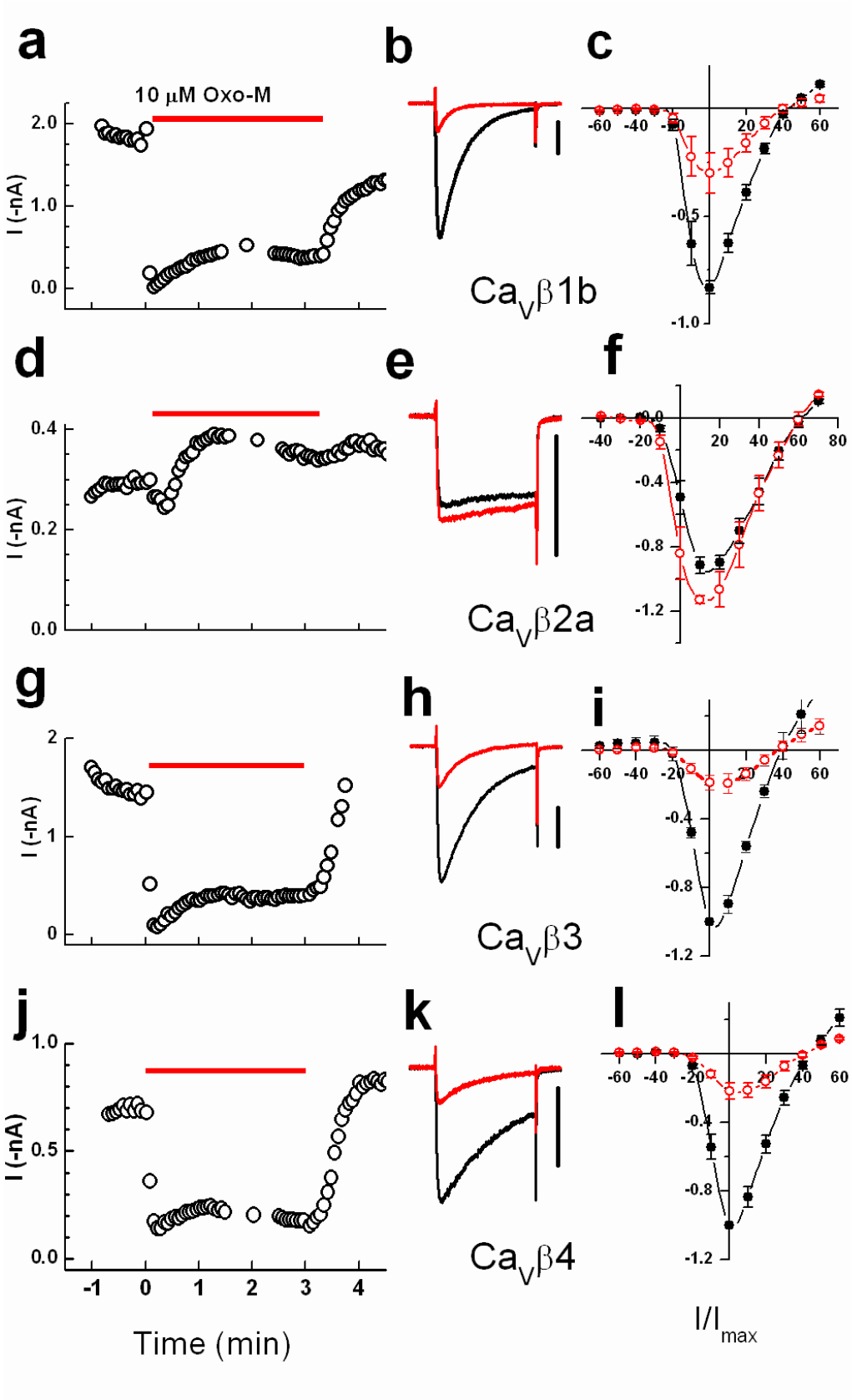
a
10 μM Oxo-M
I (-nA)
2.0
1.0
0.0
b
Ca$_V$β1b
c
-60 -40 -20 20 40 60
-0.5
-1.0
d
I (-nA)
0.4
0.2
0.0
e
Ca$_V$β2a
f
-40 -20 20 40 60 80
-0.4
-0.8
-1.2
g
I (-nA)
2
1
0
h
Ca$_V$β3
i
-60 -40 -20 20 40 60
-0.4
-0.8
-1.2
j
I (-nA)
1.0
0.5
0.0
-1 0 1 2 3 4
Time (min)
k
Ca$_V$β4
l
-60 -40 -20 20 40 60
-0.4
-0.8
-1.2
I/I$_{max}$

Figure 3-3. $Ca_V\beta$ Subunit Determines N-current response to Modulation by Exogenous Arachidonic Acid (AA). HEK-M1 cells were transiently transfected with $Ca_V2.2e$, α_2-δ-1 and various $Ca_V\beta$ subunits. Modulation of N-current in cells expressing $Ca_V\beta1b$ by AA application is demonstrated by (**a**) time courses of peak inward current using 5 mM Ba as charge carrier; before, during and after a 3 min bath application of oxo-M (10 μM), (**b**) representative whole-cell current traces taken from the respective time course prior to (**—**) and 3 min after (**—**) AA application and, (**c**) normalized I-V plots before (●) and after (**o**) AA application (n = 4). Currents were elicited every 4 sec by stepping to a test potential of 0 mV for 100 msec. Washout of AA was enhanced by the addition of 1 mg/ml BSA. (**d-e**) Modulation of N-current by AA from cells expressing $Ca_V\beta2a$. The charge carrier was increased to 20 mM Ba and the test potential was adjusted to 10 mV for surface-potential shift. (**f**) Averaged normalized I-V plots for cells expressing $Ca_V\beta2a$ (n = 5). (**g-i**) N-current modulation from cells expressing $Ca_V\beta3$ in 5 Ba, averaged normalized I-V plots (n = 5). (**j-l**) Demonstration of N-current modulation from cells expressing $Ca_V\beta4$ in 5 Ba. averaged normalized I-V plots (n = 5). Again, washout of AA was enhanced by the addition of 1 mg/ml BSA. For current-voltage plots, the test potential was stepped in 10 mV increments from -60mV to +70 mV. Black bars in representative sweeps correspond to 0.4 nA.

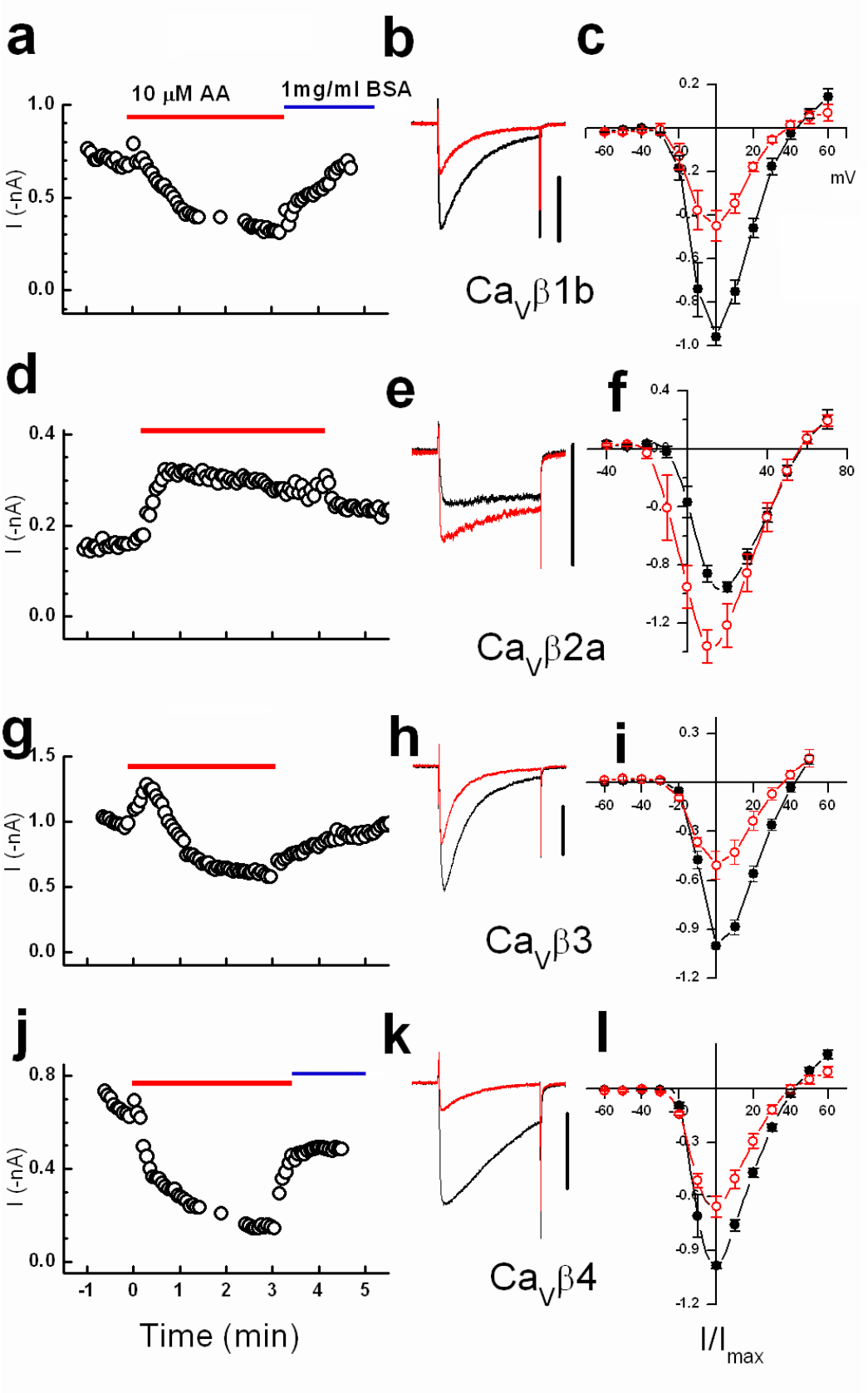
a
b
c
10 μM AA
1mg/ml BSA
I (-nA)
CaVβ1b
mV
d
e
f
CaVβ2a
g
h
i
CaVβ3
j
k
l
CaVβ4
Time (min)
I/Imax

Figure 3-4. Summary of Data from Whole-Cell Recordings from HEK-M1 Cells Expressing N-channels Comprising Various Wild-type $Ca_V\beta$. Shown are (**a**) a summary of inhibition by oxo-M after 3 minutes, and (**b**) a summary of inhibition after a three minute exposure to AA. ** denotes statistical significance ($p \leq 0.005$) as determined by one way ANOVA.

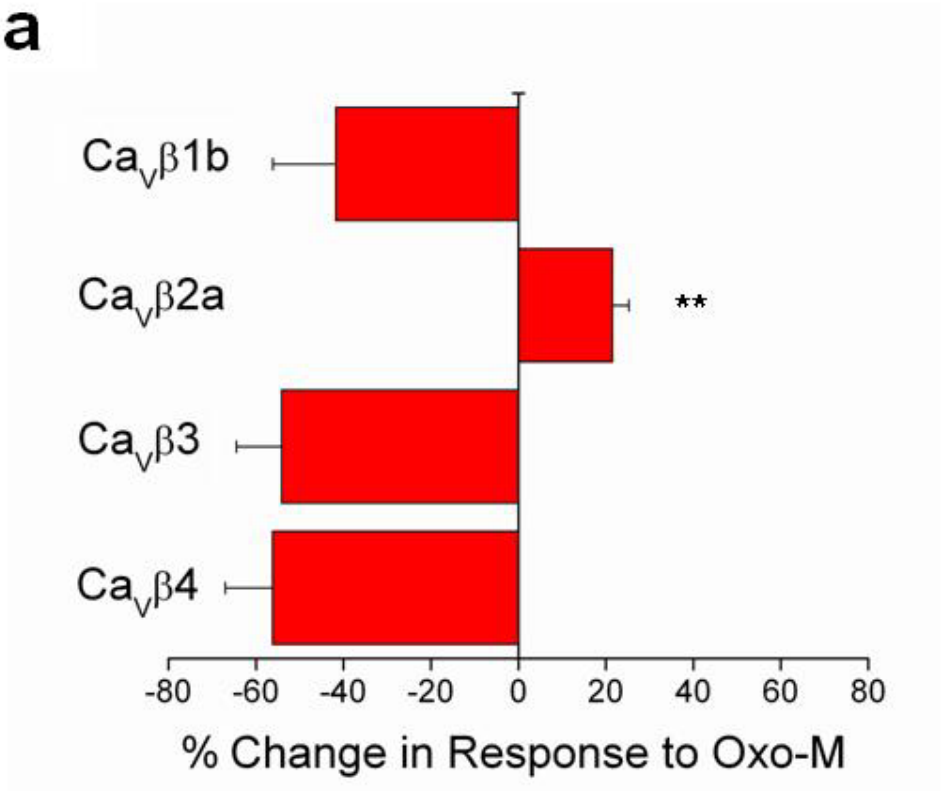
a
Ca$_V$β1b
Ca$_V$β2a
Ca$_V$β3
Ca$_V$β4
**
-80 -60 -40 -20 0 20 40 60 80
% Change in Response to Oxo-M

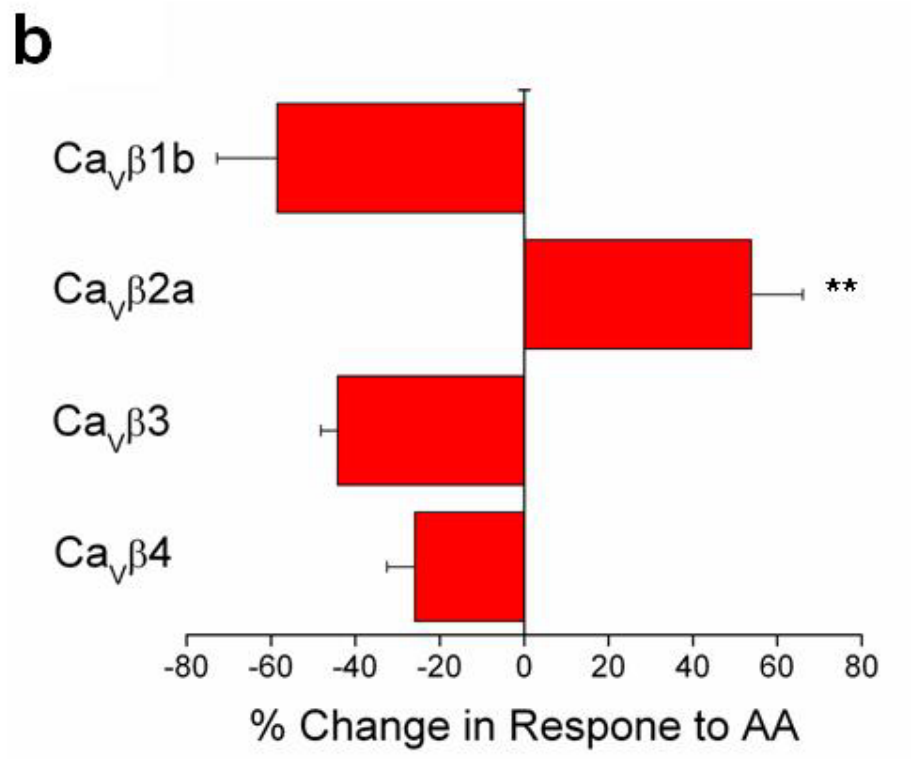
b
Ca$_V$β1b
Ca$_V$β2a
Ca$_V$β3
Ca$_V$β4
**
-80 -60 -40 -20 0 20 40 60 80
% Change in Respone to AA

Figure 3-5. Absorption of AA Minimizes Enhancement of Current. HEK-M1 cells were transiently transfected with $Ca_V2.2e$, α_2-δ-1 and $Ca_V\beta2a$. Modulation of N-current by AA application is demonstrated by (**a**) time courses of peak inward current using 20 mM Ba as charge carrier; before, during and after two separate 3 min bath applications of AA (10 μM) washout of AA was achieved by bath application of 1 mg/ml BSA, (**b**) representative whole-cell current traces taken from the respective time course prior to (—), 3 min after (—) AA application and 1 min after washout (—). Currents were elicited every 4 sec by stepping to a test potential of 0 mV for 100 ms to accentuate enhancement of current. As shown BSA reverses potentiation by AA and second application of AA repeats enhancement. (**c**) Comparison of I-V plots before (●) and after (o) AA application shows characteristic enhancement at negative potentials. (**d**) Comparison of I-V plots taken after washout of AA by BSA (●) and after (o) second application of AA shows same characteristic enhancement at negative potentials.

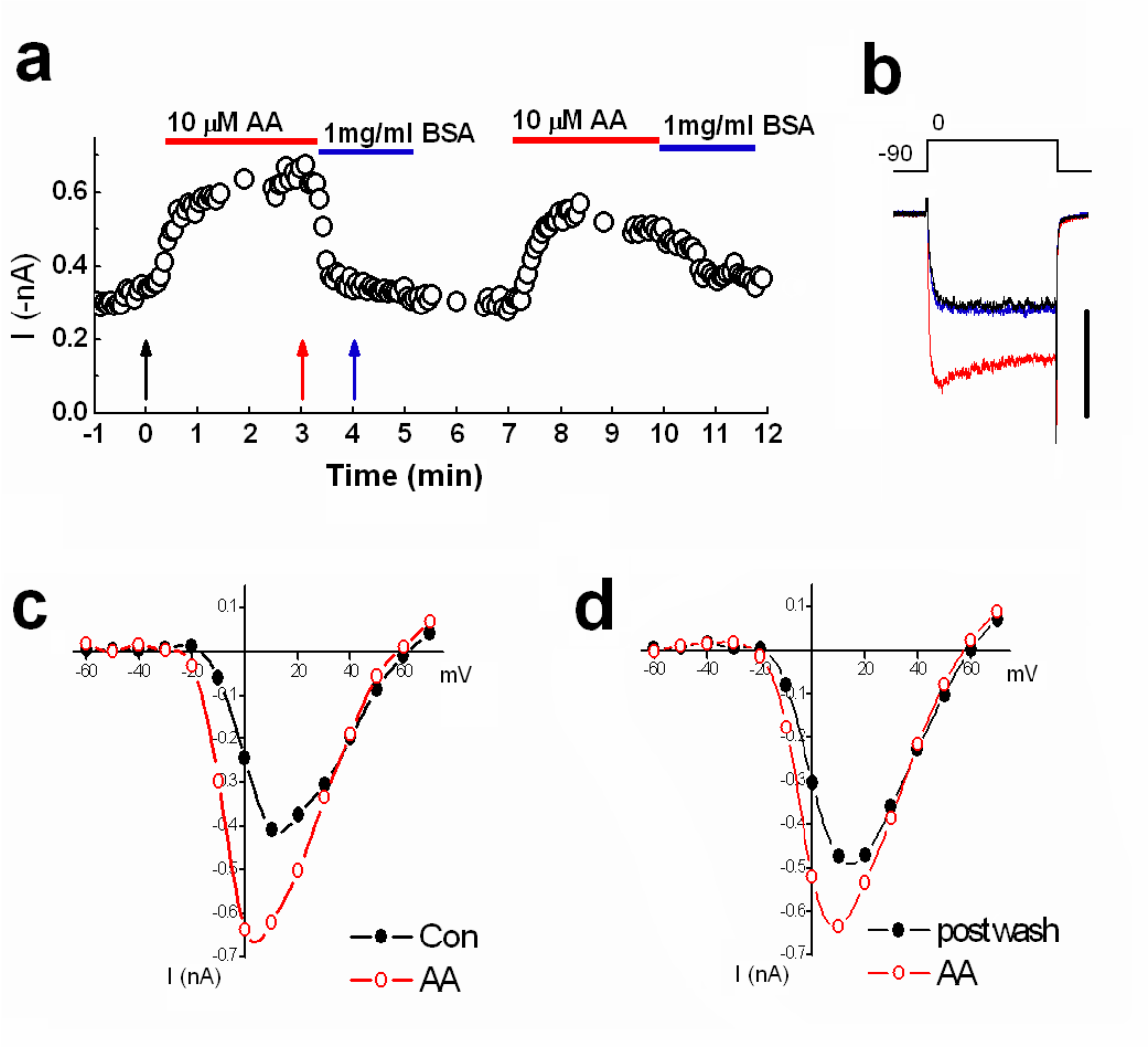
a
10 μM AA
1mg/ml BSA
10 μM AA
1mg/ml BSA
I (-nA)
Time (min)
b
0
-90
c
mV
I (nA)
Con
AA
d
mV
I (nA)
postwash
AA

Figure 3-6 $Ca_V\beta2a$ Blocks Inhibition of N-current Revealing Latent Enhancement. Using a modified Ohm's law $G = I/(V_m - V_{rev})$ where I is the peak current at each test potential, V_m is the test potential, V_{rev} is the apparent reversal potential, and G_{max} as the maximal conductance we plotted G/G_{max} vs V_m for whole-cell recordings before and after AA application and found both (**a**) $Ca_V\beta2a$ and (**b**) $Ca_V\beta3$ containing cells exhibited a negative shift in conductance as a response to AA modulation. These findings indicate that both channels exhibit enhancement. (**c**) Schematic representation of working model. Previous work had shown that extracellular events control enhancement and intracellular events control inhibition. We reasoned that since $Ca_V\beta$ binds to cytoplasmic regions of $Ca_V2.2e$ the anomalous response of $Ca_V\beta2a$ was due to alterations in inhibition. We therefore propose a model in which $Ca_V\beta2a$ allows enhancement by blocking a normally dominant inhibition.

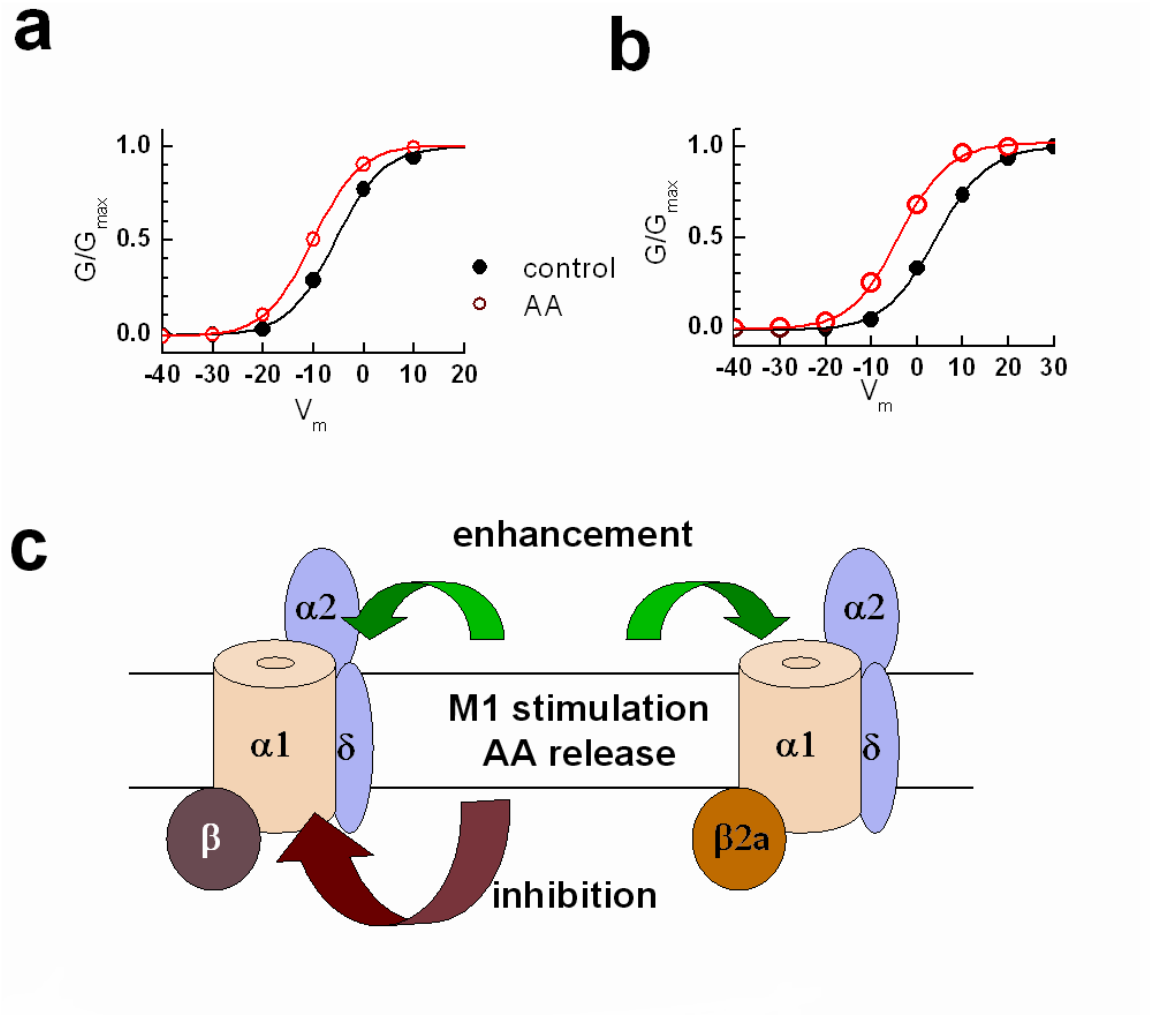
a
b
c
1.0
0.5
0.0
G/G max
-40 -30 -20 -10 0 10 20
V m
control
AA
-40 -30 -20 -10 0 10 20 30
enhancement
α2
α1
δ
β
β2a
M1 stimulation
AA release
inhibition

Figure 3-7. Multiple $Ca_V\beta$ Subunit Expression Recapitulates Modulation Pattern of SCG Neurons. HEK-M1 cells were transiently transfected with N-channel subunits comprising multiple $Ca_V\beta$ subunits. Modulation of N-current by application of AA (10 μM) is in HEK-M1 cells expressing $Ca_V2.2e$, α_2-δ-1, $Ca_V\beta2a$, and $Ca_V\beta3$ in a 12:12:10:1 ratio demonstrated by representative whole-cell current traces using 20 Ba as a charge carrier, stepping to a test potential of (**a**) -10 mV or (**b**) +10 mV, prior to (**—**) and 90 seconds after (**—**) AA application, and (**c**) normalized I-V plots before (●) and after (**o**) AA application. Modulation of N-current by application of Oxo-M (10 μM) is in HEK-M1 cells expressing $Ca_V2.2e$, α_2-δ-1, $Ca_V\beta2a$, $Ca_V\beta3$, and $Ca_V\beta4$ in a 12:12:10:1:1 ratio demonstrated by representative whole-cell current traces using 20 Ba as a charge carrier, stepping to a test potential of (**d**) -10 mV or (**e**) +10 mV, prior to (**—**) and 90 seconds after (**—**) AA application, and (**f**) normalized I-V plots before (●) and after (**o**) Oxo-M application.

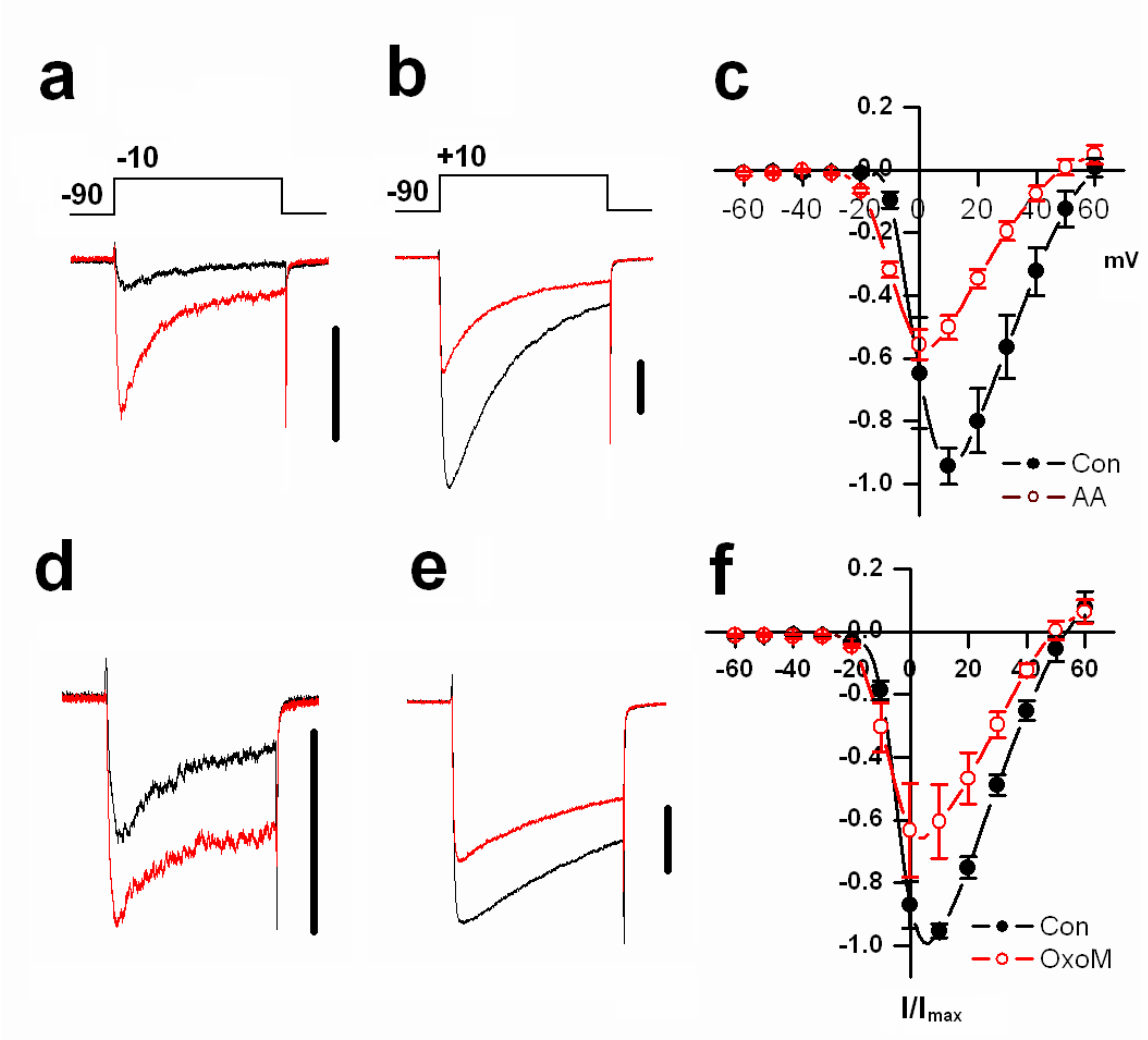
a
-10
-90
b
+10
-90
c
0.2
0.0
-0.2
-0.4
-0.6
-0.8
-1.0
-60 -40 -20 0 20 40 60
mV
Con
AA
d
e
f
0.2
0.0
-0.4
-0.6
-0.8
-1.0
-60 -40 -20 0 20 40 60
Con
OxoM
I/I max

Figure 3-8 Loss of Palmitoylation Restores Inhibition of N-current by M_1R Stimulation or AA Application. HEK-M1 cells were transiently transfected with $Ca_V2.2e$, α_2-δ-1 and $Ca_V\beta2a$(C3,4S), mutated at the two sites of palmitoylation. (**a,b**) Representative whole-cell current traces using 20 Ba as a charge carrier, stepping to a test potential of 10 mV taken prior to (—) three minutes after application of oxo-M or AA (—) and one minute after washout of oxo-M or AA (—) show similar pattern of inhibition and recovery. Vertical portion of black bars in representative sweeps correspond to 0.4 nA, horizontal portion corresponds to 20 msec. In time courses (**c**) oxo-M inhibits current transiently continued exposure to oxo-M returns current near level before oxo-M application. (**d**) AA initially enhances but, unlike wild- type $Ca_V\beta2a$ subsequently inhibits current. Washout of AA with 1 mg/ml restores current.

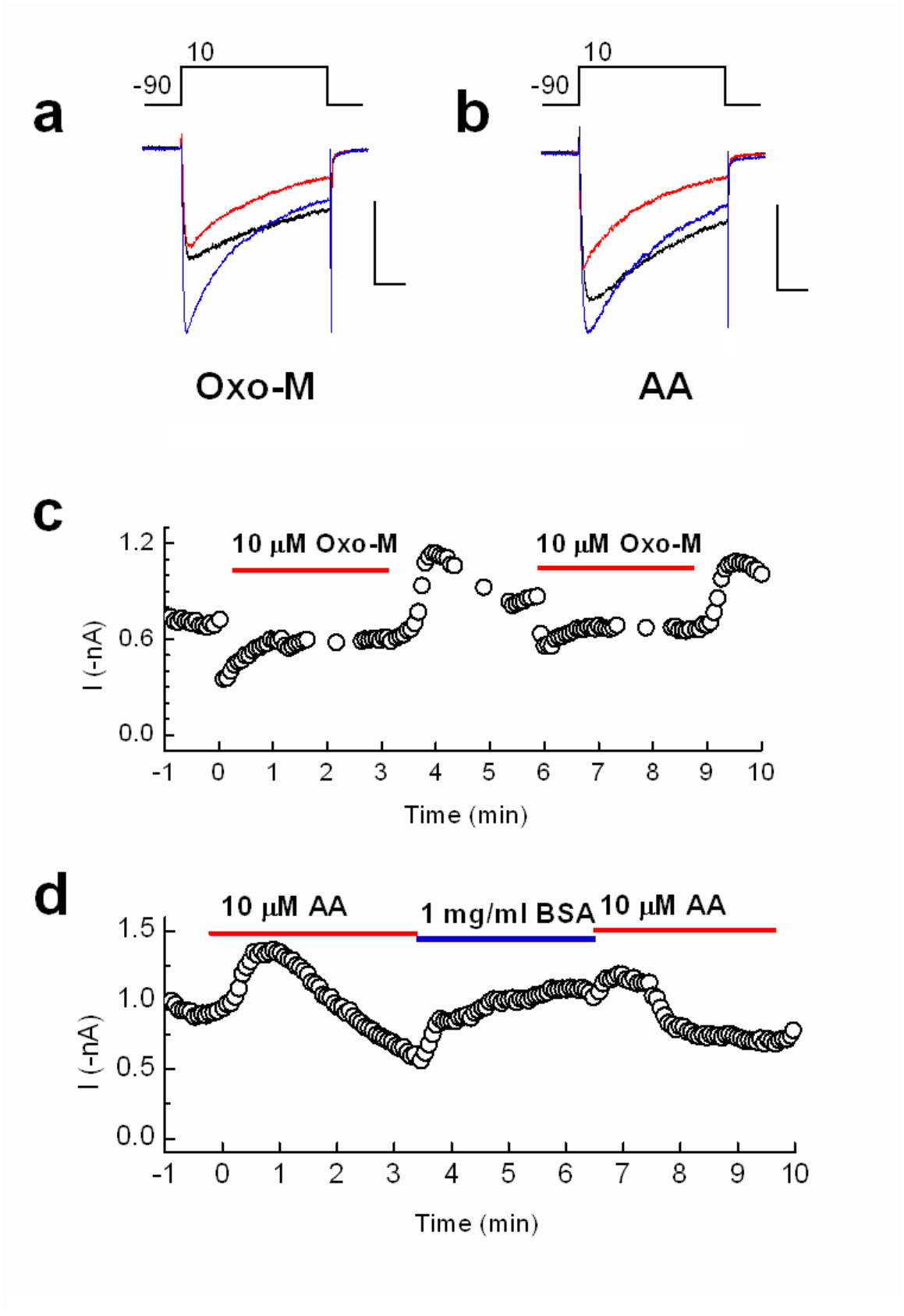
a
10
-90
Oxo-M
b
10
-90
AA
c
10 μM Oxo-M
10 μM Oxo-M
I (-nA)
1.2
0.6
0.0
-1
0
1
2
3
4
5
6
7
8
9
10
Time (min)
d
10 μM AA
1 mg/ml BSA
10 μM AA
I (-nA)
1.5
1.0
0.5
0.0
-1
0
1
2
3
4
5
6
7
8
9
10
Time (min)

Figure 3-9. Addition of Palmitoylation to Chimeric $Ca_V\beta$ Attenuates Inhibition. HEK-M1 cells were transiently transfected with $Ca_V2.2e$, α_2-δ-1 and either $Ca_V\beta2a\beta3$ chimera or $Ca_V\beta2a\beta1b$ chimera. Modulation of N-current by Oxo-M (10 μM) from cells expressing $Ca_V\beta2a\beta3$ chimera is shown through (**a**) time courses of peak inward current; before, during and after a 3 min bath application of oxo-M, (**b**) representative whole-cell current traces taken from the respective time course prior to (—), 3 min after (—) oxo-M application and, 1 min after wash (—). (**c**) Averaged normalized I-V plots before (●) and after (o) oxo-M application (n = 4). (**d,e,f**) Modulation of N-current by AA (10 μM) from cells expressing $Ca_V\beta2a\beta3$ chimera is shown as above by representative time course, sweeps, and averaged normalized I-V (n = 7). (**g,h,i**) Modulation of N-current by Oxo-M (10 μM) from cells expressing $Ca_V\beta2a\beta1b$ chimera is shown as above by representative time course, sweeps, and averaged normalized I-V (n = 4). (**j,k,l**) Modulation of N-current by AA (10 μM) from cells expressing $Ca_V\beta2a\beta1b$ chimera is shown as above by representative time course, sweeps, and averaged normalized I-V (n = 4). All data was obtained using 5 mM Ba as charge carrier Currents were elicited every 4 sec by stepping to a test potential of 0 mV for 100 ms. Black bars in representative sweeps correspond to 0.4 nA.

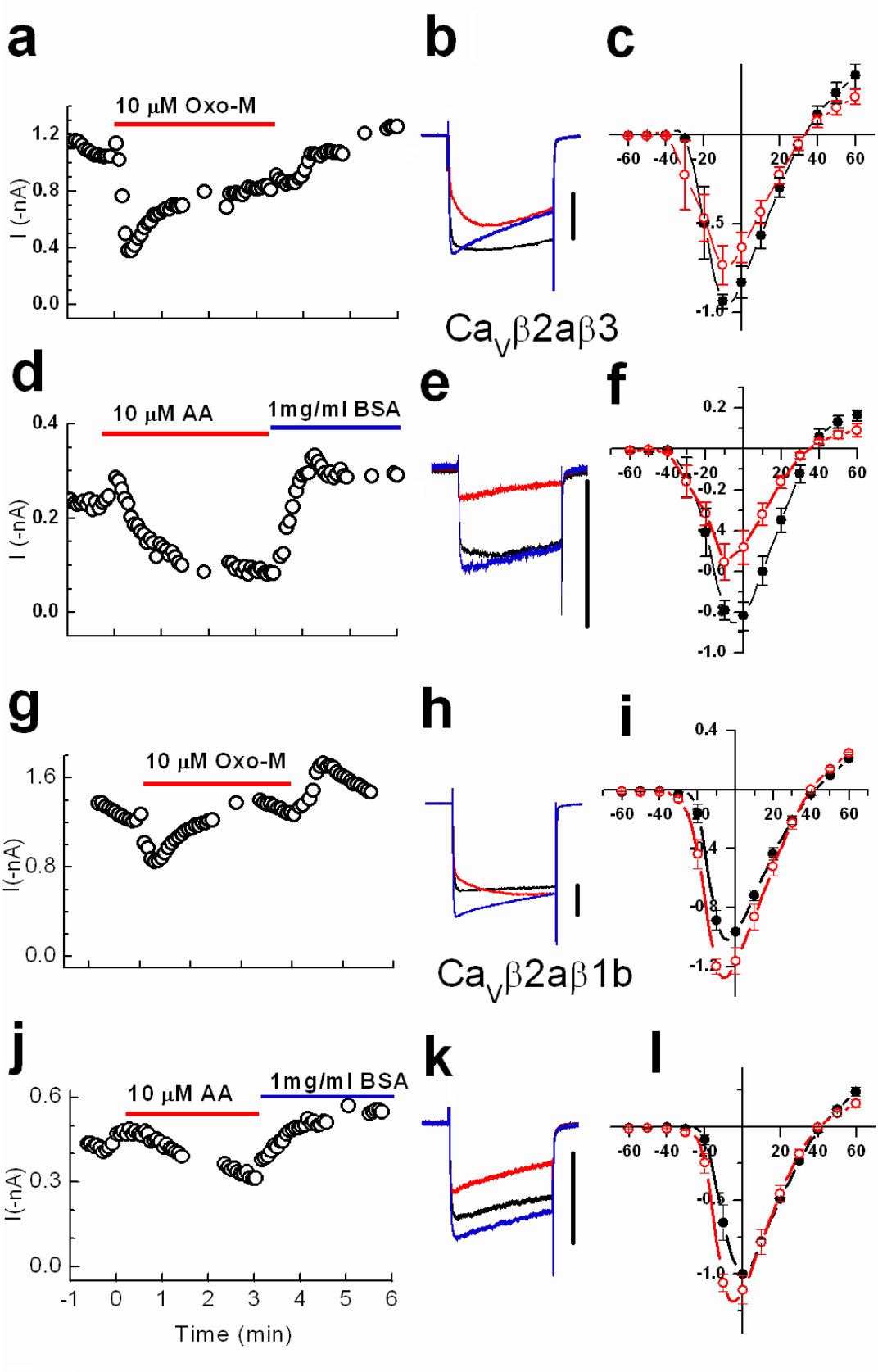
a
10 μM Oxo-M
I (-nA)
1.2
0.8
0.4
0.0
b
c
-60 -40 -20 20 40 60
-0.5
-1.0
Ca$_V$β2aβ3
d
10 μM AA
1mg/ml BSA
I (-nA)
0.4
0.2
0.0
e
f
0.2
-60 -40 -20 20 40 60
-0.2
-0.4
-0.6
-0.8
-1.0
g
10 μM Oxo-M
I(-nA)
1.6
0.8
0.0
h
i
0.4
-60 -40 -20 20 40 60
-0.4
-0.8
-1.2
Ca$_V$β2aβ1b
j
10 μM AA
1mg/ml BSA
I(-nA)
0.6
0.3
0.0
-1 0 1 2 3 4 5 6
Time (min)
k
l
-60 -40 -20 20 40 60
-0.5
-1.0

Figure 3-10 Summary of Inhibition by Oxo-M or AA of Cells Expressing Mutated or Chimeric $Ca_V\beta$ Isoforms. Here is shown percent inhibition of currents from HEK-M1 cells expressing mutated or chimeric forms of $Ca_V\beta$ by (a) oxo-M or (b) AA.

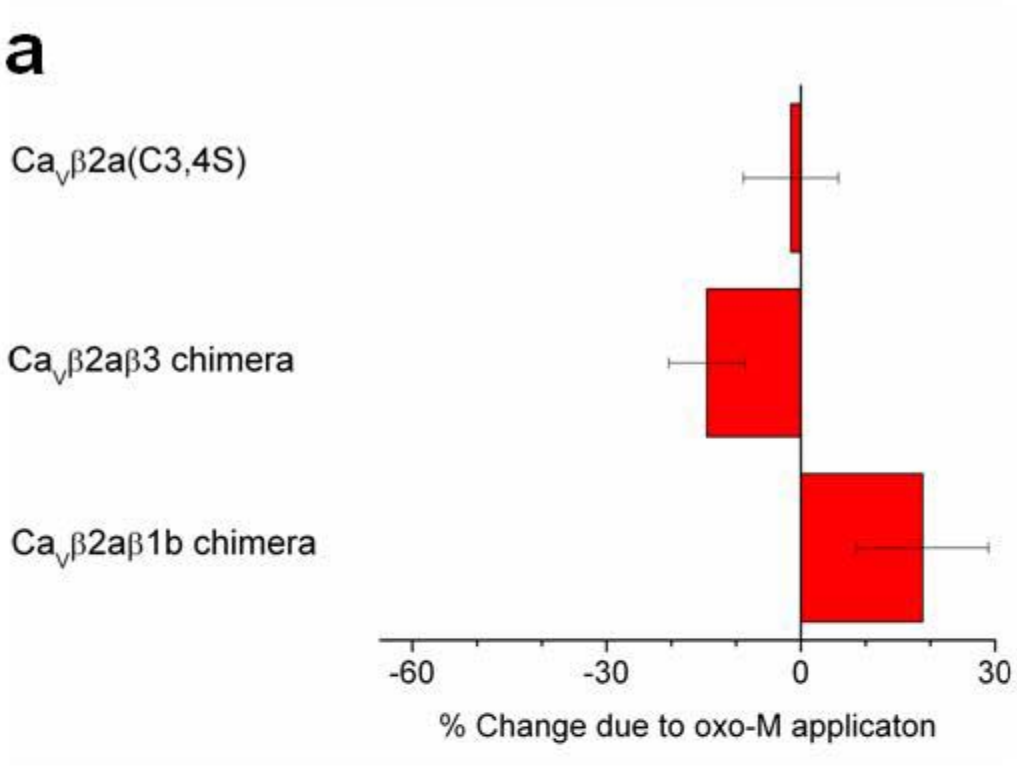
a
Ca$_V$β2a(C3,4S)
Ca$_V$β2aβ3 chimera
Ca$_V$β2aβ1b chimera
-60
-30
0
30
% Change due to oxo-M applicaton

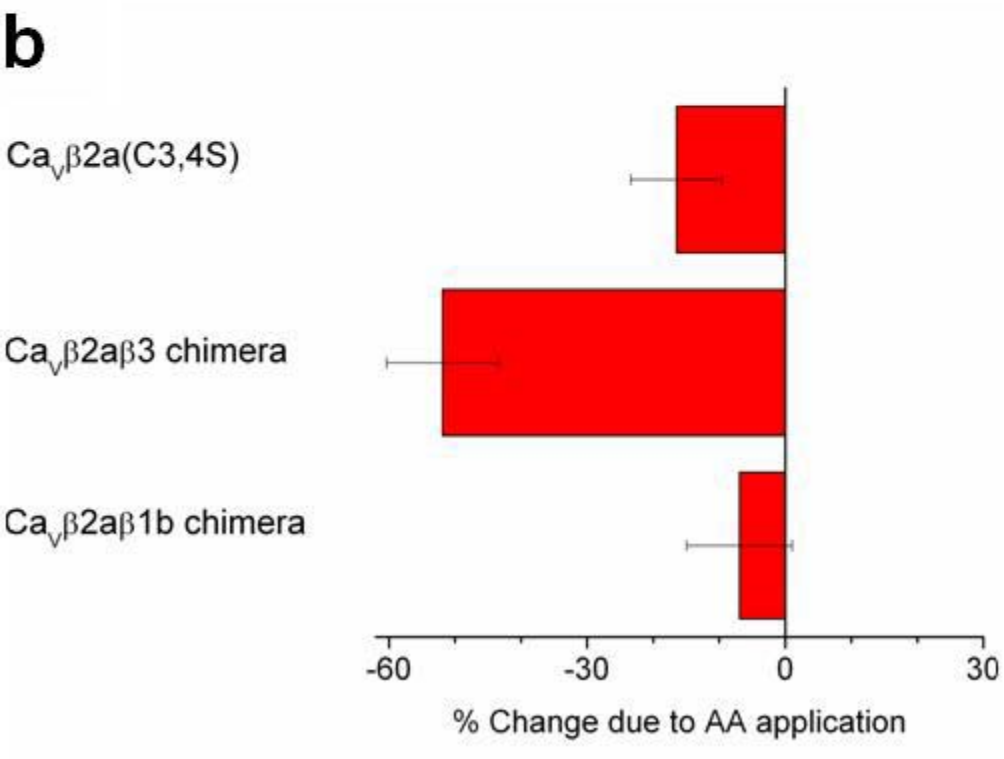
b
Ca$_V$β2a(C3,4S)
Ca$_V$β2aβ3 chimera
Ca$_V$β2aβ1b chimera
-60
-30
0
30
% Change due to AA application

CHAPTER IV

DAG Lipase is Necessary for M_1 Muscarinic Inhibition of N-and L-, but not M-Current

Abstract

M1 muscarinic receptors (M_1R) affect cognition, learning and memory and are an important therapeutic target in the treatment of Alzheimer's disease. M_1R stimulation modulates currents through various types of voltage-gated ion channels, among them: KCNQ potassium channels (M-current) and both N- and L-type calcium channels (N- and L- current). M_1Rs couple to $G_{q/11}$ which activates phospholipase C (PLC). Consequently PLC causes a depletion of phosphatidylinositol-4,5-bisphosphate (PtdIns(4,5)P_2). PtdIns(4,5)P_2 hydrolysis during M_1R stimulation suffices to elicit modulation of M-current. However, we've shown previously that events additional to PtdIns(4,5)P_2 hydrolysis are necessary for N- and L- current modulation; particularly the release of arachidonic acid (AA) after the activation of phospholipase A2 (PLA_2). Here we examined the effect of another AA liberating enzyme, diacylglycerol lipase (DAGL), on M-, N- and L-current modulation. We documented the presence of DAGL in superior cervical ganglion (SCG) neurons, and then tested the selective DAG lipase inhibitor, RHC-80267, for its capacity to block M_1R mediated inhibition of currents. We found while RHC-80267 has no effect on M-current modulation, it significantly reduces inhibition of both N- and L-currents. Furthermore, RHC-80267 does not affect inhibition of N- or L- current elicited by exogenously applied AA. These data corroborate our previous finding; indicating a divergence in signaling pathways for inhibition of M-current versus N- or L- current. Moreover, these are the first data indicating a role for DAGL in modulation of N- and L-currents elicited by M_1R stimulation.

Introduction

The release of acetyl choline (ACh) in the central nervous system (CNS) is crucial for cognition, learning and memory (Woolf 1996). ACh stimulates various muscarinic receptors which are encoded by five different genes (M_1-M_5; Caulfield and Birdsall 1998) all of which are expressed in the CNS (Levey et al., 1991; Wei et al., 1994). The M_1 muscarinic receptor (M_1R) is of particular interest, as it is the most prevalent subtype expressed in hippocampus and cortex regions of the brain associated with learning and memory (Levey et al., 1991; Wei et al., 1994). Also, severe cognitive and memory deficits occur in knockout mice lacking M_1Rs (Anagnastoras et al. 2003). Clinically the M_1R is a therapeutic target for Alzheimer's disease (AD). At the present time the majority of drugs approved to treat AD act by increasing ACh at M_1Rs (Ibach & Haen 2004).

M_1Rs affect numerous neural functions including the modulation of voltage gated ion channels. In the early 1980s, M-current, a low threshold potassium current inhibited by muscarinic stimulation was identified in frog sympathetic neurons (Brown and Adams 1980) and rat superior cervical ganglion (SCG) neurons (Constanti and Brown 1981). Since that time the signaling pathway that causes inhibition of M-current has been the subject of intense study (reviewed in Delmas and Brown, 2005). The present understanding is a depletion of phosphatidylinositol-4,5-bisphosphate ($PtdIns(4,5)P_2$) during M_1 stimulation causes a concentration gradient of $PtdIns(4,5)P_2$ in the membrane, and inhibition occurs as $PtdIns(4,5)P_2$ disengages and diffuses from KCNQ channels. (Zhang et al. 2003; reviewed in Delmas and Brown 2005; Suh and Hille 2005)

M_1R stimulation also inhibits certain voltage gated calcium currents. Since the activation of the receptor and time course of inhibition were equivalent for M-current and calcium currents, the mechanisms of inhibition were thought to be the same (Hille 1994). Recent reports indicating a depletion of PtdIns(4,5)P_2 inhibits both P/Q- or N- currents, while increases in PtdIns(4,5)P_2 concentration stabilizes P/Q- or N- currents (Wu et al., 2002; Gamper et al., 2004) were seen as evidence that loss of PtdIns(4,5)P_2 itself is both necessary and sufficient to cause inhibition of Ca_V2 channels (Suh and Hille, 2005a; Delmas et al., 2005; Delmas and Brown, 2005).

However, our lab has presented evidence that downstream events after the metabolism of PtdIns(4,5)P_2 are required for modulation of N- and L-currents. We have demonstrated stimulation of M_1Rs by oxotremorine-M (Oxo-M) in SCG neurons produces a pattern of inhibition nearly identical to exogenous application of arachidonic acid (AA), inhibiting current at positive potentials and enhancing currents at negative potentials (Liu and Rittenhouse 2003a). Absorption of AA with essentially fatty acid free bovine serum albumin (BSA) attenuates inhibition of N- or L- current by oxo-M. We examined the role of phospholipase A2 (PLA_2), an enzyme known to be instrumental in AA release. We found that PLA_2 antagonists block M_1R mediated inhibition of both N- and L-current in SCG neurons (Liu and Rittenhouse 2003a, Liu et al 2004). Moreover, inhibition of L- but not M- is lost in cytoplasmic PLA_2 knockout ($cPLA_2^{-/-}$) mice (Liu et al 2006).

Since in many systems AA release depends on both PLA_2 and diacylglycerol lipase (DAGL) (Ambs et al 1995; Caraway et al 2006, Liu 1999); we hypothesized DAGL would be essential for N- and L- current modulation by M_1Rs. Here we present

evidence that DAGL is necessary for M_1 mediated inhibition of N- and L- current. We first verified the presence of DAGL in SCG and then examined its role in modulating M-, N- and L- currents. We used a combination of pharmacological tools and electrophysiological protocols to isolate each of the currents. We then used potent and specific inhibitor RHC-80267 (RHC) to determine whether DAGL is necessary for current modulation. We found RHC blocks N- and L- current modulation but not M-current modulation. These data confirm our previous finding of diverging pathways for modulation of M- current and N- or L- current.

Results

DAG lipase is present in SCG neurons

To determine whether DAGL plays a role in current modulation we tested whether DAGL is present in SCG neurons. We first determined that the message for DAGL is present in SCG by *in situ* hybridization. A labeled oligonucleotide probe indicated substantial DAGLα mRNA in SCG neurons (**Fig 4-1 a**). To control for non-specific binding of the probe we repeated the experiment with a 250 fold excess of unlabeled oligonucleotide during hybridization (**Fig 4-1 b**). These data confirm DAGLα is transcribed in SCG neurons. To determine whether or not DAGLα protein is expressed in SCG we performed immunoctochemistry with a DAGLα specific antibody (Bisogno et al 2003) and found strong DAGLα expression in SCG neurons (**Fig 4-1 c,d**).

Pharmacological strategy for determining a role of DAGL in current inhibition

Having established DAGL expression in SCG neurons we next designed a pharmacological approach shown in figure 4-2 to examine the role of DAGL in inhibition of M-, L-, and N- currents. Stimulation of muscarinic receptors in SCG neurons results in inhibition that occurs through two separate pathways: 1) the fast pathway, mediated by M_2 and M_4 receptors, inhibits N-current; 2) the slow pathway, mediated by M_1Rs, affects both N- and L- currents (Marrion et al. 1989; Mathie et al., 1992; Hille, 1994). FPL and Nimodipine (NMN) were used to isolate L- or N-current and PTX was used to block the fast pathway. RHC-80267 [1,6-di(O-(carbamoyl)cyclohexanone oxime)hexane, (RHC)] is a potent and highly selective inhibitor of DAGL (Sutherland and Amin 1982). As

shown, M-current inhibition should be unaffected by RHC as it results purely from a breakdown of PtdIns(4,5)P_2. Conversely, since both N- and L-current inhibition were shown to be sensitive to AA production we hypothesized antagonizing DAGL would attenuate Oxo-M induced inhibition of either current.

RHC-80267 does not block inhibition of M-Current in neonate rat SCG neurons

M-current is inhibited by a signaling pathway which involves the stimulation of M_1Rs, (Marrion et al. 1989; Bernheim et al. 1992) the activation of $G\alpha_q$ (Haley et al. 1998), the subsequent activation of PLC, the hydrolysis of PtdIns(4,5)P_2 and its dissociation of PtdIns(4,5)P_2 from the KCNQ potassium channel (Zhang et al., 2003; Ford et al., 2004). A requirement for AA release in M-current inhibition has not been identified. Moreover, RHC does not affect M-current inhibition in reconstitued KCNQ in tsA cells (Suh and Hille 2006). Therefore, we anticipated M-current inhibition in SCG neurons would be the same in the presence or absence of the RHC. M-current was measured in neonatal SCG neurons as previously described (Brown and Adams, 1980). Application of Oxo-M (10 μM) inhibited M-current by 54 ± 8 % (n = 4; **Fig. 4-3 a,b,e**). When neurons were exposed to RHC (20 μM) for at least 3 minutes Oxo-M inhibited M-current by 48 ± 7 % (n =4; **Fig. 4-3 c,d,e**). There was no significant difference in the percent change in current elicited by oxo-M between measurements taken in the absence or presence of RHC (p = 0.61, **Fig. 4-3 e**). These data confirmed our hypothesis and corroborate the recently published results with reconstituted KCNQ in tsA cells (Suh and Hille 2005). More importantly, the inhibition of M-current in the presence of RHC shows the signaling pathway remains intact when DAG lipase is inhibited.

RHC-80267 blocks whole cell calcium current inhibition by M_1R

Our previous work showed AA mediates muscarinic inhibition and enhancement of whole-cell barium (Ba^{2+}) currents in SCG neurons (Liu and Rittenhouse, 2003a). Therefore, we reasoned DAGL could be important for M_1R mediated modulation of I_{Ba} in these same neurons. To test this hypothesis we measured inhibition of whole-cell current using 20 mM Ba as the charge carrier in the absence and presence of RHC (20 μM). Cells were exposed to PTX (0.2 μg/ml) for five hours before recording whole-cell currents. This preincubation blocked downstream effects of M_2 and M_4 receptors, (**Fig. 4-2**) leaving the M_1 initiated pathway intact. RHC was bath applied for at least three minutes before oxo-M. We found oxo-M elicited no change in current amplitude or kinetics (**Fig. 4-2 a,b**). Since AA and oxo-M elicit the same distinctive pattern of modulation in SCG neurons, enhancement at negative potentials and inhibition at positive potentials, we ran IVs before and 90 seconds after oxo-M application (**Fig. 4-4 c**). In the presence of RHC, oxo-M did not cause inhibition at any voltage (n =5). There was a slight enhancement of current at -10 mV (+34 ± 14 %) but the change from control was not statistically significant ($p = 0.08$).

RHC-80267 blocks L-current inhibition by Oxo-M

The voltage gated calcium current of SCG is mainly N-current with a small percentage L-current (Plummer et al., 1989). Since there was virtually no change in current elicited by oxo-M in whole cell currents as shown in the last experiment the data indicated both N- and L-current inhibition are sensitive to RHC and thus inhibition for both types of currents requires DAGL activity. This would agree with our previous work

showing both N- and L-current inhibition are sensitive to AA release during M_1R stimulation (Liu and Rittenhouse 2003a, Liu et al 2004, Liu et al 2006). Still to verify that both N- and L- currents are sensitive to RHC we used experimental protocol that tests the two types of current independently. Bath application of the L-channel agonist FPL (1 μM) together with the voltage protocol shown in figure 4-5 produces a long lasting tail current consist entirely of L-current (Liu et al 2001). The peak current observed during the initial depolarization is indicative of mainly N- current and is thus less sensitive to FPL. Accordingly, FPL typically caused a substantial increase in tail current and a slight increase in peak current (**Fig. 4-5 a**). We compared inhibition of peak and tail currents by oxo-M as shown (**Fig. 4-5 a,b**). Since PTX was not used in these experiments we used the inhibition of peak current, mainly due to fast pathway inhibition of N-current, as an internal control verifying the potency of the muscarinic agonist. Bath application of oxo-M (10 μM) inhibited peak current by 50.9 ± 8.4%. A 90 second exposure to RHC (25 μM) reduced peak current inhibition slightly to 40.2 ± 4.9%. It is expected that RHC does slightly attenuate peak current inhibition given that peak current inhibition is due to the total effect of M_1, M_2, and M_4 receptors. However, this decrease is not significant since inhibition of N-current by M_2 and M_4 muscarinic receptors dominates the peak current inhibition. Conversely, tail current in the absence of RHC is inhibited 43.0 ± 4.0% by oxo-M while tail current in the presence of RHC inhibited only 9.0 ± 2.6% (**Fig. 4-5 a,b,e**). Thus, the inhibition of tail current is significantly reduced; signifying M_1R mediated inhibition of L-current requires DAGL (**Fig. 4-5 c**).

RHC-80267 does not block L-current inhibition by AA

So far we have shown that RHC blocks M_1R mediated inhibition of whole-cell Ba^{2+} currents, which is made up of N- and L- current. Both the M-current inhibition and N-current inhibition via the fast pathway occur in the presence of RHC, demonstrating that RHC does not interfere with signaling at the level of the muscarinic receptors. The lack of interference of M-current inhibition by RHC also demonstrates the M_1R downstream effects of PLC activation and PtdIns(4,5)P_2 hydrolysis are unperturbed. The question remaining then is whether or not RHC effects slow pathway inhibition at the channel itself.

The block of N- and L- current inhibition by RHC indicates AA production by DAGL is necessary. Therefore, we hypothesized inhibition of N- or L- current should be recovered by exogenous application of AA. Since AA release occurs downstream of DAGL (**Fig. 4-2**) inhibition by AA should be unaffected by RHC. To test our hypothesis we applied AA (5 μM) to SCG neurons using both FPL and the tail protocol. We found in the presence of RHC (25 μM) AA inhibits both peak and tail currents in a time frame consistent with previous experiments using AA (**Fig. 4-6 a**). The amount of inhibition of peak current elicited by AA was the same in the absence (50.6 ± 3.0 %) or presence (41.4 ± 7.3 %) of RHC (**Fig. 4-6 b**). Also, the amount of tail current inhibition was the same in the absence (41.5 ± 5.8 %) or presence (46.0 ± 9.4 %) of RHC (**Fig. 4-6 b**). As a final test of pharmacological interference of the slow pathway, we examined the inhibition of N-current by AA in the presence of RHC and PTX. We isolated N-current by bath application of nimodipine [NMN (1 μM)], an antagonist that minimizes L-current (**Fig. 4-2**). In the presence of RHC (25 μM) application of AA (5 μM) inhibited N-current by

56.4 ± 5.0 % (**Fig. 4-7 a,b**). These data are comparable to previously reported levels of N-current inhibition elicited by AA (Liu et al 2001) and indicate inhibition of N- or L-current by AA is unaffected by RHC.

RHC blocks inhibition of N-current in a recombinant system

Previously we found M_1R stimulation inhibits reconstituted N-current in HEK cells with a stably transfected M_1Rs (Peralta et al) transiently transfected with these N-channel subunits: $Ca_V2.2e$, $Ca_V\beta3$, and $\alpha_2\delta$-1 (Chapter III). Inhibition of N-current was 54 ± 10% (n = 9; Figure **4-8 a,b)**. We next reasoned that if DAG lipase is an important component of slow pathway RHC should also block M_1R induced N-current inhibition in the recombinant system. Therefore, we compared the inhibition of N-current elicited by M_1R stimulation in the absence and presence of RHC. Following a three minute application of RHC (20 μM), application of oxo-M (10 μM) elicited an initial large rapid inhibition of current as observed previously. However the inhibition subsided so that within three minutes there was virtually no inhibition left -4.8 ± 6.4% (n=6). (Figure **4-8 c,d**). Comparison of inhibition in the absence and presence of RHC showed block of inhibition to be significant ($p \leq 0.003$).

Discussion

Here we have shown DAGL as essential in mediating M_1R mediated inhibition of N- and L- currents, but not M-current. We first verified the presence of DAGLα in SCG neurons using both *in situ* hybridization and immunohistochemistry. Next, we showed inhibition of M-current is insensitive to RHC, indicating RHC does not block M_1R signaling or downstream molecular mechanisms that lead to M-current inhibition. Conversely, RHC antagonizes inhibition of both N- and L- currents in neonatal SCG neurons indicating DAG lipase activity is necessary for inhibition. RHC does not interfere with current inhibition by AA. These data taken together indicate AA release during M_1R stimulation is both necessary and sufficient for inhibition of N- or L-current.

Our findings with native M-current corroborates the recent report that DAGL does not participate in M_1R inhibition of activity of KCNQ channels expressed in tsA cells (Suh and Hille, 2006). Taken together, these findings support the general model that M-current inhibition results from a depletion of PtdIns(4,5)P_2 and its subsequent dissociation from the KCNQ channels (reviewed in Suh and Hille, 2005a; Delmas and Brown, 2005).

On the other hand, our data that RHC attenuates inhibition of N- and L- current seems to conflict a long held hypothesis that M- and N- current inhibition are mediated by a well conserved signaling pathway (Hille, 1994; Delmas and Brown 2005). However, two recent reports indicate a divergence in signaling pathways. First, a series of palmitoylated cationic peptides designed to sequester PtdIns(4,5)P_2 were effective in blocking M-current but not N-current inhibition (Robbins et al., 2006). Second, L-current

inhibition by M_1R stimulation is absent in SCG neurons harvested from $PLA_2^{-/-}$ mice, whereas M-current inhibition remains intact.

Our data using exogenous AA corroborate other published observations using AA or its corresponding amide anandamide. For example, whole-cell currents from adult rat SCG neurons are enhanced at negative potentials and inhibited at positive potentials by anandamide (Guo and Ikeda 2004). In T-type channels, AA also simultaneously shifts activation towards negative potentials and increases steady state inactivation (Talavera et al 2004). These data substantiate our observation that M_1R stimulation and exogenous AA produce a similar, distinctive pattern of dual modulation of N-current.

Our data identifying DAGL as an important component of slow pathway inhibition complements our previous work demonstrating a similar requirement for PLA_2 activity. Previously we reported inhibition of the AA producing PLA_2 enzyme by oleyloxyethyl-phosphorylcholine (OPC) diminishes inhibition of N- current by oxo-M in SCG neurons (Liu and Rittenhouse 2003, Liu et al 2004). These data have been openly questioned as OPC did not block the slow pathway the same cells but with different experimental conditions (Gamper et al., 2004). We have endeavored to duplicate the experimental conditions in which OPC did not reduce inhibition. When the using the perforated patch technique and solutions employed by Gamper and colleagues (2004), we found that a slightly longer preincubation with OPC was required in order to observe a loss of N-current inhibition (Liu, unpublished data). Moreover, we identified a role for PLA_2 in L-current inhibition using OPC, dialyzed antibodies specific for $cPLA_2$, and neurons harvested from $cPLA_2^{-/-}$ knockout mice. Taken together these data indicate $cPLA_2$ activation is necessary for L-current inhibition.

Our data do not diminish a proposed role for PtdIns(4,5)P_2 in N-current inhibition but document a role for AA. Our experimental conditions have yielded results indicting AA is both necessary and sufficient for slow pathway modulation (Liu et al 2003; Liu et al 2004; Liu et al., 2006). Other labs have yielded results which led to the conclusion PtdIns(4,5)P_2 depletion is both necessary and sufficient for slow pathway modulation (Wu et al., 2002; Gamper et al., 2004). These data show that inhibition is not observed when PtdIns(4,5)P_2 levels are kept high by exogenous application. Likewise, sequestering of PtdIns(4,5)P_2 with antibodies or cationic peptides results in inhibition.

Recently, a model was proposed for modulation of voltage-gated potassium channels in which PtdIns(4,5)P_2 depletion and AA formation exert bidirectional control of modulation (Oliver et al., 2004). This study showed PtdIns(4,5)P_2 stops the typical fast-inactivation of K_V channels by binding to the N-terminal "ball" of the channel. AA or anandamide reverses the effect of PtdIns(4,5)P_2. The authors had determined a PtdIns(4,5)P_2 binding site on the inactivation ball domain by mutating cationic residues, and had not proven a binding site for AA or anandamide, but postulated AA interferes with PtdIns(4,5)P_2 through allosteric modification.

Two opposing modulatory effects for PtdIns(4,5)P_2 or AA on Ca_V2 channels have now been reported. Wu and colleagues (2002) reported PtdIns(4,5)P_2 sustains Ca_V2 currents and causes an activation shift to positive potentials. Our lab has reported AA inhibits currents and causes an activation shift to negative potentials (Liu and Rittenhouse 2003a, Liu et al 2001, Barrett et al 2001). There may be some conserved mechanism by which channels respond to both PtdIns(4,5)P_2 depletion and free AA. Such a mechanism would seem an evolutionary advantage. Since PtdIns(4,5)P_2 depletion and AA formation

occur simultaneously sensitivity to both effects could make the channel more responsive to M1R stimulation.

AA and PtdIns(4,5)P_2 may act on distinct sites of the calcium channel α_1 subunit and AA may interfere with a PtdIns(4,5)P_2 effect via an allosteric mechanism as proposed for Kv channels. Alternatively, AA and PtdIns(4,5)P_2 may compete at the same site. This is a distinct possibility since AA occupies the sn-2 position in PtdIns(4,5)P_2 molecules. A binding of PtdIns(4,5)P_2 to the Ca_V2 subunit may involve a binding site for the arachidnoyl moiety present in all PtdIns(4,5)P_2 molecules. If so, sufficient concentrations AA or anandamide could supplant PtdIns(4,5)P_2 at this site. Then again both PtdIns(4,5)P_2 and AA are bioactive molecules each with multiple effects, so either or both could act on the channel through another effector.

Figure 4-1. DAGLα message and protein is expressed in SCG neurons. (**a**) In situ hybridization of DAGLα in from adult rat SCG. Binding of labeled oligonucleotide shows considerable levels of DAGLα mRNA in neurons but minimal amounts in the fiber tract (FT). (**b**) A competition control as described in the methods section. Low levels of nonspecific binding are observed over the entire section when a 250-fold excess of unlabelled oligonucleotides are added to the probe during hybridization. (**c** and **d**) Immunohistochemistry of adult rat SCG with DAGLα specific antibody shows strong labeling of protein in neurons but minimal in fiber tract. Images represent duplicate experiments.

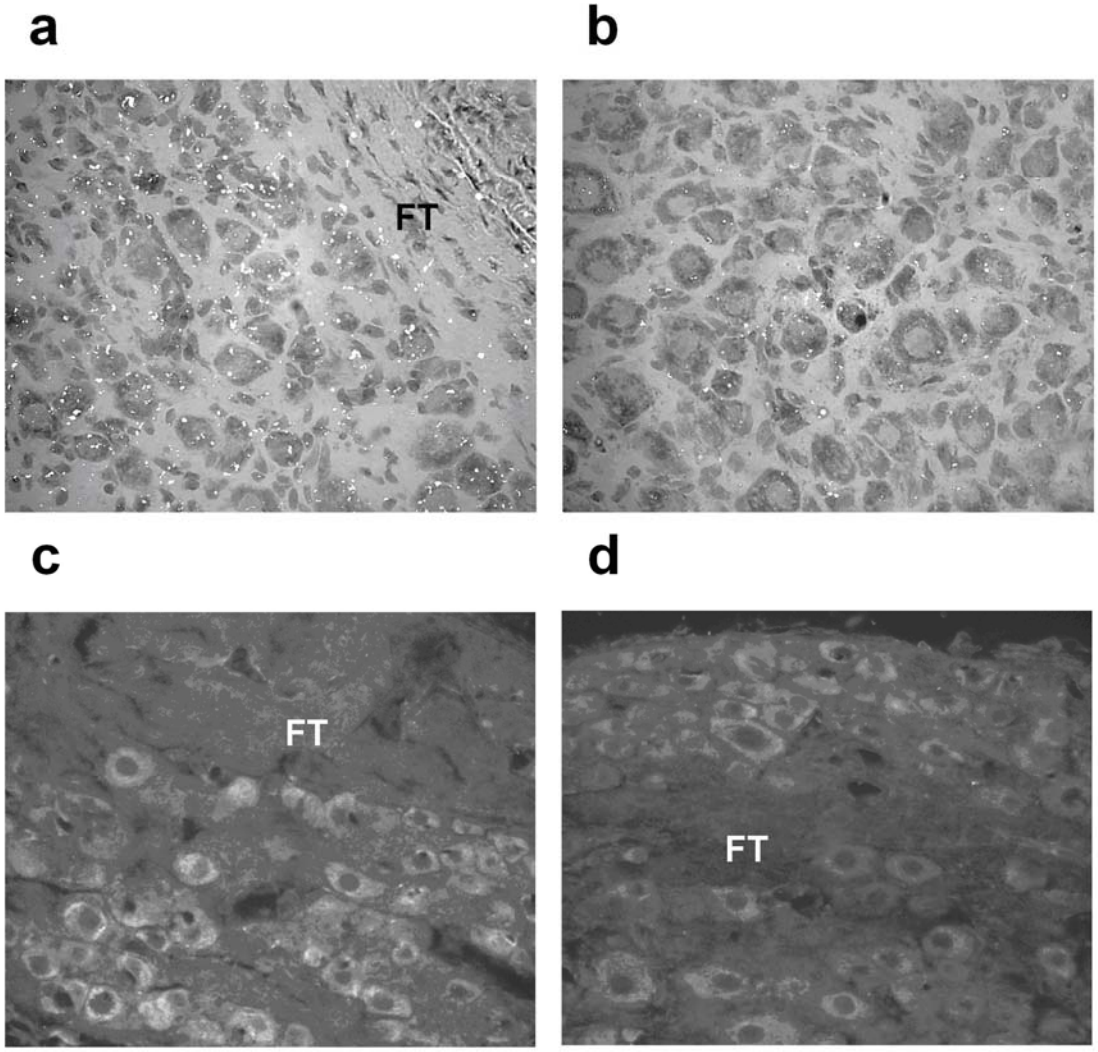
a
b
FT
c
d
FT
FT

Figure 4-2. Pharmacological strategy for dissecting DAG lipase from M_1R induced pathways of current inhibition. Muscarinic stimulation of SCG neurons by Oxo-M activates several pathways that inhibit ion channel activity. M-current inhibition results from PLC induced depletion of PtdIns(4,5)P_2 (Delmas and Brown 2005; Suh and Hille 2005) and thus should be insensitive RHC-80267 (RHC). Conversely, both L- and N-current inhibition are sensitive to AA production (Liu et al 2004; Liu et al 2006) and hypothetically may be sensitive to DAGL antagonism by RHC. Inhibition of L- or N-current should be restored with exogenous AA in the presence of RHC. The L-channel agonist FPL 64176 (FPL) elicits long lasting tail currents consisting L-current thus highlighting L-current modulation and the L-channel antagonist nimodipine (NMN) diminishes L-current thus allowing observation of N-current modulation. Pertusis toxin (PTX) blocks a second pathway of N-current inhibition mediated by M_2Rs or M_4Rs.

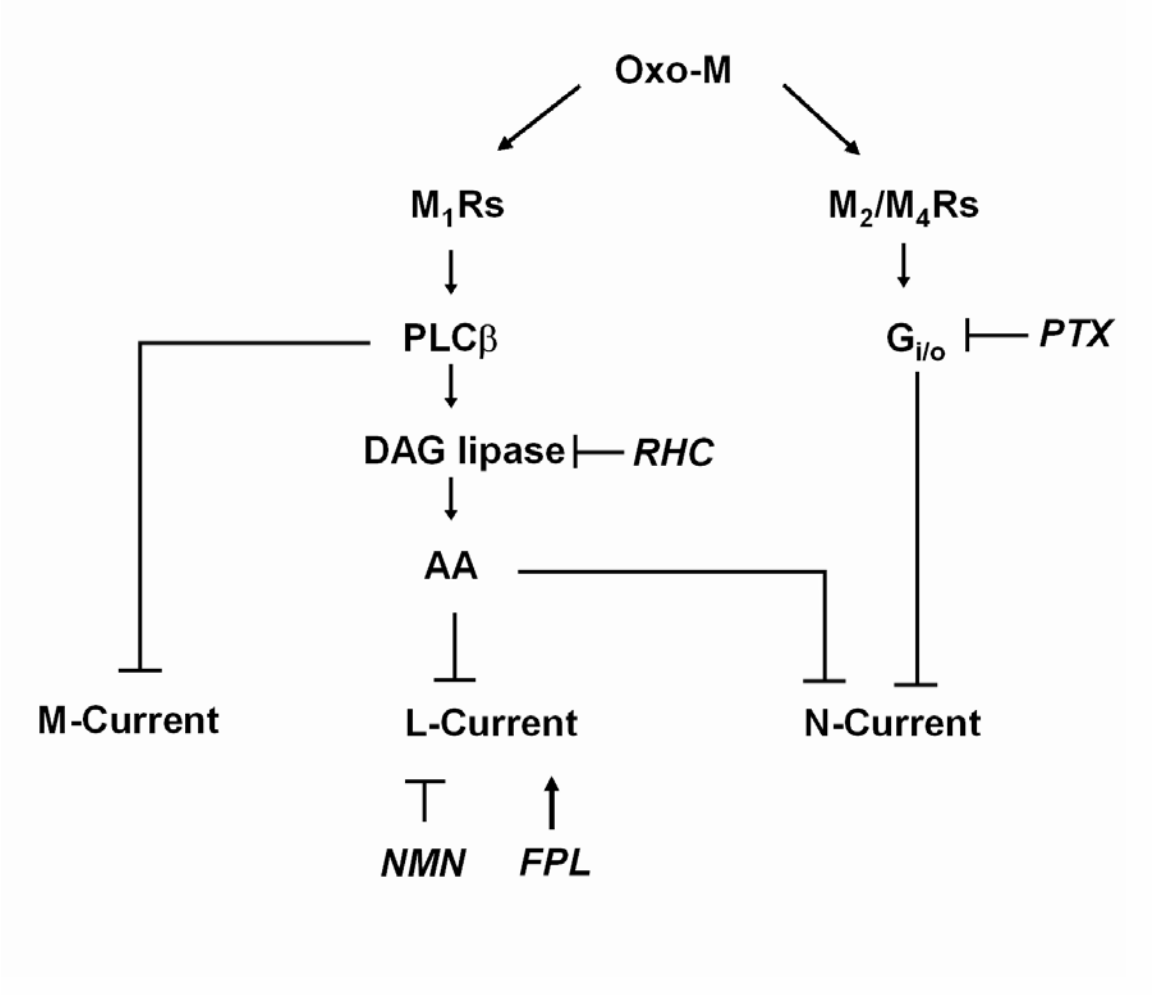
Oxo-M
M1Rs
M2/M4Rs
PLCβ
Gi/o
PTX
DAG lipase
RHC
AA
M-Current
L-Current
N-Current
NMN
FPL

Figure 4-3. M-Current inhibition by Oxo-M is unaffected by RHC. M-current was measured in neonatal SCG neurons as previously described (Brown and Adams 1980). (**a**) Time course of current measured 400 ms after repolarization shows two applications of 10 μM Oxo-M. (b) Representative sweeps just prior to Oxo-M application (—), 1 minute after Oxo-M (—) and 3 minutes after washing of Oxo-M (—). (**b**) RHC did not block inhibition of M-current. Time course and representative sweeps as described for **a**. (**c**). Summary of recordings comparing % inhibition of current occurring 1 minute after Oxo-M application in absence (n = 4) and presence (n = 4) of RHC (p=0.6).

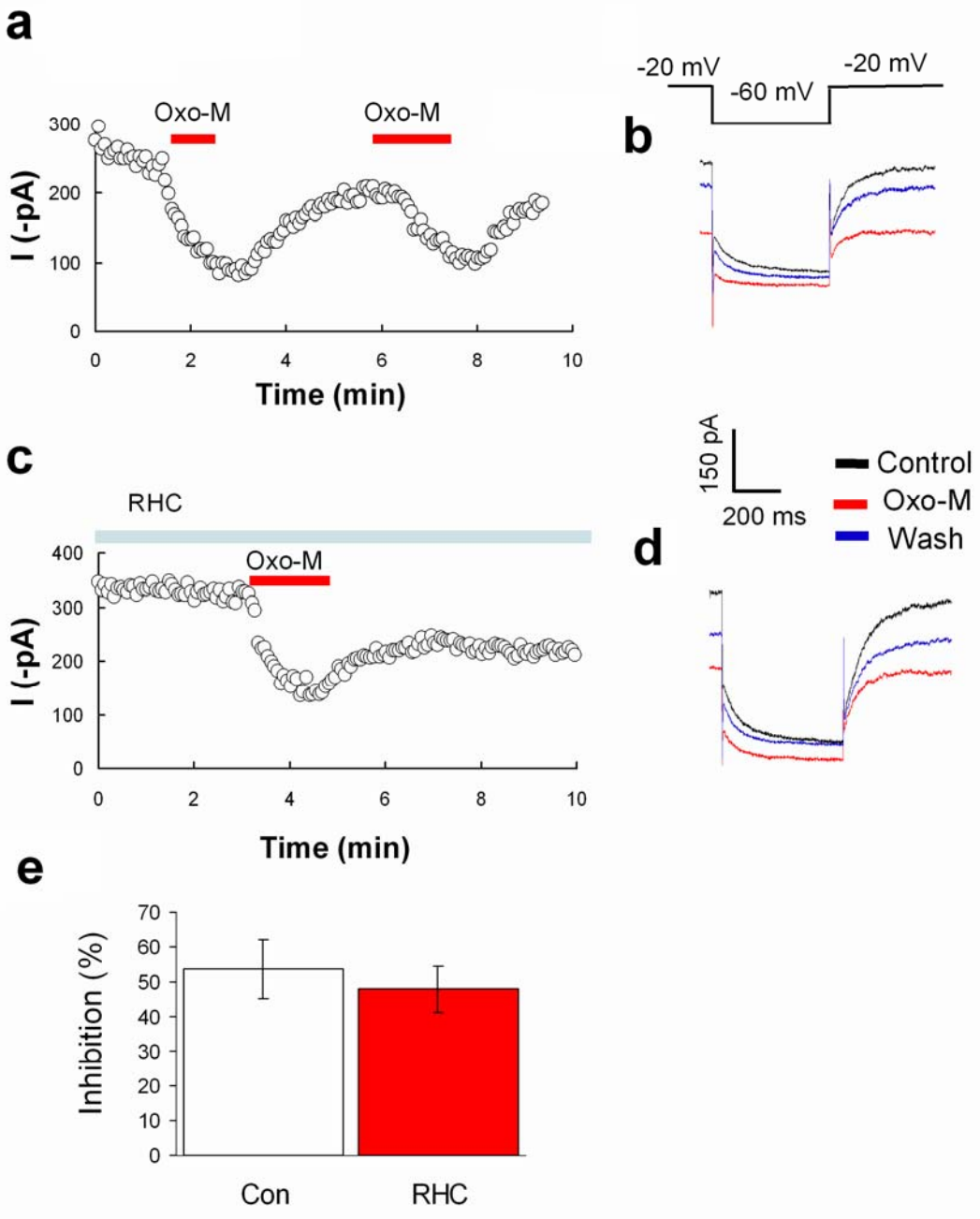
a
Oxo-M
Oxo-M
I (-pA)
Time (min)
b
-20 mV
-60 mV
-20 mV
150 pA
200 ms
Control
Oxo-M
Wash
c
RHC
Oxo-M
I (-pA)
Time (min)
d
e
Inhibition (%)
Con
RHC

Figure 4-4. RHC blocks Oxo-M inhibition of the whole-cell current. Neonatal SCG neurons were pretreated with PTX for 5 hours to eliminate the fast pathway. (**a**) Representative time course of whole cell Ba^{2+} does not show significant inhibition during application of Oxo-M (10 μM) in the presence of RHC. (**b**) Representative sweeps taken prior to Oxo-M (—), 3 min after Oxo-M (—) and 1 min after washout (—). (**c**) Average IV data from PTX-treated SCG neurons. RHC blocks inhibition at positive potentials. At -10 mV a slight enhancement remains although not statistically significant (p=0.08), n=5.

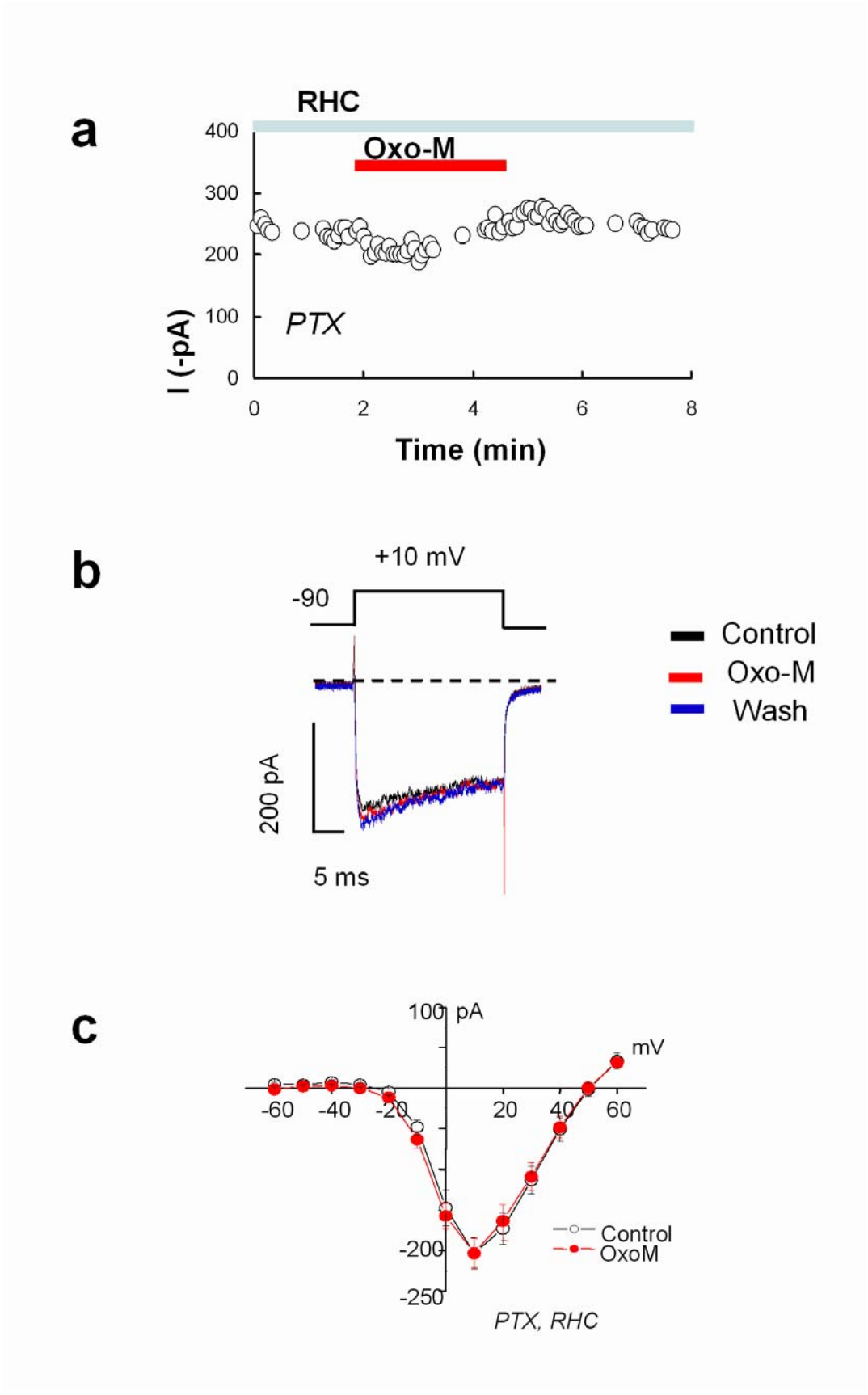
a
RHC
Oxo-M
PTX
I (-pA)
Time (min)
b
+10 mV
-90
200 pA
5 ms
Control
Oxo-M
Wash
c
100 pA
mV
Control
OxoM
PTX, RHC

Figure 4-5. RHC attenuates Oxo-M inhibition of whole-cell L-type current. (**a**) Representative time course showing bath application of 25μM RHC blocks Oxo-M inhibition of tail currents in FPL treated SCG neurons, which is entirely made of L-type Ca2+ current. Conversely, Oxo-M still inhibits the peak current, due to membrane delimited inhibition of N-current. (**b**) Voltage protocol used to measure peak and tail currents with representative sweeps, from a holding potential of –90 mV the voltage is stepped to +10 mV for 20 milliseconds and then back to -40 mV. Peak current amplitudes were measured 15 ms after the start of the test pulse (C1). The long-lasting component of the tail current was measured approximately 13 ms following the test pulse (C2). The long-lasting component of the control tail current (in the absence of the L-type Ca2+ channel agonist) typically measured approximately ~5 pA in amplitude. (**c**) Summary of the effects of Oxo-M on the currents in the absence of or in presence of RHC. N=4~5 recordings. *P<0.05

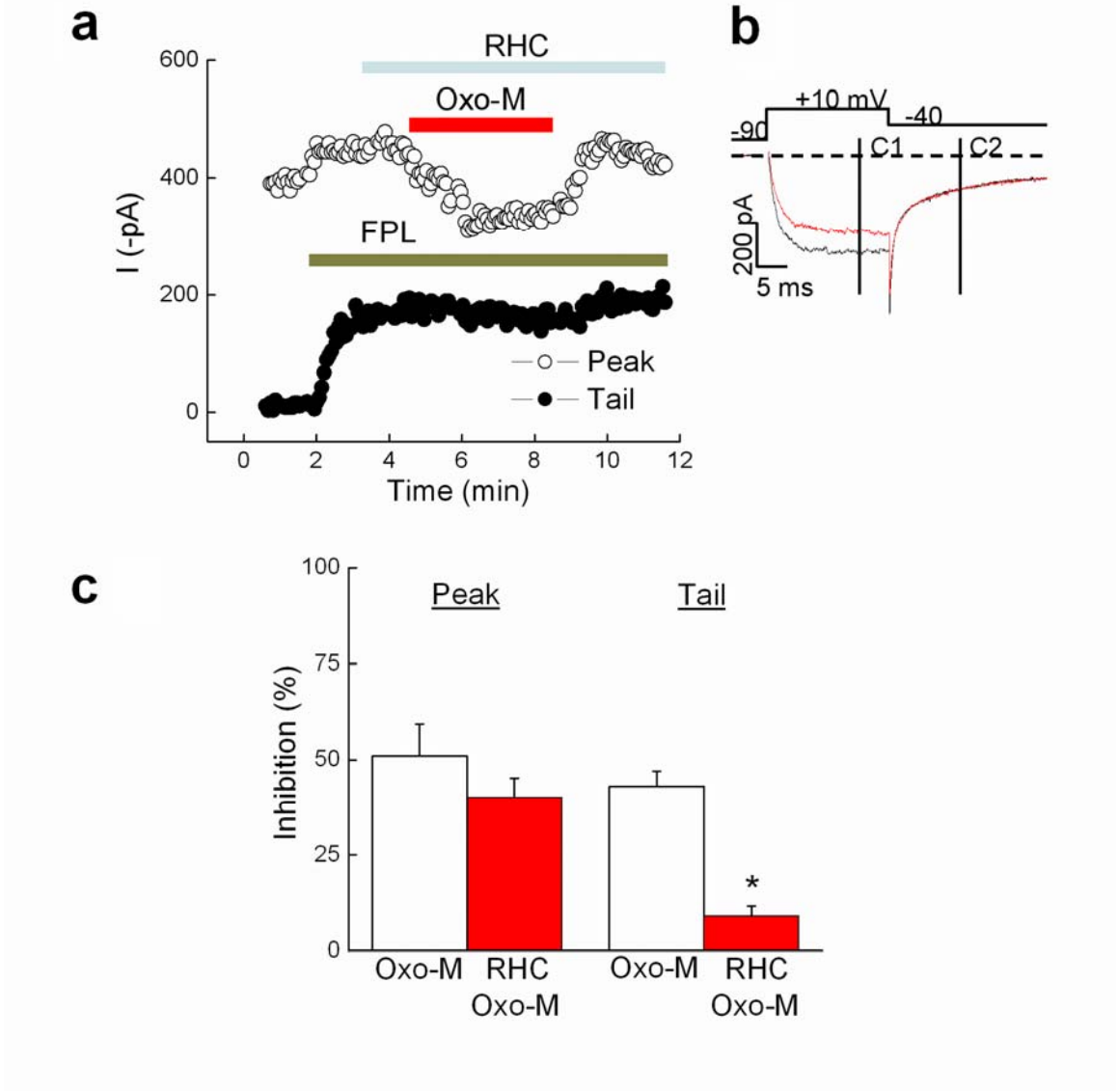
a
RHC
Oxo-M
FPL
I (-pA)
600
400
200
0
0
2
4
6
8
10
12
Time (min)
Peak
Tail
b
+10 mV
-40
-90
C1
C2
200 pA
5 ms
c
Peak
Tail
Inhibition (%)
100
75
50
25
0
Oxo-M
RHC
Oxo-M
Oxo-M
RHC
Oxo-M
*

Figure 4-6. RHC does not interfere with Inhibition of AA on whole-cell current. (**a**) Representative time course shows bath application of 25μM does not affect inhibition of peak current or the long-lasting component of the tail current by 5 μM AA on SCG neurons. (**b**) Summary of the effects of AA on the currents in the absence of or in presence of RHC. N=3~5 recordings.

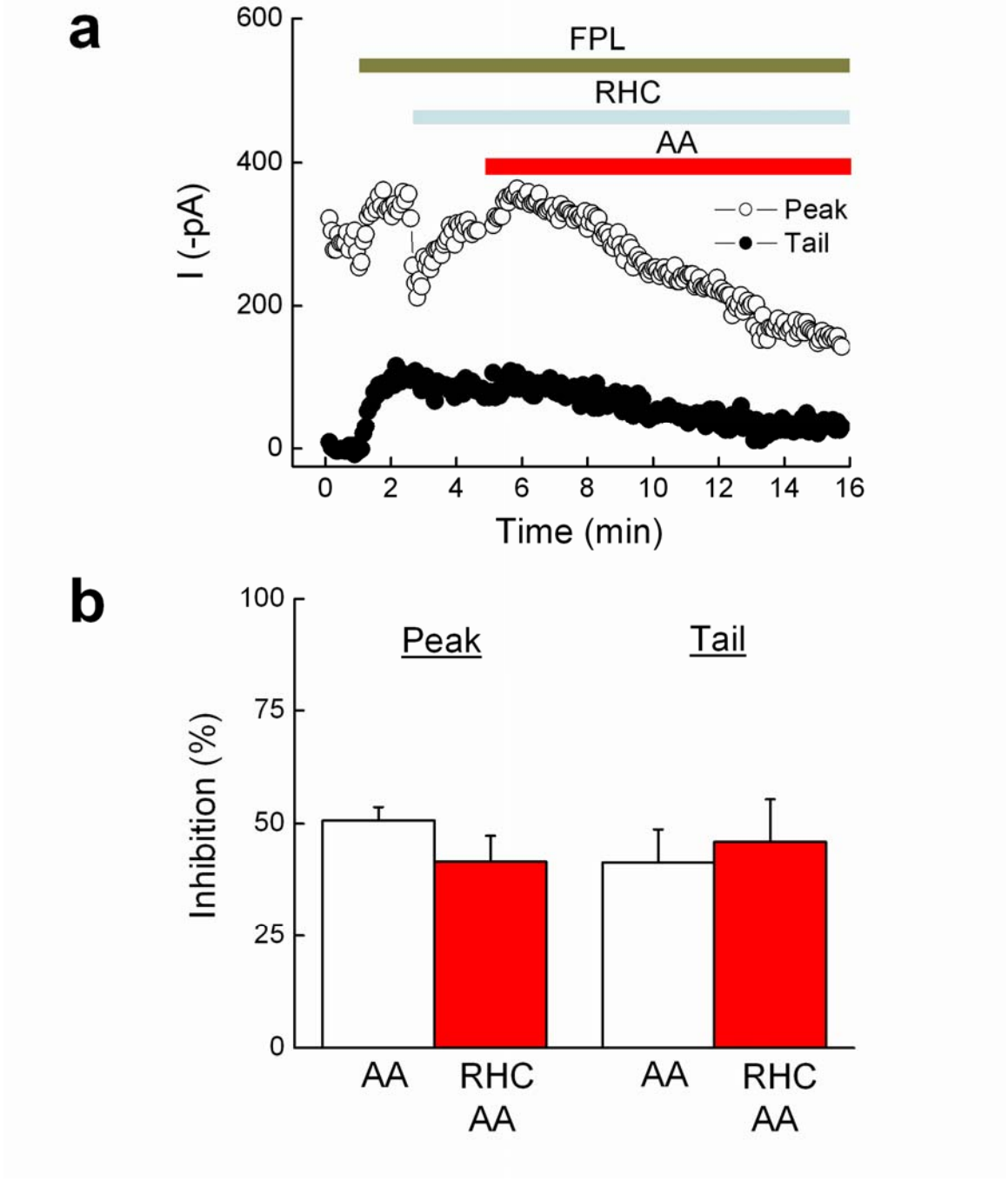
a
600
400
200
0
I (-pA)
FPL
RHC
AA
Peak
Tail
0
2
4
6
8
10
12
14
16
Time (min)
b
100
75
50
25
0
Inhibition (%)
Peak
Tail
AA
RHC
AA
AA
RHC
AA

Figure 4-5. RHC Does not block the inhibition of whole-cell N- current by AA. (**a**) Bath application of RHC (25 μM) did not interrupt the effect of AA (5 μM) on N-type current in PTX-treated neonatal rat SCG neurons. Recordings were performed in the presence of 1 μM NMN to block L-current (**b**) Summary of the effects of AA (5 μM) on the currents in presence of RHC in the bath solution. n=5 recordings. *$p \leq 0.05$

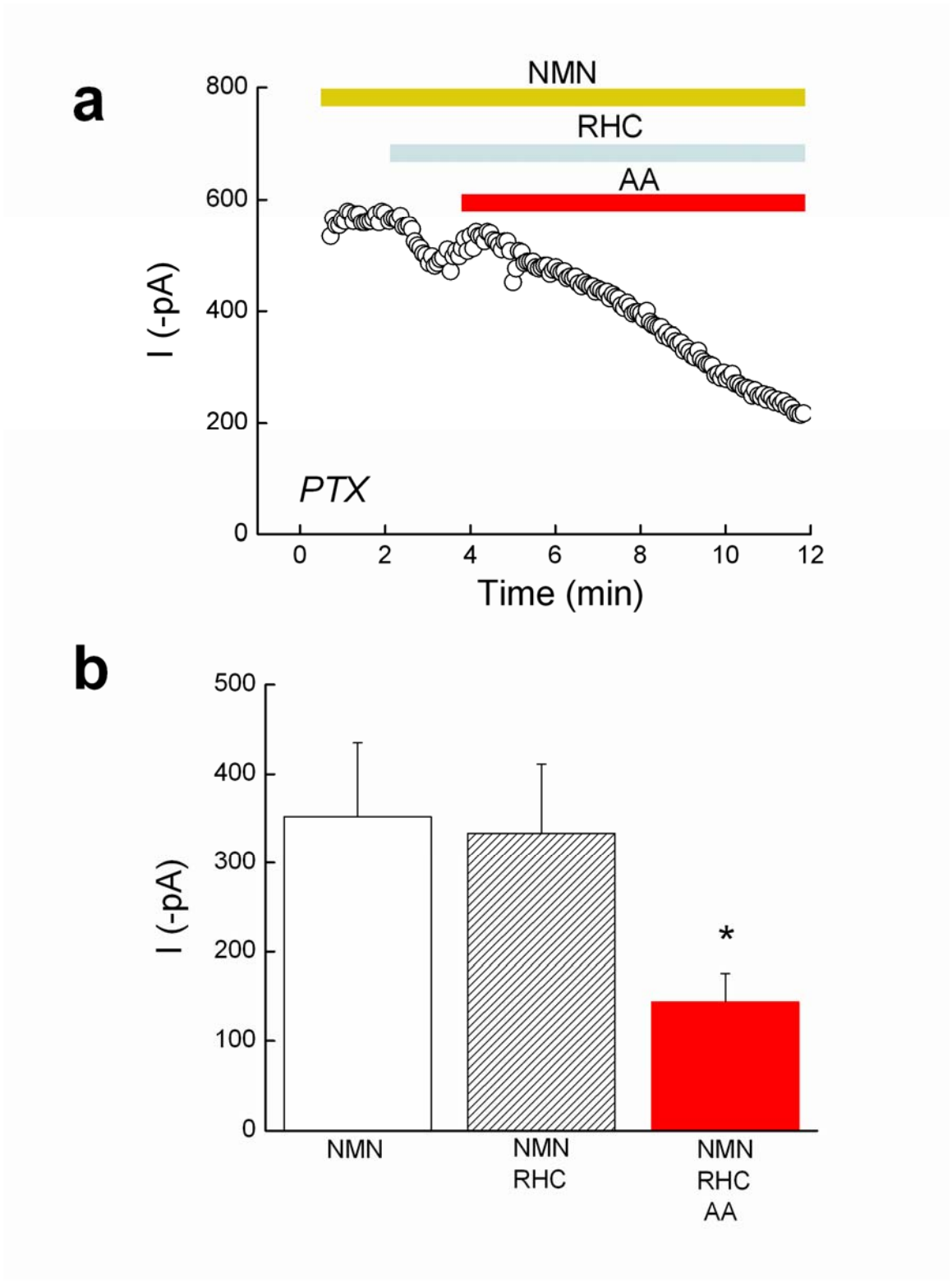
a
NMN
RHC
AA
800
600
400
200
0
I (-pA)
PTX
0
2
4
6
8
10
12
Time (min)
b
500
400
300
200
100
0
I (-pA)
*
NMN
NMN
RHC
NMN
RHC
AA

Figure 4-8. RHC blocks Oxo-M inhibition of N-type current in recombinant cells. HEK cells with a stably transfected M1 receptor (HEK-M1) were transiently transfected with N-channel subunits Cav2.2e, α2δ and Cav β3. Currents were recorded using 5 mM Ba^{2+} as the charge carrier. (**a**) time course of peak current before, during and after application of 10 μM Oxo-M shows transient inhibition followed by stable inhibition. (**b**) representative sweeps just prior to Oxo-M application (—), 3 minutes after oxo-M (—) and 1 minute after washing of oxo-M (—). RHC blocks stable inhibition in recombinant cells. (**c**) Time course and (**d**) representative sweeps as described above (**e**) Summary of recordings comparing % inhibition of current occurring 3 minute after Oxo-M application in absence (n=9) and presence (n=6) of RHC $^{**}p<0.005$.

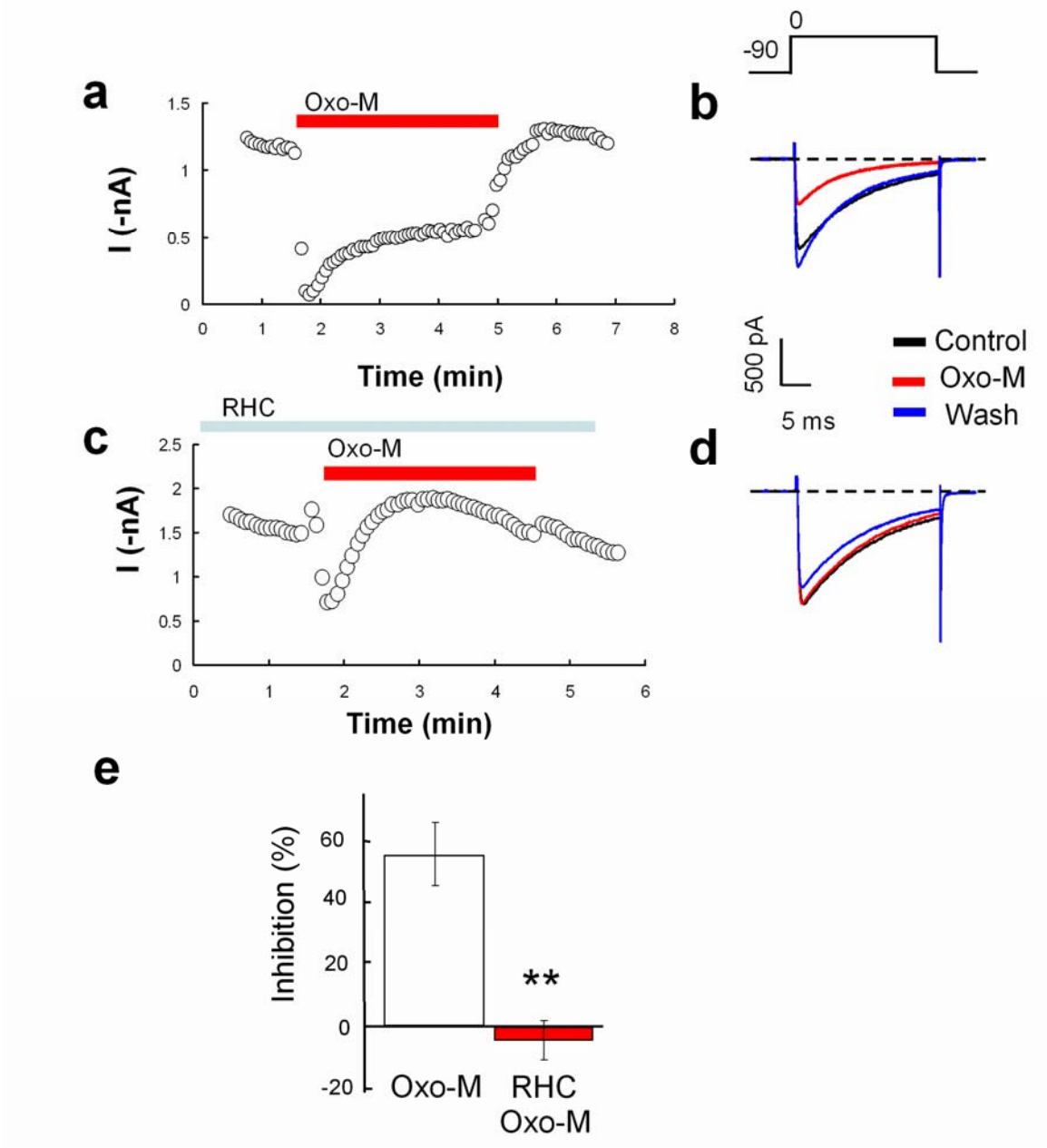
a
Oxo-M
I (-nA)
Time (min)
b
0
-90
500 pA
5 ms
Control
Oxo-M
Wash
c
RHC
Oxo-M
I (-nA)
Time (min)
d
e
Inhibition (%)
**
Oxo-M
RHC
Oxo-M

CHAPTER V

M_1 Muscarinic Stimulation Blocks Fast Pathway Inhibition of N- Current

Abstract

Direct binding of the Gβγ subunit of G-proteins to the α_1 subunit of the N-type calcium channels ($Ca_V2.2$) inhibits their activity. During basal conditions Gβγ complexes bind to a portion of N-channels giving rise to tonic inhibition. Gβγ binding to $Ca_V2,2$ increases with stimulation of particular G-protein coupled receptors (GPCRs). This classical signaling cascade was originally referred to as membrane-delimited or voltage-dependent inhibition, but is now more commonly known as the fast pathway. Phosphorylation of $Ca_V2.2$ by protein kinase C (PKC) antagonizes Gβγ binding, thus reversing inhibition. Evidence for the role of PKC in current modulation has relied on phorbol esters to stimulate PKC. Comparable effects using neurotransmitters (NTs), predicted to activate PKC, have been elusive. M_1 muscarinic receptors (M_1Rs) activate PKC through a signaling pathway reliant on phospholipase C (PLC). However, the activation of PLC by M_1Rs has multiple downstream effects, some of which may obscure the N-current modulation by PKC. Specifically, activation of PLC participates in a diffusible second messenger pathway, also called the slow pathway that inhibits N-current. Our lab found that bath application of either the specific DAG lipase inhibitor RHC-80267 (RHC), or the phospholipase A_2 (PLA_2) inhibitor oleoyloxyethyl phosphocholine (OPC) minimizes inhibition of N-current by the slow pathway. Both of these agents act by limiting the release of arachidonic acid (AA). Since neither RHC nor OPC is reported to inhibit PLC activity, I hypothesized either these agents could be used to block inhibition by M_1Rs leaving PKC activation intact. An attenuation of fast pathway could be used as an indication of PKC phosphorylation. When this pharmacological strategy is employed in freshly dissociated neurons, M_1R stimulation blocks inhibition normally elicited by the

membrane-delimited/fast pathway. These data are consistent with activation of PKC and subsequent phosphorylation of the N-channel.

Introduction

Calcium influx through N-type calcium channels (N-channels; $Ca_V2.2$) affects numerous neuronal functions including synaptic transmission (Hirning et al., 1988; Takahashi and Momiyama, 1993; Turner et al., 1993), regulation of neuronal excitability (Wisgirda and Dryer, 1992), control of intracellular biochemical processes, including enzyme activation (Rittenhouse and Zigmond, 1999) and gene transcription (Brosenitsch and Katz, 2001; West et al., 2002). The modulation of $Ca_V2.2$ activity by signaling cascades initiated by G-protein coupled receptors (GPCRs) is a key mechanism for fine tuning calcium influx (Elmslie 2003).

N-channels are sensitive to inhibition via a signaling pathway now commonly referred to as the fast pathway, but also known as the membrane delimited pathway. This type of inhibition is characterized by direct binding of β and γ subunits of G-proteins to the $Ca_V2.2$ subunit (Herlitze et al., 1996; Ikeda, 1996). Under basal conditions a certain percentage of β and γ subunits of trimeric G-proteins bind to N-channels giving rise to what is known as tonic inhibition. Prolonged depolarization relieves the inhibition as does challenging inhibition with a strong prepulse (Bean, 1989; Elmslie et al., 1990). Repetitive neuronal activity also reverses Gβγ inhibition of N-current, which may underlie short term plasticity (Brody et al., 1997; Brody and Yue, 2000).

Pretreatment of neurons with protein kinase C (PKC) activating phorbol esters prevents fast pathway inhibition (Swartz, et al., 1993; Swartz, 1993). The phosphorylation of $Ca_V2.2$ by PKC at a region called the I-II linker appears to be the key molecular event in blocking membrane-delimited inhibition (Zamponi et al., 1997; DeWaard et al 1997, Hamid et al 1999). Although it is has been studied extensively,

evidence of a role for PKC in N-current modulation has relied on phorbol esters to stimulate PKC. Release of DAG typically activates PKC, which occurs when $PtdInsP_2$ is hydrolyzed by phospholipase C (PLC). Activation of PLC has multiple downstream effects, which may obscure N-current modulation by PKC. Specifically, activation of PLC induces a diffusible second messenger that causes current inhibition.

M_1 muscarinic receptors (M_1Rs) stimulate PKC (Caulfield and Birdsall 1998). Moreover M_1 stimulation increases synaptic release by a mechanism reliant on PKC (Costa et al 1993). Therefore, I examined the possibility that M_1Rs modulate N-channels by activating PKC. Here I report that M_1R stimulation blocks N-current inhibition normally elicited by norepinepherine. Moreover, the block of inhibition is consistent with activation of PKC.

Results

Fast pathway inhibition by muscarinic receptors is transient in SCG neurons

The working hypothesis for this work is that M_1 stimulation of SCG neurons activates PKC, which subsequently phosphorylates N-channels. Recently our lab has found bath application of either the specific diacylglycerol (DAG) lipase inhibitor RHC-80267 (RHC), or the (PLA_2) inhibitor oleoyloxyethyl phosphocholine (OPC) minimizes inhibition of current by the diffusible second messenger pathway (Liu and Rittenhouse 2003a; Liu et al 2004; Chapter IV). I hypothesized that by using this pharmacology I could block N-current inhibition by the diffusible second messenger during PLC stimulation revealing the effects of PKC on channel activity.

N-channel phosphorylation should enhance current but normally inhibition of the slow pathway overshadows potentiation of N-current. PKC stimulation could be observed if slow pathway inhibition was blocked downstream of PtdIns(4,5)P_2 hydrolysis and DAG release. Since muscarinic stimulation of SCG neurons activates both slow and fast pathways of inhibition (Mathie et al., 1992), I first tried to use the muscarinic agonist oxotremoreine–methiodone (oxo-M) for both the stimulation of membrane-delimited inhibition and the activation of PKC (**Fig 5-1a**). I hypothesized inhibition elicited by M_2 and M_4 receptors would diminish as PKC, activated by M_1 receptors, phosphorylated the channel, and thus displaced Gβγ subunits. With the slow pathway blocked by OPC, the activation of PKC would be observed as recovery of current.

In freshly dissociated SCG neurons, whole-cell current was measured every 4sec by stepping to +10 mV for 100 msec from a holding potential of -90 mV. I found bath application of oxo-M (10 μM) elicits rapid inhibition marked by a change in whole-cell

kinetics to slowed activation, which diminishes over the course of several minutes with continued exposure to oxo-M (**Fig 5 1 b,c**). Both the rapid inhibition and slowed activation kinetics are indicative of membrane-delimited inhibition and the recovery of current amplitude and activation kinetics are both indicative of a dissociation of Gβγ from Cav2.2 (Barrett and Rittenhouse 2000). Thus, these two effects could be interpreted as an indication of M_1 stimulation of PKC. Exposure to oxo-M for 30 seconds inhibited the current 30.8 ± 7.5% (n = 5), but after 3 minutes the current was inhibited by 0.64 ± 18% vs. control.

To determine whether the recovery of current was due to M_1 stimulation, dissociated SCG neurons were preincubated with the potent and selective M_1 inhibitor MT-7 (100 nM) for at least an hour at 37°C. This toxin binds to and irreversibly blocks M_1Rs (Adem and Karlsson 1997). In the presence of MT-7, current inhibition by the fast pathway still reversed over the course of several minutes (**Fig 5-2 a, b**). Current was inhibited after 30 seconds by 47.1 ± 9.1% (n = 3), but by three minutes inhibition vs. control had diminished to 2.2 ± 4.8%.

These findings suggested that the reversal of inhibition occurred independently of M_1R signaling. In a separate control experiment I repeated the experiment with OPC to block slow pathway inhibition and the PKC inhibitor bisindolylmaleimide HCl I (BLM; 100 nM) present in the bath. Under these conditions, Oxo-M inhibited whole-cell current by 31.6 ± 9.8% (n = 5) after a 30 second exposure but after three minutes currents returned to control levels (-1.6 ± 9.5%). Since the inhibited current recovered seemingly without stimulation of PKC or M_1Rs, I concluded the original observation of transient N-current inhibition was due to a mechanism such as receptor desensitization. M_2Rs are

known to desensitize in a time frame of seconds to minutes (Hosey et al 1995). Therefore, I had to reassess the pharmacological strategy for maintaining fast pathway inhibition of N-current.

Norepinepherine elicits a steady inhibition of current via the fast pathway

I next sought a neurotransmitter or agonist that could elicit stable inhibition over the course of several minutes, so that changes in inhibition could be attributable to a downstream effect of M_1Rs. In SCG neurons norepinepherine (NE) binds to α_2 adrenergic receptors, stimulating membrane-delimited inhibition of N-current but not slow pathway inhibition (Mathie et al 1992). Since membrane-delimited inhibition is voltage dependent, I used a prepulse protocol to examine N-current inhibition apart from rundown. The prepulse protocol (Elmslie et al., 1990) utilizes a strong depolarizing step to +80 mV (100 msec); a brief return to -90 mV (5 msec); followed by a test pulse to +10 mV. The strong depolarizing step reverses inhibition elicited by membrane-delimited inhibition (Elmslie et al., 1990). Currents elicited after the depolarization are referred to as "facilitated". Whole-cell current was measured every 4 sec at +10 mV from a holding potential of -90 mV. The prepulse protocol was used for every other measurement so as to alternate between facilitated and unfacilitated whole-cell current measurements. The representative time course shown in (**Fig 5-2 a,b**) is typical with application of NE. NE (10 μM) caused both a large voltage-dependent and small voltage-independent inhibition; however voltage-independent inhibition was transient while voltage-dependent inhibition was stable for several minutes. The stable inhibition by NE indicated a continuous association of Gβγ with the channel. Thus changes in NE induced inhibition could be

interpreted as a dissociation of Gβγ from the channel presumably due to PKC activation. We previously showed that the M_2R antagonist methoctramine (METH) blocks M_2Rs thereby eliminating fast pathway inhibition by oxo-M in SCG neurons (Liu and Rittenhouse 2003a). Thus hypothetically, oxo-M could be used to stimulate M_1Rs without causing membrane-delimited inhibition and if the downstream effects of M_1Rs that cause further inhibition were blocked, PKC stimulation should be unaffected (**Fig. 5-2 c**).

PKC stimulation elicited with the phorbol ester phorbol 12-myristate 13-acetate (PMA) is reported to block inhibition by NE (Swartz, 1993). Therefore, PMA was used to stimulate PKC effect with which the oxo-M effect could be compared. Application of NE (10 μM) caused a strong voltage-dependent inhibition as previously described (Kammermeier et al 2000) but also a slight voltage independent inhibition (**Fig. 5-4 a**). As shown the application of NE before PMA (500 nM) elicited a large voltage-dependent inhibition but a five minute exposure to PMA blocked any facilitation of current by a prepulse (**Fig. 5-4 a**). These data agree with previous studies that PKC activation and prepulse facilitation are equivalent in reversing membrane-delimited inhibition (Barrett and Rittenhouse 2000).

Since membrane-delimited inhibition is voltage-sensitive, prepulse facilitation was used as a determination of Gβγ binding. Facilitation is the percent increase in current which occurs after the +80 mV depolarization (see methods). During the first application of NE prepulse facilitation was 103 ± 31 % (n = 4). A five minute exposure to PMA reduced the prepulse facilitation to 26 ± 14 % (**Fig. 5-4 c**). Changes in kinetics were determined by measuring the time to peak current during the 100 millisecond test pulse.

Membrane delimited inhibition causes slow activation of current, thus the time to peak is delayed. Conversely, relief of inhibition, either by a strong depolarization or by PKC phosphorylation, decreases the time to peak. During NE, the time to peak was 65 ± 10 ms (n = 4). After a five minute exposure to PMA and the time to peak elicited by NE was 17 ± 6 ms. (**Fig. 5-4 d**).

Oxo-M blocks inhibition by NE

To stimulate PKC via M_1Rs, I tried different concentrations of oxo-M in conjunction with METH (100 nM) and either OPC (10 μM) or RHC (20 μM). 10 μM oxo-M had been previously shown to be sufficient to elicit both fast and slow pathway inhibition in SCG neurons (Liu and Rittenhouse 2003a). However this concentration of oxo-M did not block the inhibition of NE (**Fig. 5-5 a,b**). Therefore the concentration of oxo-M was increased. Previously Liwang in our lab reported 30 μM oxo-M is necessary to elicit maximal inhibition of N-current via the slow pathway (Liu and Rittenhouse 2003b). Since the slow pathway and PKC activation are both hypothetically downstream of M_1Rs 30 μM oxo-M might also be necessary to elicit PKC activation. Accordingly, a three minute exposure to oxo-M (30 μM) dramatically blocked inhibition by NE **(Fig. 5-5 c,d)**. As shown in the representative time course in (**Fig. 5-5 c**), there was a brief spike of inhibition which subsided. This brief spike of inhibition may not be the result of Gβγ inhibition. In the previous experiments with NE and prepulses NE elicited a small voltage-independent inhibition (see **Fig. 5-4 a** and **Fig 5-3 a**)**.** The voltage–independent inhibition has been ascribed to incomplete dissociation of Gβγ by the strong depolarization (Kammermeier, et al 2000). However I found the voltage-independent

and voltage-dependent inhibition caused by NE to be fundamentally different. First, the voltage-independent inhibition was transient over the course of a few minutes. Second, after a five minute exposure to PMA the voltage-dependent inhibition was lost, but the voltage-independent inhibition recurred (**Fig. 5-3 a**) Therefore it appears under the recording conditions NE elicits two types of inhibition. To avoid spurious effects of inhibition not due to Gβγ, inhibition of current was measured 25 seconds after application of NE. Following a three minute exposure to oxo-M (30 μM) in the presence of RHC (20 μM) and METH (100 nM), NE (10 μM) elicited an inhibition of 8.4 ± 4.4 % (n = 5).

To ensure the block of inhibition was not due to non-specific effects of the combination of RHC and METH two separate control experiments were run. First, the inhibition of current by NE (10 μM) was measured when RHC (20 μM) and METH (100 nM) were in the bath but no oxo-M exposure. Under these conditions NE inhibited current 39 ± 4.3 % (n = 8). Second, the inhibition by NE (10 μM) was measured without any of other aforementioned drugs. Under these conditions NE inhibited current 32 ± 2.8 % (n = 30). Inhibition by NE after 30 μM oxo-M was significantly different from either control condition ($p < 0.001$).

To see if the kinetic changes were blocked by oxo-M the time to peak was determined for each of the conditions described above. Under control conditions with out any other drugs in the bath NE causes the time to peak to shift on average to 76 ± 4.2 msec (n = 30), whereas in the experimental conditions using oxo-M the time to peak was 26 ± 4.5 msec (n = 5) a significant change ($p < 0.001$). However, after exposure to RHC and METH, without oxo-M the time to peak was variable, so that the average was 47 ± 10 msec (n = 8). These data suggest the kinetic and amplitude changes may be separable

effects, the kinetic changes being somewhat sensitive to the presence of RHC and METH. Pretreatment with oxo-M elicited a consistent block of the slowed activation, coupled with the dramatic block of inhibition suggested that PKC had been stimulated.

Having established a concentration of oxo-M which mimicked PKC activation experiments were set up with the prepulse protocol similar to the ones described earlier to test activation of PKC by PMA. Breifly, during whole cell recordings from SCG neurons, NE (10 μM) was applied to before and after a three minute exposure to 30 μM oxo-M. RHC (20 μM) and METH (100 nM) were present in the bath solutions during the entire experiment (**Fig.5-6 a**).

As before Gβγ inhibition was indicated by increased facilitation and the time to peak shifted toward the end of the 100 msec pulse. These parameters were calculated for cells exposed to NE before and after oxo-M. The prepulse facilitation caused by NE was reduced from 91 ± 16 % before oxo-M to 47 ± 24 % (n = 6). Also the time to peak during NE stimulation was shortened from 56 ± 9.7 msec to 24 ± 9.3 msec. These data further suggested an activation of PKC.

PKC inhibitors do not stop loss of NE modulation

To show the loss of NE induced inhibition was truly due to PKC activation, the next step was to repeat the experiment and block the effect with PKC inhibitors. First a pharmacological strategy was tried. In our lab, BLM had been used successfully to block PKC activation of PMA (Barrett and Rittenhouse 2000). For those reported experiments BLM (100 nM) had been dissolved in dimethyl sulfoxide (DMSO). DMSO because it has non-specific effects, and there was some evidence that DMSO interferes with M_1Rs

in our cell prep and recording conditions (comm. Liwang Liu). Therefore the water-soluble, hydrochloride salt of BLM was used in an attempt to block the PKC effect. The same protocol as before with prepulses, two separate applications of NE (10 μM) separated by an application of oxo-M (30 μM), was used in conjunction with RHC (20 μM), METH (100 nM) and with the addition of BLM (100 nM; **Fig 5-7 a**). Under these conditions during the first application of NE the facilitation was 148 ± 14 % after a three minute application of oxo-M facilitation was 58 ± 7 % (n=4; **Fig 5-7 b**). The time to peak during the first application of NE was 84 ± 3.3 msec, and 38 ± 10 msec during the second application of NE (**Fig 5-7 c**). These data did not indicate addition of BLM blocked the apparent PKC effect.

The experiment in which 30 μM but not 10 μM oxo-M blocked NE effects indicated there was a specific effect of oxo-M, but paired compared comparisons on the same cell requires holding cells much longer. Also, the water soluble form of BLM had not been characterized in our lab. Therefore several possibilities arose that could explain why there was not a loss of NE induced modulation. First holding a cell in the whole-cell configuration for extended periods of time could result in dialysis of factors necessary for inhibition by NE. Second, a longer exposure to the pharmacological agents could possibly cause non-specific effects. Third, it was possible that the water-soluble form of BLM required was not as effective as the hydrophobic form used earlier and thus higher concentrations of the inhibitor could be necessary. Experiments were set up to determine which if any of these effects contributed to the loss of NE induced modulation.

First, to determine if prolonged whole-cell recordings were dialyzing essential factors out of the cell, paired applications of NE separated by a three minute wash with

bath solution without any drug were compared. There were no significant differences between the two applications of NE (data not shown). Therefore, the loss of NE effect was not caused by dialysis of some factor out of the neuron during the whole-cell measurement. Next, a similar experiment was conducted examining the effect of two applications of NE separated by a three minute wash, with METH and RHC in the bath during the entire recording. Under these conditions prepulse facilitation during NE application was significantly reduced. These data indicate prolonged exposure to METH and RHC might also induce some PKC activity. A long exposure to RHC might inhibit basal activity of DAG lipase, increase DAG concentrations and thereby activate PKC if given a sufficient period of time. If the loss of NE induced modulation was due to PKC activation by prolonged exposure to RHC or a shorter exposure to oxo-M then either effect should be blocked by a sufficiently effective PKC inhibitor.

Therefore, the concentration of BLM was increased and retested for its capacity to block PKC activity induced by PMA. 500 nM BLM was included in both the bath and pipette solutions. The IC_{50} for BLM is reported to be 3-70 nM (Toullec et al 1991). In control conditions facilitation of current induced by NE (10 μM) was 87 ± 12 %, but after a five minute exposure to PMA, facilitation of current induced by NE diminished to 14 ± 5.3 % (n=12). When BLM (500 nM) was included in the solutions initial facilitation during NE was 86 ± 19 %, and after PMA exposure the facilitation during NE was 56 ± 13 % (n = 7; **Fig 5-8 a**). The kinetic shift was also affected. Under control conditions the time to peak elicited by NE went from 73 ± 8.2 msec to 7.9 ± 0.7 msec before and after PMA. With BLM on board the time to peak went from 61 ± 13 msec to 39 ± 13 msec

(**Fig 5-8 b**). These data indicate the presence of 500 nM BLM (approximately ten times the IC_{50}) greatly attenuates but does not eliminate PMA's capacity to block effects of NE.

Inhibition of PKCε attenuates PKC effect

Since BLM did not completely block the apparent effect of PKC other inhibitors of PKC were sought. It is reported that PKCε is bound to the carboxy-terminus of $Ca_V2.2$ (Maeno-Hikichi et al., 2003). Moreover, PKC modulation of whole-cell calcium currents in hippocampal neurons is completely disrupted by dialysis of 10 μM PKCε translocation inhibiting peptide (PKCε-TIP). Therefore, whole cell currents from SCG neurons were measured with 10 μM PKCε-TIP in the pipette using paired applications of NE (10 μM) to stimulate membrane delimited inhibition and PMA 500 nM to stimulate PKC. With 10 μM PKCε-TIP in the pipette facilitation during NE application went from 97 ± 9.4 % before PMA to 33 ± 9.2 % after PMA (n=3). This concentration did not eliminate NE induced changes in current, so the concentration was and retested. When 20 μM PKCε-TIP was in the pipette the facilitation went from 102 ± 23 % before PMA to 72 ± 28 % after PMA (n=3). Since facilitation recurred robustly this was a considerable improvement in blocking the PKC effect. The higher concentration of PKCε-TIP also had a significant effect on kinetic changes. When 10 μM PKCε-TIP was included in the pipette time to peak elicited by NE went from 86 ± 3.6 msec before PMA, to 22 ± 6.7 msec after PMA. Conversely, when 20 μM PKCε-TIP was included in the pipette time to peak went from 73 ±14 msec before PMA to 40 ± 25 msec after PMA.

Discussion

Here I have presented evidence of a muscarinic agonist resulting in an attenuation of membrane-delimited inhibition. I used a pharmacological approach to block the diffusible second messenger pathway, to observe a reversal of G-protein mediated N-current inhibition. Initially, I found that recovery of membrane-delimited current inhibition, induced by the classic muscarinic agonist Oxo-M, is not caused by PKC activation but is more likely evidence of M_2R receptor desensitization. Still, 30 μM Oxo-M, presumably through M_1Rs, successfully blocked NE-induced N-current inhibition by the membrane-delimited pathway when the M_2R antagonist, METH and the DAG lipase inhibitor, RHC-80267 were included in the bath.

The pharmacological strategy using 30 μM oxo-M blocked both the changes in current amplitude and current kinetics normally elicited by NE. Moreover, the pharmacological strategy produced results similar to the PKC activating phorbol ester PMA. Therefore, these data are consistent with an activation of PKC. I found the application of the PKC inhibitor BLM did not reverse the action of 30 μM oxo-M. However, I found the apparent affects of PKC activation by PMA were also resistant to block with BLM.

The experiments I presented here were based on a combination standard electrophysiological techniques and pharmacological agents. Each of the drugs I used in this study has been used previously in other studies. However, a combination of drugs can produce non-specific effects. For example I found the combination of OPC and METH destabilized the membranes of neurons during whole-cell current measurements. Also, RHC and METH together reduced the changes in kinetics produced by NE, and

when applied for long periods of time reduced the amount of inhibition elicited by NE. Therefore, I've taken care to run proper controls. I found a combination of RHC and METH partially blocked inhibition of N-current by NE indicating a possible increase in basal PKC activity. However, the PKC activity elicited by 30 μM oxo-M is more robust. These data are consistent with phosphorylation of N-channels by PKC activated by M_1Rs.

In the same way reversal of Gβγ induced inhibition by neuronal activity constitutes a putative mechanism for short term plasticity (Brody and Yue 2000), the activation of PKC to attenuate tonic inhibition of calcium current and block further inhibition elicited by GPCRs may also constitute a mechanism for short term plasticity. Therefore identification of the receptors which activate PKC to phosphorylate channels is a key to understanding basic neural function. Not surprisingly, attempts to discern the neuronal receptors that induce phosphorylation of Ca_V2 channels via PKC comprise an active field of research.

Recently it was reported that M_1Rs do not cause phosphorylation of $Ca_V2.2$ channels so as to block fast pathway inhibition (Kamatchi et al., 2004). In this study potentiation of current in oocytes expressing M_1Rs and either $Ca_V2.2$ or $Ca_V2.3$ was gauged during muscarinic stimulation or PMA application. The authors found that while PMA potentiates $Ca_V2.2$ current, M_1 stimulation does not. Conversely both M_1 stimulation and PMA potentiate $Ca_V2.3$ current. The authors of this study concluded that specific residues of the II-III linker of $Ca_V2.3$ are phosphorylated by M_1R stimulation but the PKC consensus sites on the I-II linker of $Ca_V2.2$ and $Ca_V2.3$, which have been implicated in the block of Gβγ binding (Hamid et al., 1999) are not phosphorylated

during M_1R stimulation. They came to the conclusion that M_1 stimulation activates conventional forms of PKC (α, β_I, β_{II}, and γ) whereas other receptors stimulate novel PKC isoforms such as PKCε.

There are several reasons for the disagreement in findings. First is the use of oocytes in the alternate study. Although oocytes have been used well to elucidate many aspects of channel function, they may not contain all the necessary signaling components to be applicable to neuronal preps. The second possible reason for the discrepancy is the use of RHC to block the slow pathway. If DAG lipase is normally active during M_1 stimulation then DAG may be to low to activate PKC. A third possibility is that muscarinic stimulation interferes with NE signaling through a mechanism that does not require PKC. A fourth possibility for the disagreement is that they may not have had the right conditions in their expression system to observe potentiation. Enhancement of current by PKC requires tonic inhibition due to G$\beta\gamma$ bound to the channel (Swartz et al., 1993; Barrett and Rittenhouse 2000). The expression of certain $Ca_V\beta$ subunits in recombinant systems can adversely affect G$\beta\gamma$ binding (Roche et al., 1995; Roche and Treistman 1998). If Kamatchi and colleagues did not have sufficient tonic inhibition then phosphorylation could occur without any change in current amplitude or kinetics (Barrett and Rittenhouse 2000).

Figure 5-1. Muscarinic activated membrane-delimited inhibition is transient in SCG neurons (a) Shown is a pharmacological strategy to dissect PKC activation from other pathways. Muscarinic activated fast pathway inhibition can be antagonized by activation of PKC. Hypothetically, PKC may be activated by M_1 stimulation. Fast pathway is activated through M_2 and M_4 receptors while PKC is activated by M_1 receptors. Typical slow pathway inhibition of voltage gated calcium currents is blocked by PLA_2 antagonist OPC. (b) Representative time course of whole-cell current is transiently inhibited by oxo-M in the presence of OPC. (c) Representative sweeps take from time course show slowed activation kinetics typical of membrane delimited inhibition recovering within several minutes. For the representative time course and all subsequent time courses current was measured 7 msec after the start of the test pulse.

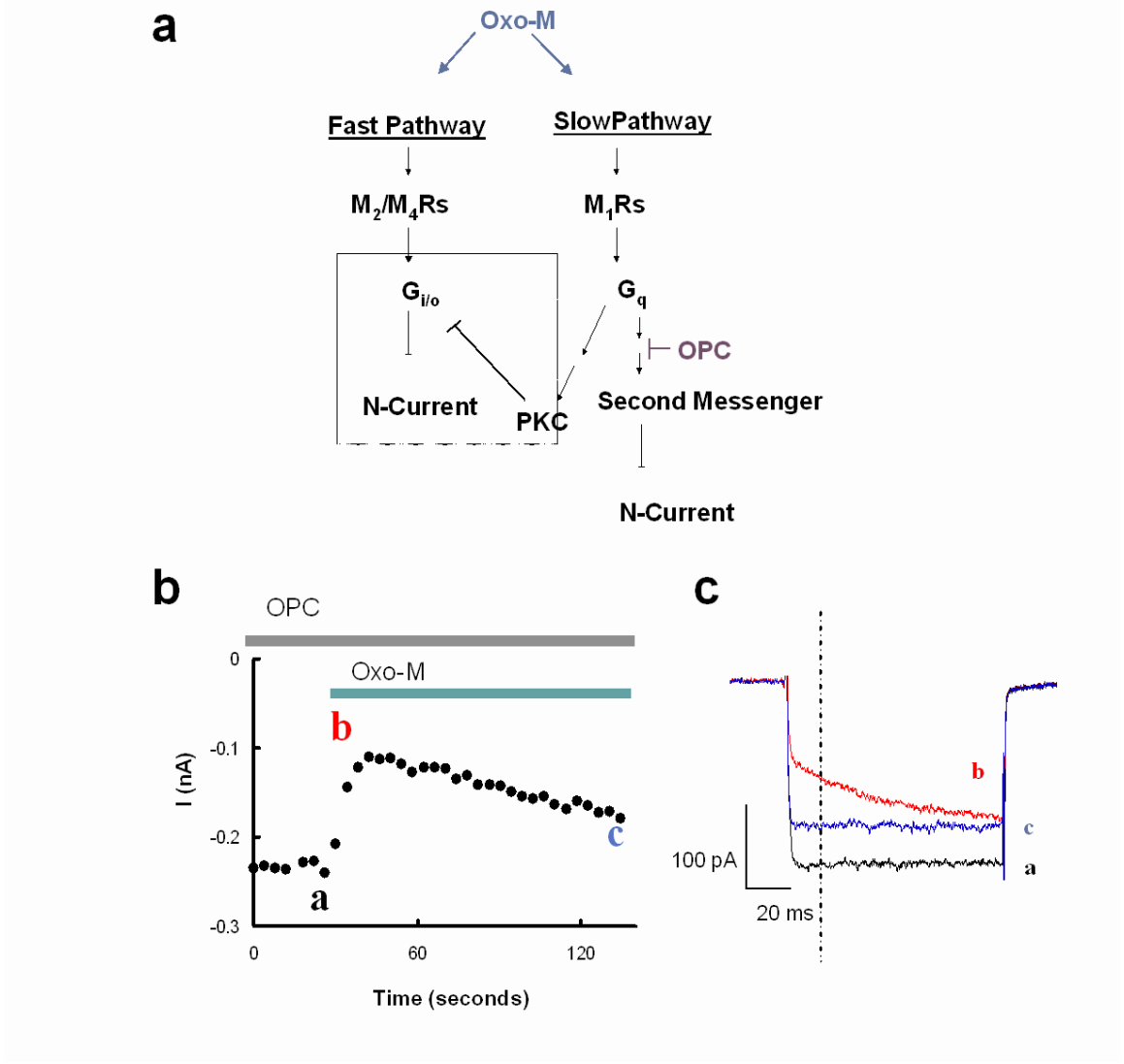
a
Oxo-M
Fast Pathway
SlowPathway
M2/M4Rs
M1Rs
Gi/o
Gq
OPC
N-Current
PKC
Second Messenger
N-Current
b
OPC
Oxo-M
0
-0.1
-0.2
-0.3
I (nA)
b
c
a
0
60
120
Time (seconds)
c
b
c
a
100 pA
20 ms

Figure 5-2. Membrane–delimited inhibition is transient without M_1 simulation. (**a**) time course shows unfacilitated (●) and facilitated (■) whole-cell currents measured in the presence of MT-7. (**b**) representative sweeps taken prior to (0 s) application of oxo-M, 30 seconds after oxo-M application and 3 minutes after oxo-M. Each representative sweep depicts an overlay of an unfacilitated (—) and facilitated (—) recording taken 4 seconds apart (**c**) summary of inhibition elicited by oxo-M at 30 seconds and 3 minutes after onset of application, in the presence of OPC, MT-7 or OPC and BLM

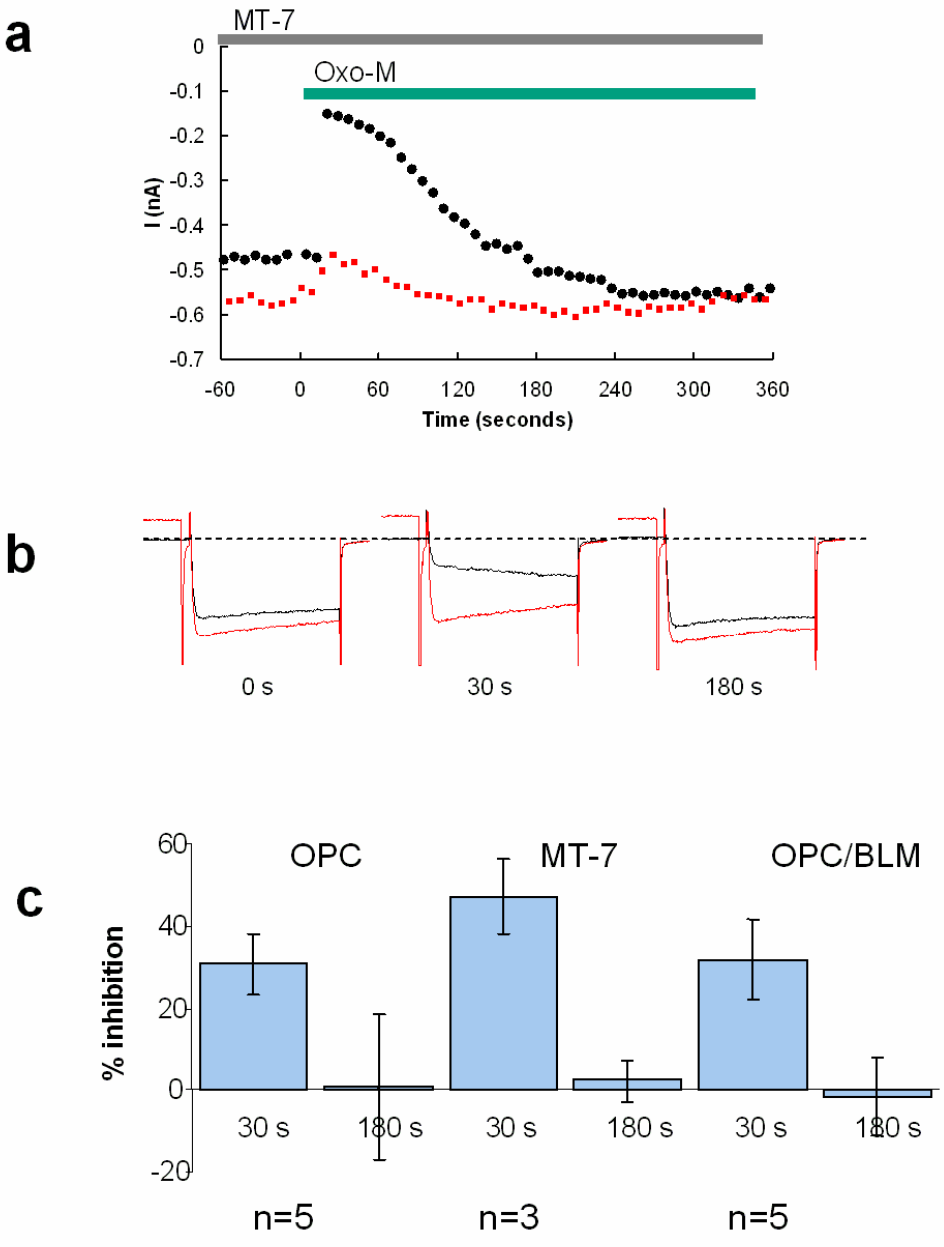
a
MT-7
Oxo-M
0
-0.1
-0.2
-0.3
-0.4
-0.5
-0.6
-0.7
I (nA)
-60
0
60
120
180
240
300
360
Time (seconds)
b
0 s
30 s
180 s
c
OPC
MT-7
OPC/BLM
% inhibition
60
40
20
0
-20
30 s
180 s
30 s
180 s
30 s
180 s
n=5
n=3
n=5

Figure 5-3. NE causes stable inhibition of whole-cell currents. (**a**) time course shows unfacilitated (●) and facilitated (■) whole-cell currents measured before and after application of 10 μM NE (b) representative sweeps of unfacilitated (—) and facilitated (—) recordings taken 4 seconds apart taken prior to (0 s) application of NE, 30 seconds after oxo-M application and 3 minutes after NE. (c) revised pharmacological strategy for dissecting PKC from M_1 stimulated pathways in SCG neurons. Fast pathway inhibition activated by M_2 receptors can be blocked with 100 nM METH while slow pathway inhibition of M_1 receptors can be blocked with 20 μM RHC. Fast pathway inhibition can be induced with 10 μM NE after PKC activation.

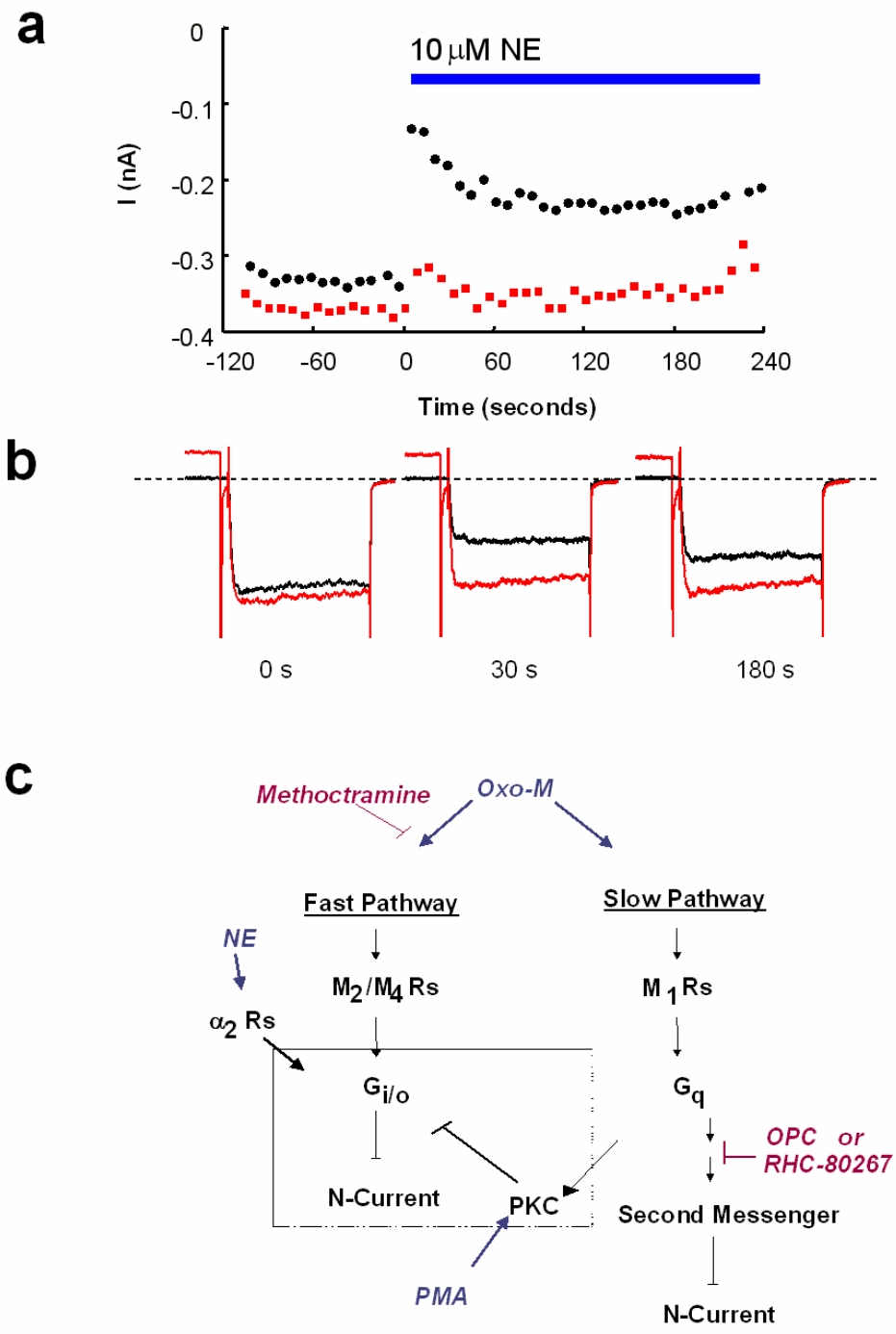
a
10 μM NE
I (nA)
0
-0.1
-0.2
-0.3
-0.4
-120
-60
0
60
120
180
240
Time (seconds)
b
0 s
30 s
180 s
c
Methoctramine
Oxo-M
Fast Pathway
Slow Pathway
NE
M2/M4 Rs
M1 Rs
α2 Rs
Gi/o
Gq
OPC or
RHC-80267
N-Current
PKC
Second Messenger
PMA
N-Current

Figure 5-4. PMA blocks voltage-dependent inhibition elicited by NE. (**a**) representative time course shows unfacilitated (●) and facilitated (■) whole-cell currents measured in the before and after two distinct applications of 10 μM NE separated by a five minute application of 500 nM PMA (**b**) representative sweeps taken prior to (control) application of NE, 30 seconds after the first application of NE (NE) and 30 seconds after the second application of NE (NE post PMA) (**c**) Inhibition by NE as represented by prepulse facilitation elicited 30 seconds after NE application before (control) and after PMA (PMA). (**d**) Change in kinetics of facilitated and unfacilitated currents as represented by time to peak elicited by NE before (control) and after PMA (PMA).

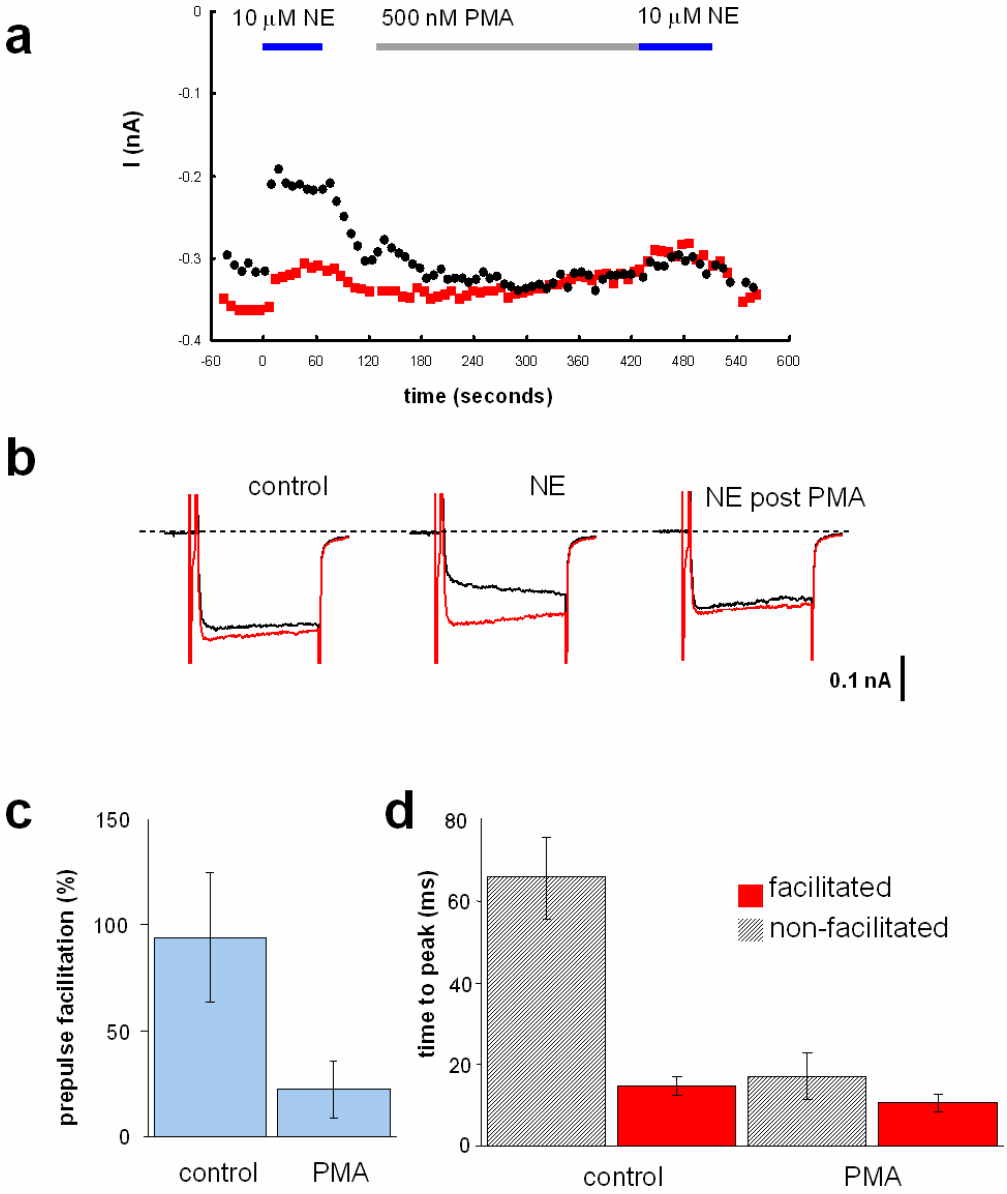
a
10 μM NE
500 nM PMA
10 μM NE
I (nA)
time (seconds)
b
control
NE
NE post PMA
0.1 nA
c
prepulse facilitation (%)
control
PMA
d
time to peak (ms)
facilitated
non-facilitated
control
PMA

Figure 5-5. 30 μM Oxo-m blocks inhibition by NE. (a) representative time course of whole-cell recordings in which M_1 receptors were stimulated for three minutes by 10 μM oxo-M in the presence of 100 nM METH and 20 μM RHC. Subsequently α_2 receptors were stimulated with 10 μM NE (b) representative sweeps taken prior to (—) application of NE, and 30 seconds after NE (—) application. (c) The same experiment as described for **a** and **b** with the substitution of 30 μM oxo-M. (d) Representative sweeps taken prior to (—) application of NE, and 30 seconds after NE (—) application. (e) Inhibition by NE was calculated as a percent change of current that occurred as a result of NE by comparing current amplitude measurements prior to and 30 seconds after NE application. Shown are averaged determinations for comparison of currents measured without METH, RHC or oxo-M, (control), with RHC and METH, but no oxo-M, and 30 μM oxo-M, with RHC and METH (f) Change in kinetics of as represented by time to peak elicited by NE under same conditions as described for **e**.

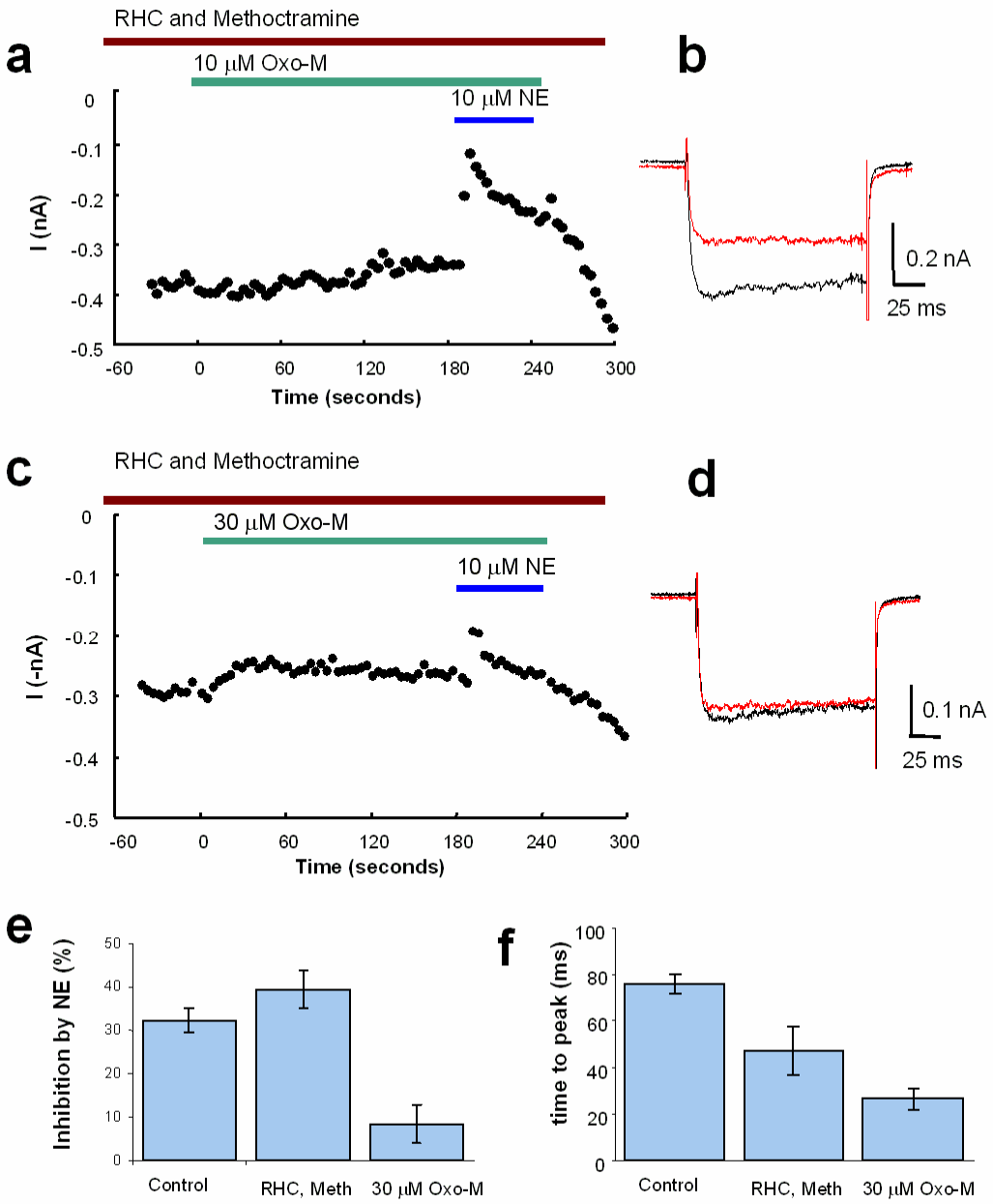
a
RHC and Methoctramine
10 μM Oxo-M
10 μM NE
I (nA)
Time (seconds)
b
0.2 nA
25 ms
c
RHC and Methoctramine
30 μM Oxo-M
10 μM NE
I (-nA)
Time (seconds)
d
0.1 nA
25 ms
e
Inhibition by NE (%)
Control
RHC, Meth
30 μM Oxo-M
f
time to peak (ms)
Control
RHC, Meth
30 μM Oxo-M

Figure 5-6. 30 μM oxo-m block of inhibition is consistent with PKC activation. (**a**) representative time course shows unfacilitated (●) and facilitated (■) whole-cell currents measured in the before and after two distinct applications of 10 μM NE separated by a three minute application of 30 μM oxo-m, in the presence of METH and RHC as described earlier (**b**) representative sweeps of unfacilitated (—) and facilitated (—) recordings taken prior to (left) application of NE, 30 seconds after the first application of NE (center) and 30 seconds after the second application of NE (right) (**c**) Inhibition by NE as represented by prepulse facilitation elicited 30 seconds after NE application before (control) and after oxo-M (Oxo-M). (**d**) Change in kinetics of facilitated and unfacilitated currents as represented by time to peak elicited by NE before (control) and after oxo-M (oxo-M).

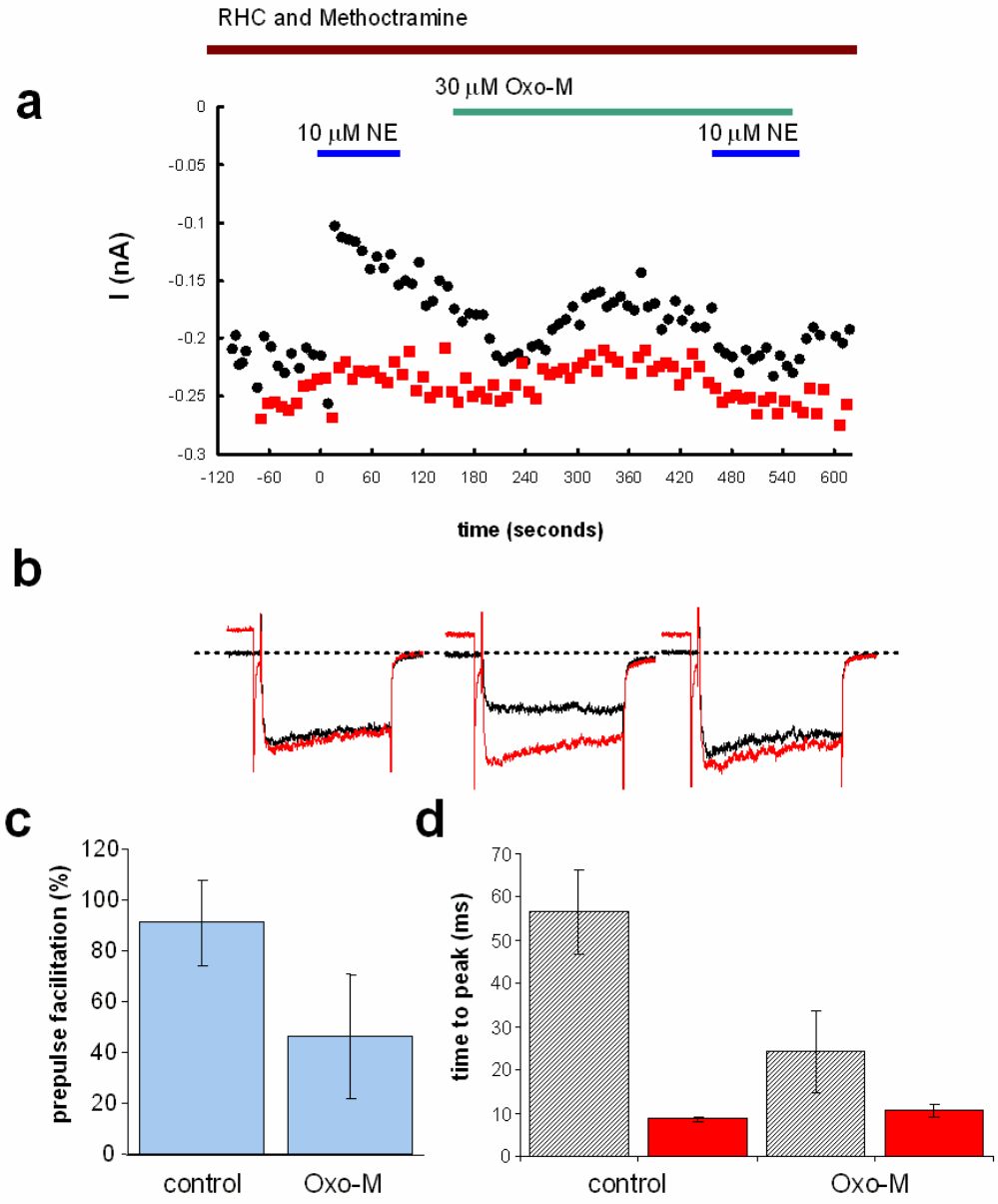
RHC and Methoctramine
a
30 μM Oxo-M
10 μM NE
10 μM NE
I (nA)
0
-0.05
-0.1
-0.15
-0.2
-0.25
-0.3
-120
-60
0
60
120
180
240
300
360
420
480
540
600
time (seconds)
b
c
prepulse facilitation (%)
120
100
80
60
40
20
0
control
Oxo-M
d
time to peak (ms)
70
60
50
40
30
20
10
0
control
Oxo-M

Figure 5-7. 100 nM BLM does not block effect of 30 μM oxo-M pretreatment. (**a**) representative time course shows unfacilitated (●) and facilitated (■) whole-cell currents measured in the before and after two distinct applications of 10 μM NE separated by a three minute application of 30 μM oxo-m, in the presence of METH and RHC as described in the previous figure with the addition of 100 nM BLM to the bath solution. (**b**) Inhibition by NE as represented by prepulse facilitation elicited 30 seconds after NE application before (pre Oxo-M) and after oxo-M (post Oxo-M). (**d**) Change in kinetics of facilitated and unfacilitated currents as represented by time to peak elicited by NE before (pre Oxo-M) and after oxo-M (post Oxo-M).

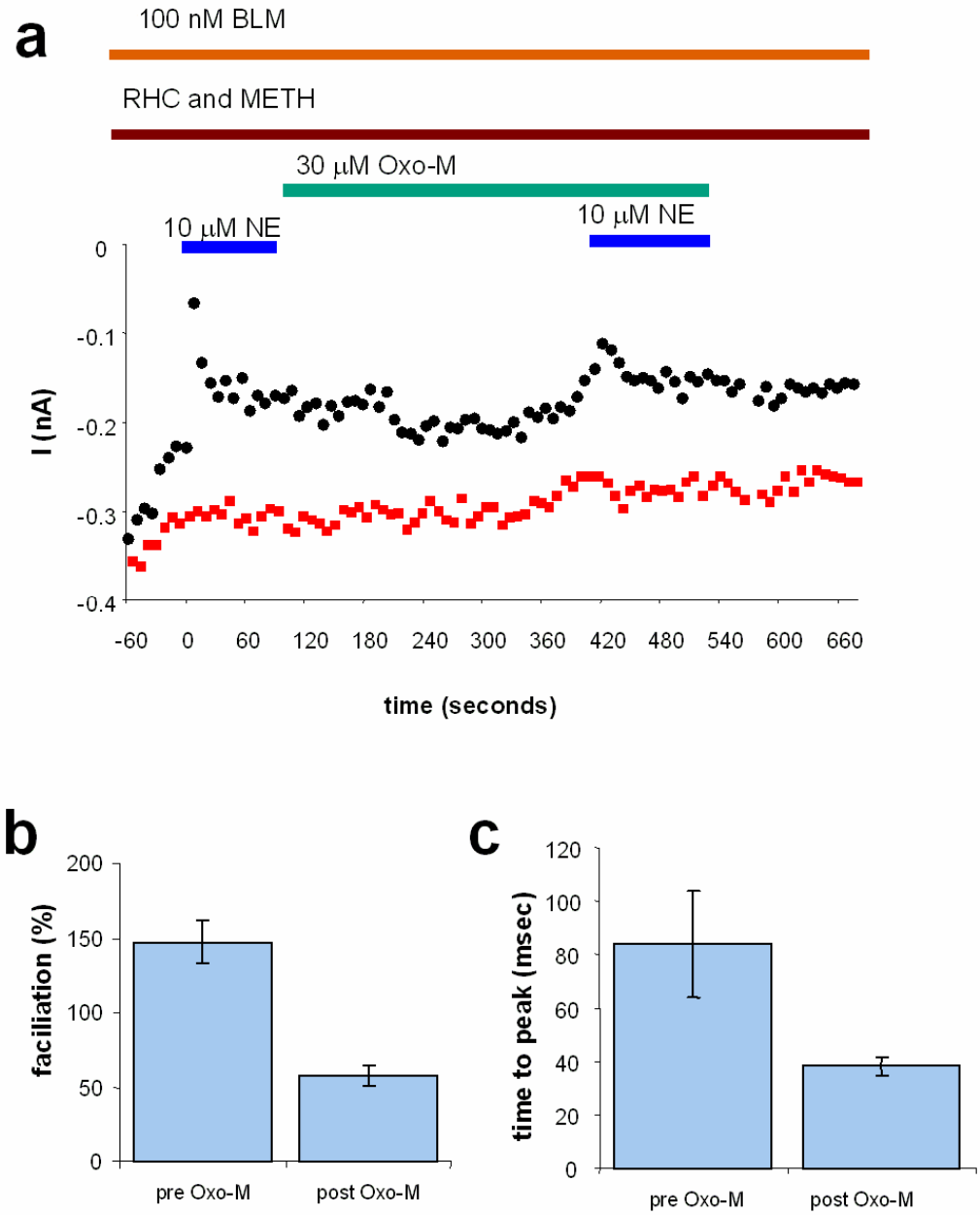
a
100 nM BLM
RHC and METH
30 μM Oxo-M
10 μM NE
10 μM NE
0
-0.1
-0.2
-0.3
-0.4
I (nA)
-60
0
60
120
180
240
300
360
420
480
540
600
660
time (seconds)
b
facilitation (%)
200
150
100
50
0
pre Oxo-M
post Oxo-M
c
time to peak (msec)
120
100
80
60
40
20
0
pre Oxo-M
post Oxo-M

Figure 5-8. 500 nM BLM partially blocks effect of 500 nM PMA pretreatment. (**a**) summary of inhibition elicited by NE as determined by % facilitation before and after a three minute application of 500 nM PMA. Shown are the data from two sets of experiments one without BLM (■) the other with 500 nM BLM in both bath and pipette solutions (■). (**b**) time to peak measurements taken from the same sets of experiments.

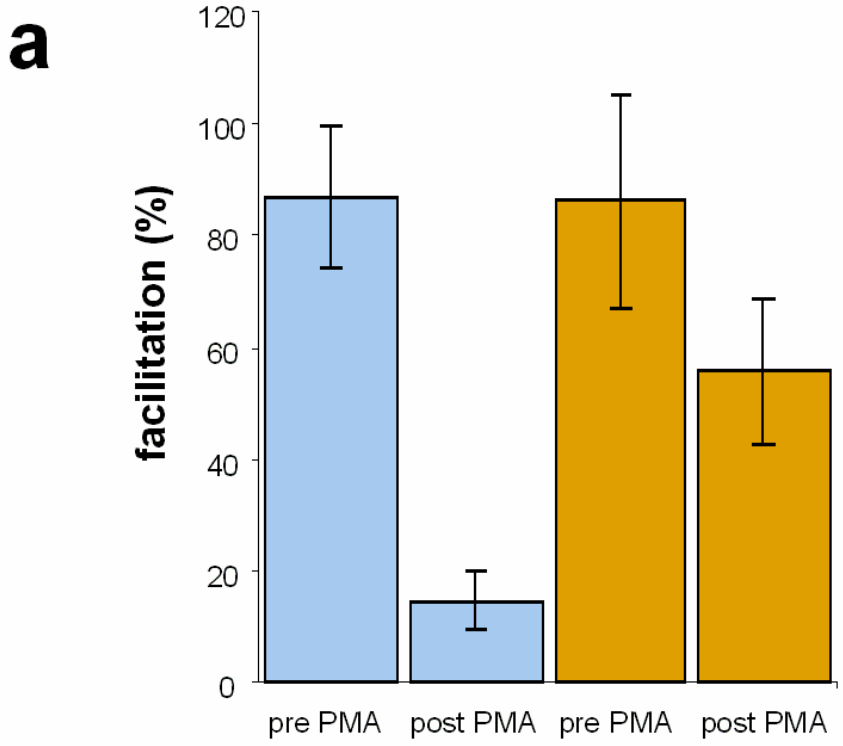
a
facilitation (%)
120
100
80
60
40
20
0
pre PMA
post PMA
pre PMA
post PMA

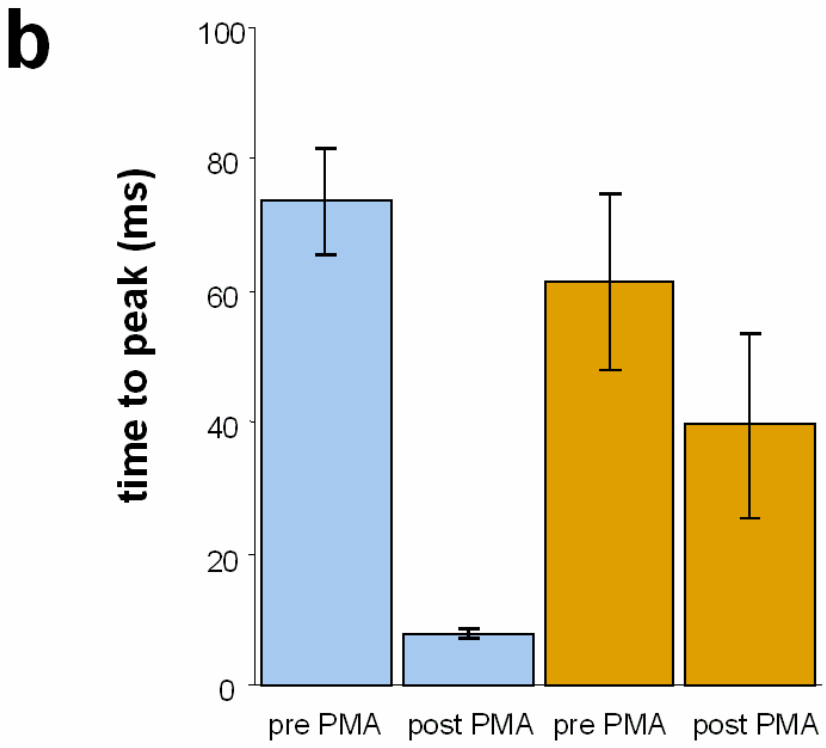
b
time to peak (ms)
100
80
60
40
20
0
pre PMA
post PMA
pre PMA
post PMA

Figure 5-9. 20 μM PKCε-TIP partially blocks effect of 500 nM PMA pretreatment. (**a**) summary of inhibition elicited by NE as determined by % facilitation before and after a three minute application of 500 nM PMA. Shown are the data from two sets of experiments one with 10 μM PKCε-TIP in the pipette solution (■) the other with 20 μM PKCε-TIP in the pipette solutions (□). (**b**) time to peak measurements taken from the same sets of experiments.

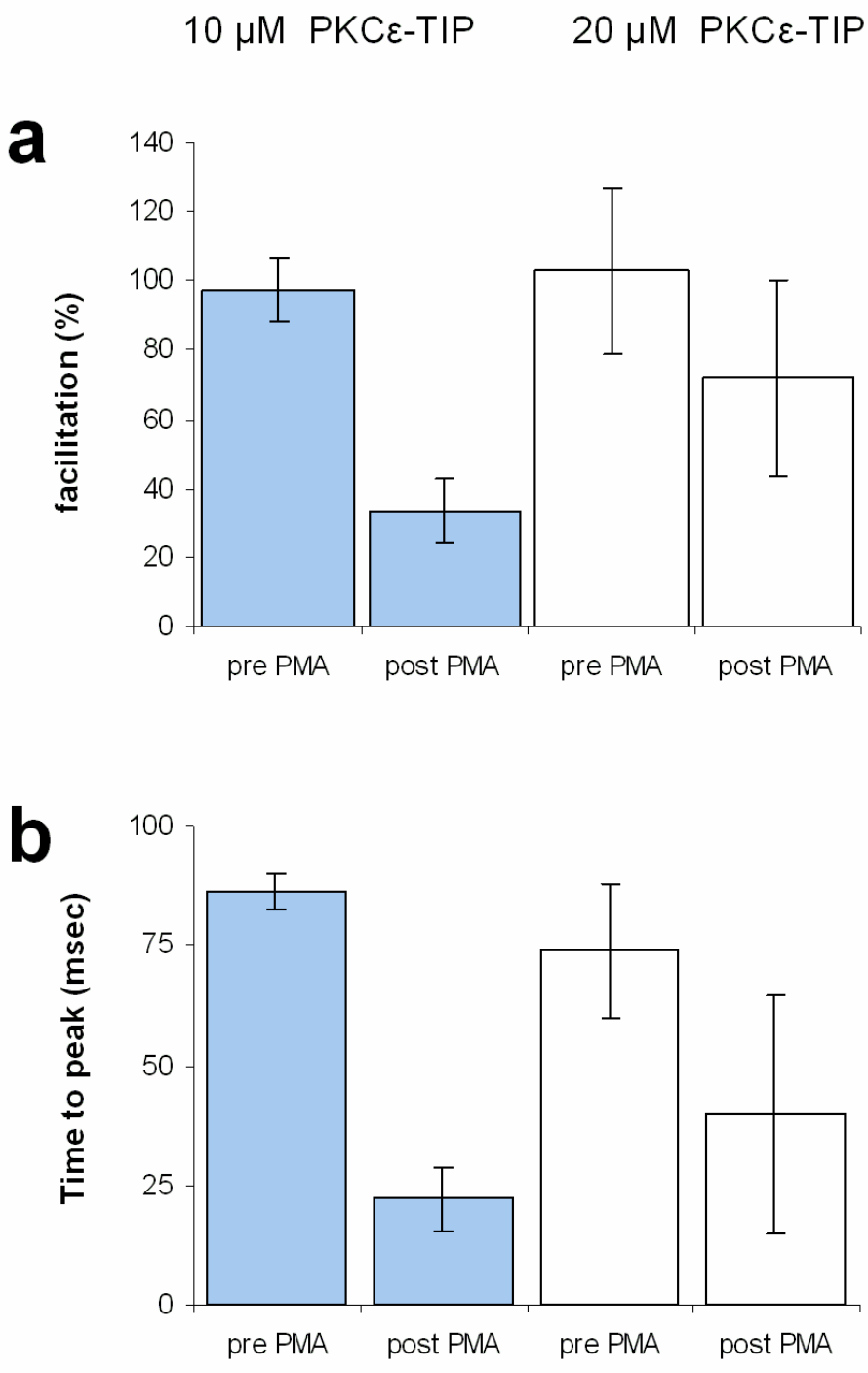
10 μM PKCε-TIP
20 μM PKCε-TIP
a
facilitation (%)
140
120
100
80
60
40
20
0
pre PMA
post PMA
pre PMA
post PMA
b
Time to peak (msec)
100
75
50
25
0
pre PMA
post PMA
pre PMA
post PMA

CHAPTER VI

General Discussion

In this thesis I have explored the modulation of N-channels by M_1 muscarinic receptors. M_1Rs have multiple downstream effects, several of which modulate $Ca_V2.2$. To study various effects independently of each other I took two approaches; a pharmacological approach, blocking various M_1R induced pathways in neurons; and a reductionist approach, expressing $Ca_V2.2e$ in non-neuronal cells with M_1Rs. Both of these approaches yielded novel results expanding the understanding of M_1 modulation of N-current. Here I've shown the expression of $Ca_V\beta$ subunit can toggle M_1R muscarinic modulation between enhancement and inhibition of N-current (chapter III). I've identified DAG lipase as a previously unrecognized component of slow pathway inhibition (chapter IV). Finally, I've demonstrated M_1 stimulation attenuates N-current inhibition typically induced by $G\beta\gamma$ binding (chapter V).

<u>AA is a component of the slow pathway</u>

Each investigation of M_1 modulation of N-current that I've described is shaped by a central premise that AA serves a vital role in the slow pathway. This premise is based on previous work published by other members of my lab (Liu et al. 2006, 2004; Liu and Rittenhouse 2003a). The investigations I've reported here corroborate those initial findings and provide further evidence of AA's importance in the slow pathway. In a recombinant system using wild type N-channel subunits, application of AA reproduces every effect of M_1R stimulation by Oxo-M, strongly suggesting AA mediates N-channel modulation. These effects are: inhibition of current with $Ca_V\beta1b$, $Ca_V\beta3$, or $Ca_V\beta4$ enhancement of current with $Ca_V\beta2a$ (Chapter III). Moreover, the discovery that DAG

lipase activity is required for slow pathway inhibition implicates a role for AA (Chapter IV).

The importance of AA in the slow pathway is at present controversial. A model for N-current modulation incorporating AA as an essential component represents a departure from a model established for M-current inhibition, in which PtdIns(4,5)P_2 depletion suffices to cause inhibition (Delmas and Brown 2005). Also, evidence for a similar model for calcium channel inhibition based on PtdIns(4,5)P_2 depletion has been accumulating (Suh and Hille 2005).

It had been postulated that the underlying mechanism for M- and N-current inhibition would prove to be the same, given a similar progression of inhibition during M_1R stimulation (Hille 1994). However, our lab has presented evidence that the modulating pathways for M- and L- current are not the same (Liu et al., 2006), specifically while L-current inhibition requires $cPLA_2$ activation M-current inhibition does not. Therefore, when examining the role of DAGL in N- and L- current modulation, I also tested M-current to show the established model is not in question, that is a block of DAGL does not affect M-current inhibition (Chapter IV).

My findings together with previous reports generated by our lab indicate a model in which PtdIns(4,5)P_2 depletion is the sole mechanism of inhibition is incomplete. If N-channels are sensitive to both PtdIns(4,5)P_2 depletion and AA formation, then experimental conditions might show either to be both necessary and sufficient for inhibition. It's possible that sufficient amounts of exogenously applied PtdIns(4,5)P_2 during M_1 stimulation blocks inhibition, and sufficient amounts of exogenously applied AA induces inhibition in vitro, but the amounts used to elicit these effects are greater than

what may be generated under normal physiological conditions (**Fig. 6-1**). Although at the present time it is not possible to accurately gauge the concentration of PtdIns(4,5)P_2 or AA at the channel, at any particular point in time.

Since PtdIns(4,5)P_2 depletion and AA formation occur simultaneously, sensitivity to both effects would make the calcium channel more responsive to M_1R stimulation, as has been proposed for a type of potassium channels (Oliver et al., 2004). Wu and colleagues (2002) reported PtdIns(4,5)P_2 sustains Ca_V2 currents and causes an activation shift to positive potentials. While our lab reported AA inhibits currents and causes an activation shift to negative potentials (Liu and Rittenhouse, 2003a; Liu et al., 2001; Barrett et al., 2001). In both types of modulation PtdIns(4,5)P_2 and AA act in opposite directions. Each lab reported that the two types of modulation were unconnected molecular effects occurring at distinct sites on the channel. Although no binding site for PtdIns(4,5)P_2 or AA has been determined, there is agreement that the site of inhibition is inside the plasma membrane (Wu et al., 2002; Barrett et al., 2001). This is supported by my discovery that the cytoplasmic $Ca_V\beta2a$ subunit blocks inhibition without affecting the voltage shift in gating (chapter III).

Finally it must be noted that the inclusion of AA in a pathway of modulation for calcium currents has implications in intercellular signaling. Unlike PtdIns(4,5)P_2 , AA can leave the plasma membrane and diffuse to an adjacent cell. In fact, AA has been implicated as a retrograde messenger for both long term potentiation (Williams et al., 1989) and long term depression (Bolshakov and Siegelbaun, 1995), two neural mechanisms thought to be the underpinnings of learning. Thus, for example, M_1 stimulation in a postsynaptic cell could elicit release of AA modulating N-current in the

presynaptic cell. Moreover the modulation by AA could be potentiation or inhibition depending on the channel composition.

$Ca_V\beta$ expression has extensive effects

My finding, that the expression of $Ca_v\beta$ subunit can toggle M_1R muscarinic modulation between enhancement and inhibition of N-current was totally unexpected and may have far reaching consequences. The discovery that switching the $Ca_V\beta$ subunit of N-channels directs modulation reveals a physiological mechanism by which modulatory effects can occur independently at different channels. The initial discovery of enhancement by AA was interesting (Liu et al 2001; Barrett et al 2001) and since it caused cells to become more sensitive to small depolarizations such as EPSPs, it suggested a role for post-synaptic modulation of N-current. The discovery that opposite responses occur in response to M_1R stimulation depending on Cavβ expression indicates a previously unrecognized mechanism of localized control of calcium influx.

At the cellular level Ca^{2+} influx through N-channels plays a key role in regulation of neuronal excitability, intracellular biochemical processes, and synaptic transmission. My findings predict the expression and localization of different $Ca_V\beta$ subunits could result in either up- or down-regulating these processes. I've shown the coexpression of multiple $Ca_V\beta$ subunits in produces a heterogeneous population of channels allowing for inhibition and enhancement presumably in different regions of the channel. For the expression of $Ca_V\beta$ not only determines the modulation of the channel, but also the localization. In Madin Darby Canine Kidney (MDCK) cells, a polarized epithelial cell line, coexpression of Cav2.1 with $Ca_V\beta$1b and $Ca_V\beta$4 resulted in transport of channels to

the apical membrane, while $Ca_V\beta 2a$ resulted in transport of channels to the basolateral membrane (Brice and Dolphin, 1999). Thus $Ca_V\beta 2a$ determines how the channels respond to cues for subcellular migration as well as modulation.

My discovery predicts changes in the expression $Ca_V\beta$ isoforms over time would alter N-current modulation in response to M_1R stimulation and thus may represent a previously unrecognized form of plasticity. Accordingly, the expression pattern of $Ca_V\beta$ subunits associated with N-channels changes during rat brain development (McEnery et al 1998). Also, the distribution of $Ca_V\beta$ isoforms changes in the hippocampi of patients with temporal lobe epilepsy (Lie et al 1999), suggesting changes in $Ca_V\beta$ expression may be activity dependent.

The control of M_1 moduation by $Ca_V\beta$ subunits may be a general mechanism by which numerous Gq coupled receptors (GqPCRs) either enhance or inhibit current. In SCG neurons, stimulation of either neurokinin receptor type I (NK-1Rs) or M_1Rs inhibit N-current through a signaling pathway which requires Gαq and the downstream activation of phopholipase Cβ (Shapiro et al. 1994; Kammermeier et al. 2000), therefore the NK-1R would likely stimulate a convergent pathway with the M_1R. In HEK-M1 cells (see Chapter III) expressing N-channels and NK-1Rs, substance P, the natural ligand for NK-1Rs, elicited enhancement when $Ca_V\beta 2a$ was expressed and inhibition when $Ca_V\beta 3$ was expressed (data not published; comm. Tora Mitra-Ganguli).

I found palmitoylation of $Ca_V\beta 2a$ alters the N-channel's response to M_1R stimulation. Since palmitoylation and depalmitoylation are known to be dynamic processes, modulation of N-current may change over the course of seconds to minutes. For example, within neurons reversible palmitoylation processes have already been

implicated in controlling ion channel clustering at synapses and in decreasing N-channel inactivation (Huang & El-Husseini 2005; Hurley et al. 2000). Thus dynamic palmitoylation of $Ca_V\beta2a$ could alter the channels response to modulation as well.

The discovery that the palmitoylated N-terminus of $Ca_V\beta2a$ plays a key role in modulation lends itself to some speculation as to how it does so. Given that M_1 mediated modulation of N-current occurs as a result of PtdIns(4,5)P_2 depletion, AA formation or a combination of the two effects, the N-terminus of $Ca_V\beta2a$ might interact with PtdIns(4,5)P_2, AA, or both. First, it seemed possible that the palmitoyl side chains could be interfering with a direct interaction of AA on the α_1 subunit of the channel (**Fig. 6-2**). However, since the non-palmitoylated $Ca_V\beta2a$(C3,4S) does not show complete recovery of inhibition it does not seem likely that interference of AA is sufficient to block inhibition. Second, the concentration of cationic residues in the N-terminus could be a docking site for PtdIns(4,5)P_2 (**Fig. 6-3**). Thus within the sixteen amino acids of the $Ca_V\beta2a$ N-terminus there are possible interaction sites for both AA and PtdIns(4,5)P_2.

If the N-terminus of $Ca_V\beta2a$ is a focal point control of modulation then it would seem that its presence would be sufficient to block inhibition. However, when I expressed the chimera with the $Ca_V\beta2a$ N-terminus on a $Ca_V\beta3$ subunit inhibition was only partially blocked. This could be due to an improper positioning of the $Ca_V\beta2a$ N-terminus (**Fig. 6-4**). It is possible that the structure of the different $Ca_V\beta$ subunits position the N-termini differently such that only the wild-type $Ca_V\beta2a$ places the N-terminus in the exact location necessary to completely block inhibition.

M_1 stimulation of PKC

The impetus for most of the research in this thesis came from an aim of determining a physiological means to elicit PKC induced phosphorylation of $Ca_V2.2$. Such a finding would be an important step in understanding neural function for the following reasons: 1) $Ca_V2.2$ is a vital component of synaptic transmission; 2) Inhibition of $Ca_V2.2$ by Gβγ binding, together with the relief of inhibition constitute a putative mechanism of short term plasticity (Brody and Yue 2000); 3) Phosphorylation of $Ca_V2.2$ by PKC blocks Gβγ inhibition and Gβγ subunits obstruct PKC phosphorylation for an elegant control of $Ca_V2.2$ activity (Barrett and Rittenhouse, 2000) 4) Efforts to show $Ca_V2.2$ phosphorylation as a downstream effect of neurotransmitters had been unsuccessful (Bean, 2000); and 5) M_1 stimulation enhances synaptic release through PKC activation (Costa et al., 1993). Taken together these data suggest the phosphorylation of $Ca_V2.2$ as a downstream effect of M_1Rs is a likely cellular mechanism for current modulation.

I used a pharmacological strategy to dissect the pathway and presented evidence consistent with block of fast pathway inhibition and thus consistent with PKC activation. My efforts to block the effect with PKC inhibitors were not initially successful; however, I found the block of inhibition as presumably elicited by phorbol esters was also difficult.

Also, during my research on PKC a competing lab published results indicating, the PKC activation elicited by M_1Rs does not phosphorylate $Ca_V2.2$ at the I-II linker thus does not potentiate N-current by relief of Gβγ (Kamatchi et al., 2004). I found the data the authors presented to be convincing. One caveat being the work was done oocytes and oocytes may lack the components for a proper recapitulation of a signaling pathway of a

mammalian neuron. Still they showed phosphorylation at the II-II linker of $Ca_V2.3$ which indicates activation of PKC. It's interesting that the I-II linker of neither $Ca_V2.3$ nor $Ca_V2.2$ was phosphorylated by M_1 stimulation, but both were phosphorylated by phorbol ester stimulation. Another caveat is that they used $Ca_V\beta1b$ in all of their studies and $Ca_V\beta$ isoforms can compete at the I-II linker with $G\beta\gamma$ subunits. If the $Ca_V\beta1b$ subunit did not allow sufficient tonic inhibition by $G\beta\gamma$, then potentiation by phosphorylation would never be apparent.

It's highly unlikely the consensus site for PKC phosphorylation site on the I-II linker evolved without a functional significance. Doubtless there is some mechanism to activate a kinase and block $G\beta\gamma$ inhibition. In addition to oxo-M I tried several other agonists for GqPCRs that might activate PKC, including bradykinin, substance P and angiotensin II. But, I was never able to show loss of tonic inhibition with any of these ligands which would indicate PKC was not being activated.

Future directions

In my opinion the most striking discovery I've made is the control of modulation by $Ca_V\beta$ subunits. This finding leads to numerous questions and research possibilities. The block of inhibition by $Ca_V\beta2a$ provides a molecular tool to probe the enhancing effects of AA and GqPCR stimulation. Interestingly neither AA nor M_1 stimulation enhances L-type channels (Ca_V1). This provides an opportunity to create chimeric α_1 subunits to determine which regions of $Ca_V2.2$ promote enhancement of current. Our lab has already gathered data indicating L-type channels associated with $Ca_V\beta2a$ have a unique response to modulation by AA (unpublished data comm. Mandy Roberts-

Crowley) but are not enhanced. In order to ascertain a site of enhancement it would also be interesting to see if selective enhancement with $Ca_V\beta 2a$ subunits occurs with $Ca_V2.1$ and $Ca_V2.3$.

I suggested that the cationic region of the $Ca_V\beta 2a$ N-terminus could act as a PtdIns(4,5)P_2 binding pocket (Chapter III). I'd be very interested in how the cationic region of the $Ca_V\beta 2a$ affects modulation. Point mutations of the arginine residues near the N-terminus might show a loss of the bock of inhibition. However, it's not a straight-forward experiment; mutations could disrupt the consensus site for palmitoylation.

To really get at how these subunits are affecting modulation it would be best to get single-channel recordings of recombinant channels. The single channel recordings would allow one to assess how modulation affects such parameters as mean open time, steady state inactivation.

Figure 6-1. A Model for M_1 Modulation of N-current. As shown M_1R stimulation elicits PtdIns(4,5)P_2 depletion and AA formation, both of which have been shown to cause modulation of N-current. Since N-current seems to be sensitive to both effects, experimental conditions involving exogenous application of either PtdIns(4,5)P_2 or AA could respectively block or elicit N-current modulation. At the present time it is impossible to ascertain what the actual concentrations of PtdIns(4,5)P_2 or AA are at the channel, or to what degree the concentrations fluctuate during M_1R stimulation.

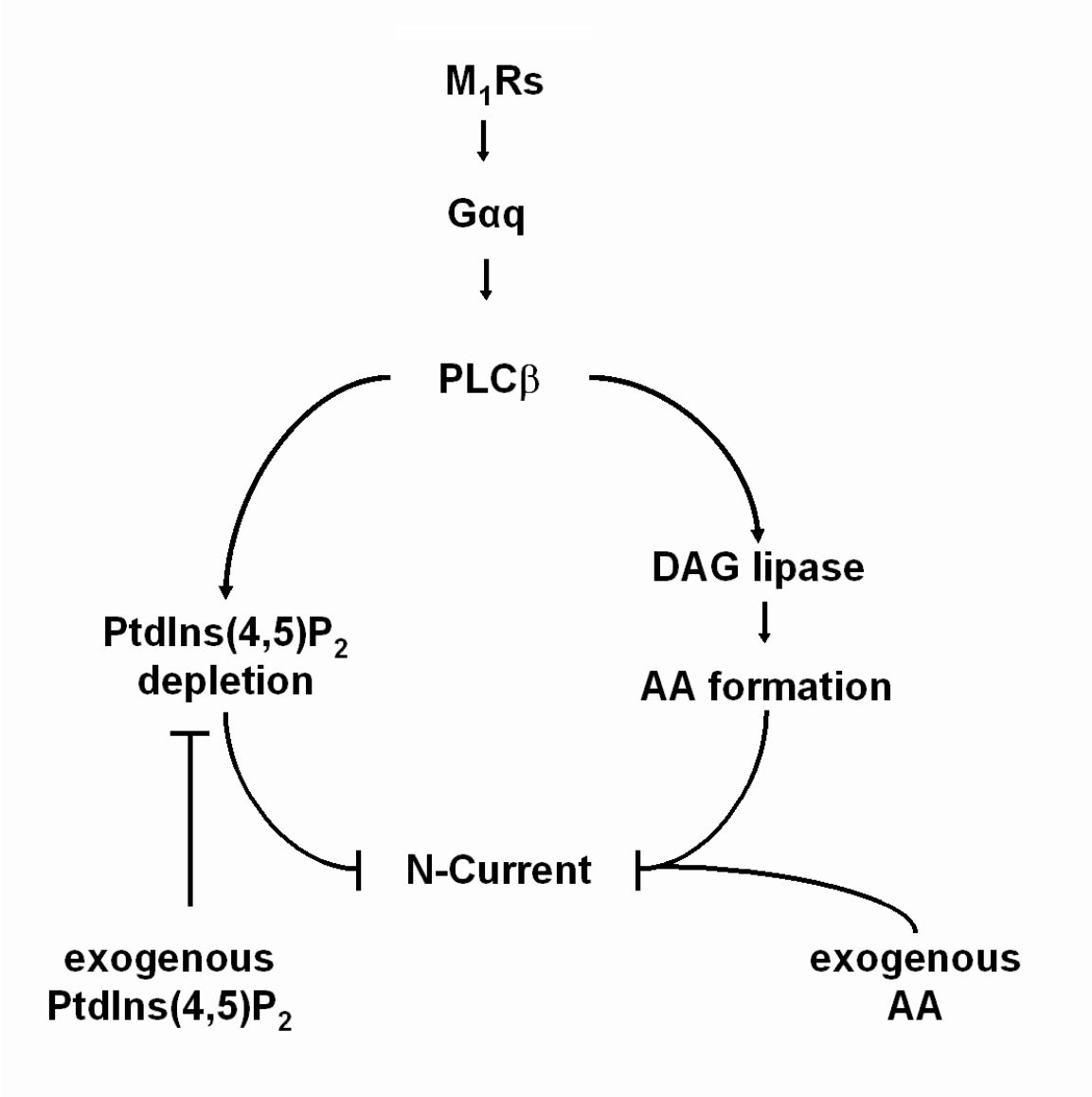
M1Rs
Gαq
PLCβ
DAG lipase
AA formation
PtdIns(4,5)P2
depletion
N-Current
exogenous
PtdIns(4,5)P2
exogenous
AA

Figure 6-2. Palmitoylation of $Ca_V\beta 2a$ may interfere with direct effect of arachidonic acid on channel. Here is depicted a model by which $Ca_V\beta 2a$ might block inhibition by causing steric hindrance to AA. With non-palmitoylated wild-type $Ca_V\beta$ subunits as show in (**a**) AA might directly bind to the α_1 subunit causing inhibition. The palmitoyl side chains of $Ca_V\beta 2a$ as show in (**b**) could conceivably block a direct effect of AA.

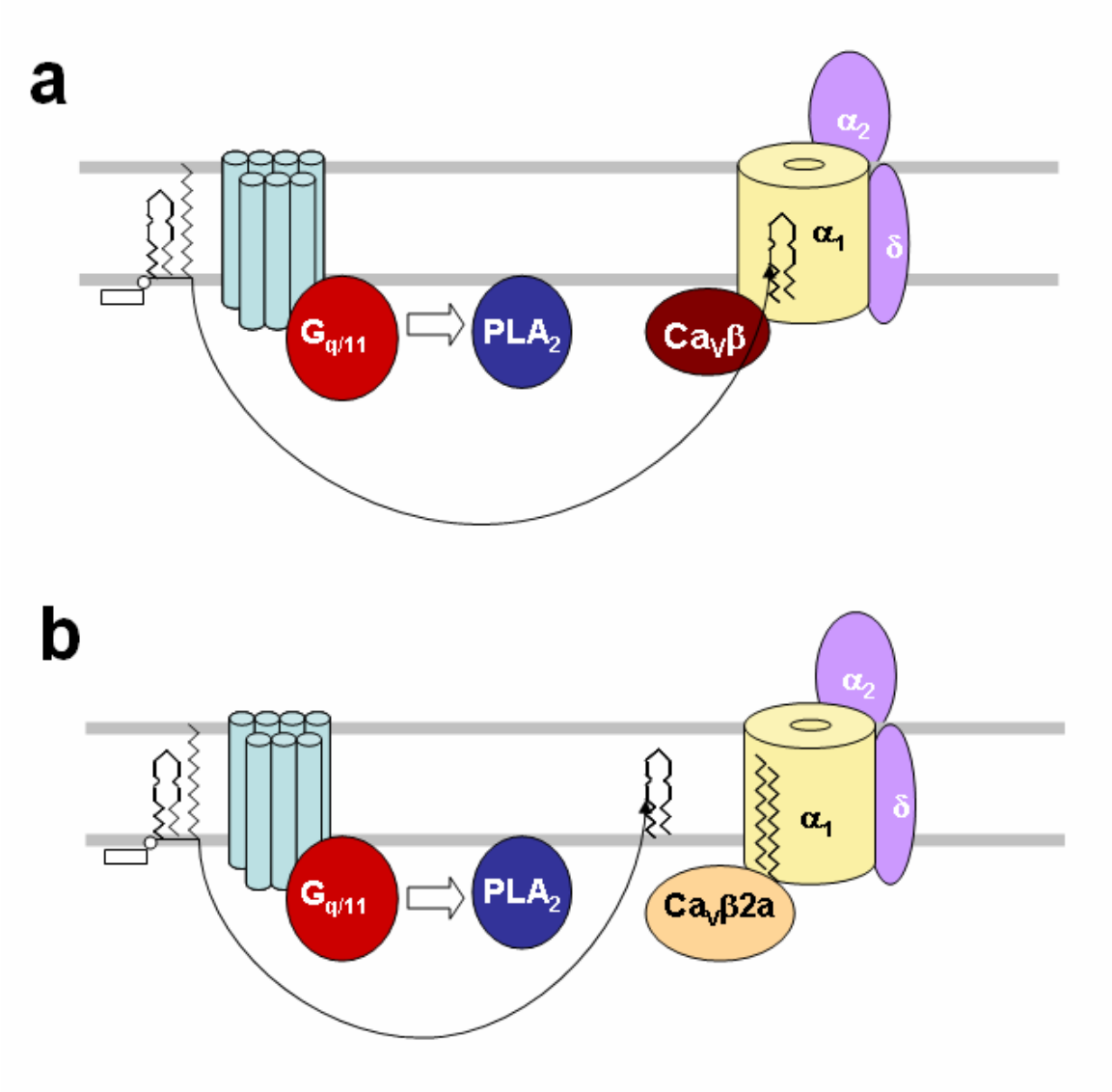
a
α2
α1
δ
Gq/11
PLA2
CaVβ
b
α2
α1
δ
Gq/11
PLA2
CaVβ2a

Figure 6-3. $Ca_V\beta 2a$ may act as PtdIns(4,5)P_2 docking site. (**a**) depiction of a widely accepted model of N-channel inhibition by PtdIns(4,5)P_2 depletion. In this model M_1Rs couple to PLC through Gαq. The stimulation of PLC causes a hydrolysis of PtdIns(4,5)P_2 and resultant concentration gradient within the membrane results in PtdIns(4,5)P_2 dissociating and diffusing away from the channel. (**b**) The N-terminus of $Ca_V\beta 2a$ contains a concentration of cationic residues which could serve to tether PtdIns(4,5)P_2 at the channel. Thus as shown in (**c**) the wild type $Ca_V\beta 2a$ would keep PtdIns(4,5)P_2 from dissociating and diffusing from the channel even if a concentration gradient had been formed by PtdIns(4,5)P_2 depletion.

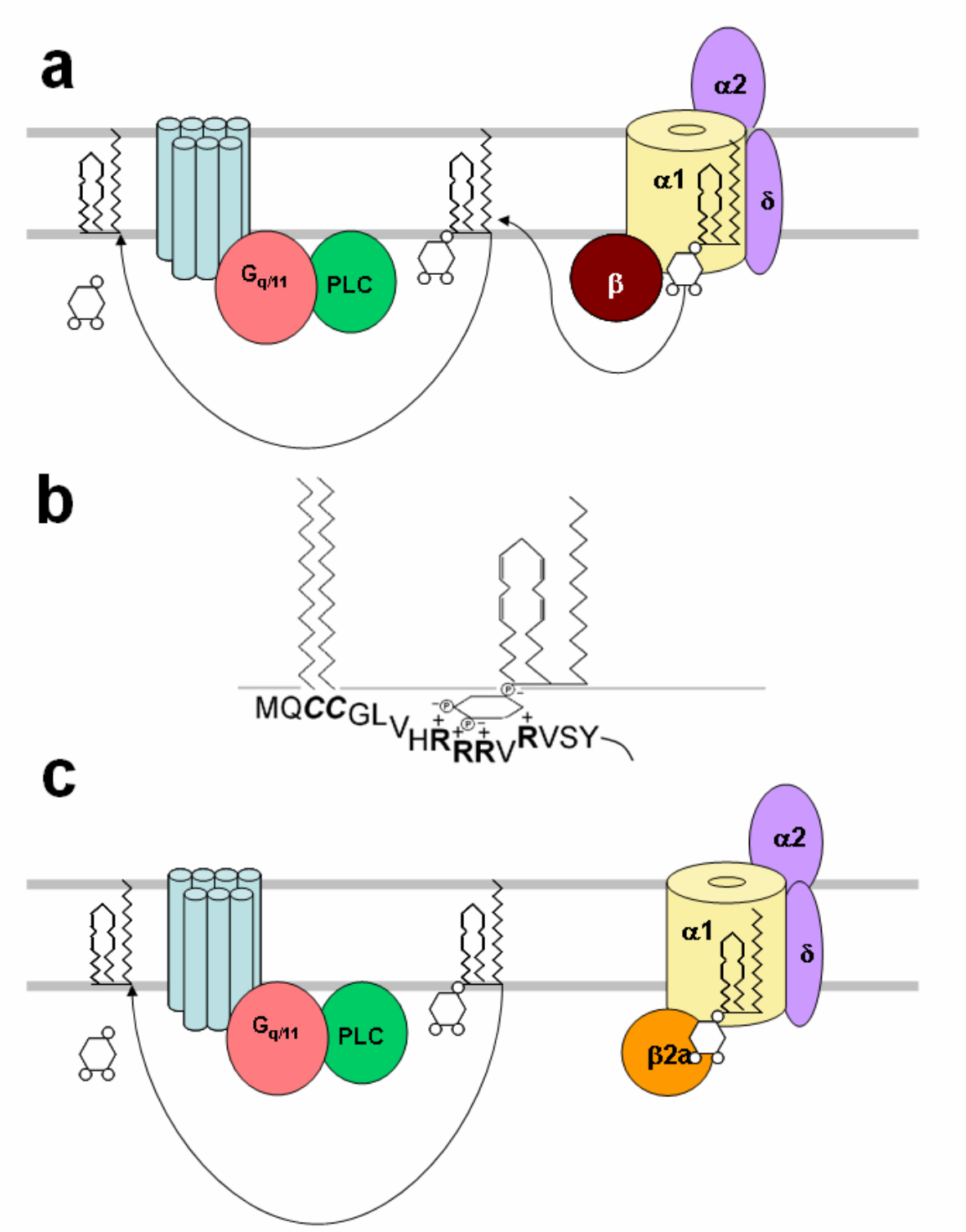
a
α2
α1
δ
β
$G_{q/11}$
PLC
b
MQCCGLVHRRRVRVSY
c
α2
α1
δ
β2a
$G_{q/11}$
PLC

Figure 6-4. $Ca_V\beta 2a$ Sequence may uniquely position N-terminus to block inhibition. The evidence obtained with the chimeric channels indicates that palmitoylation by itself does not block inhibition elicited by oxo-M or AA however we cannot discount the docking site hypothesis based on this evidence. The sequence of amino acids in the $Ca_V\beta 2a$ isoform may be uniquely adapted to position the N-terminus such that it blocks the effect of inhibition. So as depicted in (**a**) the wild type $Ca_V\beta 2a$ would have the N-terminus positioned properly to block inhibition, whereas a chimeric $Ca_V\beta$ subunit as shown in (**b**) could have the N-terminus in an unfavorable position.

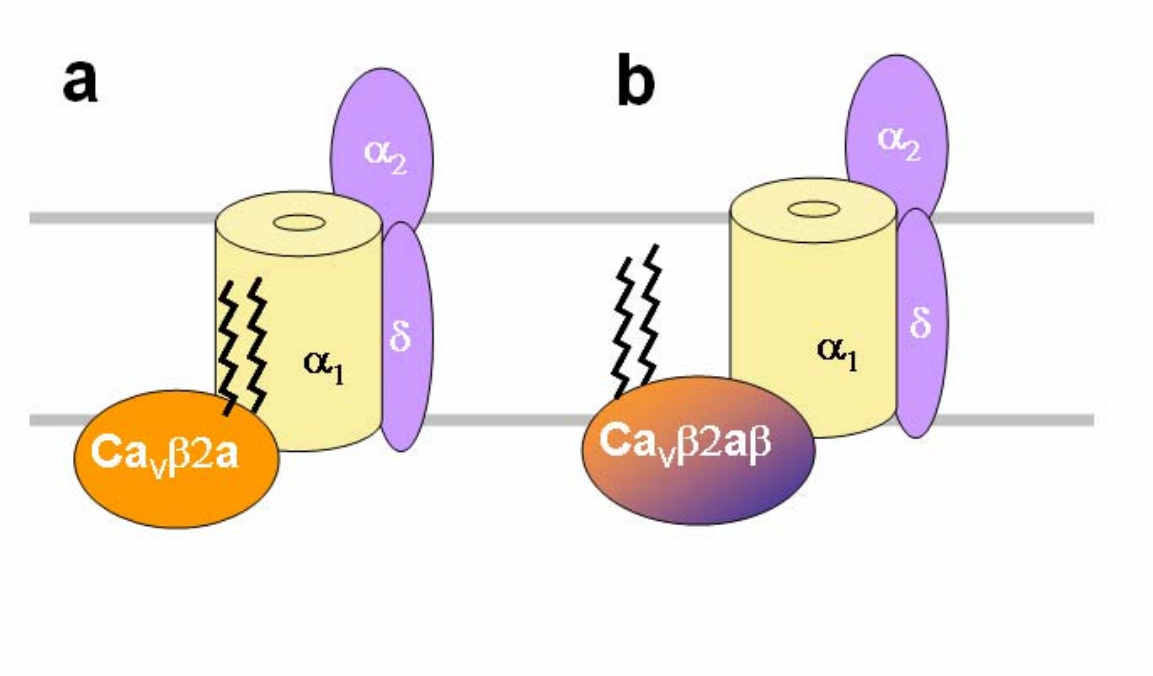
a
b
α2
α1
δ
CaVβ2a
CaVβ2aβ

References

1. Adem A., Karlsson E. Muscarinic receptor subtype selective toxins. *Life Sci.* **60,** 1069-1076 (1997).

2. Agler H.L., Evans J., Tay L.H., Anderson M.J., Colecraft H.M., Yue D.T. G protein-gated inhibitory module of N-type (Ca(v)2.2) Ca2+ channels. *Neuron*. **46**, 891-904 (2005).

3. Ambs P., Fitzke E., Dieter P. AA-release is under control of PLA2 and DAG lipase in rat liver macrophages.*Adv Prostaglandin Thromboxane Leukot Res*.**23,** 81-83 (1995).

4. Anagnostaras S.G., Murphy G.G., Hamilton S.E., Mitchell S.L., Rahnama N.P., Nathanson N.M., Silva A.J. Selective cognitive dysfunction in acetylcholine M1 muscarinic receptor mutant mice. *Nat Neurosci*., **6**, 51-58 (2003).

5. Arikkath J., Campbell K.P. Auxiliary subunits: essential components of the voltage-gated calcium channel complex. *Curr Opin Neurobiol.* **13**, 298-307 (2003).

6. Artim D.E., Meriney S.D. G-protein-modulated Ca(2+) current with slowed activation does not alter the kinetics of action potential-evoked Ca(2+) current. *J Neurophysiol*., **84**, 2417-2425 (2000).

7. Barrett C.F., Liu L., Rittenhouse A.R. Arachidonic acid reversibly enhances N-type calcium current at an extracellular site. *Am J Physiol Cell Physiol.* **280**, C1306- C1318 (2001).

8. Barrett C.F., Rittenhouse A.R. Modulation of N-type calcium channel activity by G-proteins and protein kinase C. *J Gen Physiol*. **115**, 277-286 (2000).

9. Bean B.P. Neurotransmitter inhibition of neuronal calcium currents by changes in channel voltage dependence. *Nature*. **340**, 153-156 (1989).

10. Beech D.J., Bernheim L., Mathie A., Hille B. Intracellular Ca2+ buffers disrupt muscarinic suppression of Ca2+ current and M current in rat sympathetic neurons.*Proc Natl Acad Sci U S A* **88,** 652-656 (1991).

11. Bernheim L., Beech D.J., Hille B. A diffusible second messenger mediates one of the pathways coupling receptors to calcium channels in rat sympathetic neurons. *Neuron*. **6**, 859-867 (1991).

12. Bernheim L., Mathie A., Hille B. Characterization of muscarinic receptor subtypes inhibiting Ca2+ current and M current in rat sympathetic neurons. *Proc Natl Acad Sci U S A* **89**, 9544-9548(1992).

13. Berridge M.J. Neuronal calcium signaling. *Neuron*.**21**,13-26 (1998).

14. Bichet D., Cornet V., Geib S., Carlier E., Volsen S., Hoshi T., Mori Y., De Waard M. The I-II loop of the Ca2+ channel alpha1 subunit contains an endoplasmic reticulum retention signal antagonized by the beta subunit. *Neuron*. **25**, 177-190 (2000).

15. Birnbaumer L., Qin N., Olcese R., Tareilus E., Platano D., Costantin J., Stefani E. Structures and functions of calcium channel beta subunits. *J Bioenerg Biomembr*. **30**, 357-375 (1998).

16. Bisogno T., Howell F., Williams G., Minassi A., Cascio M.G., Ligresti A., Matias I., Schiano-Moriello A., Paul P., Williams E.J., Gangadharan U., Hobbs C., Di Marzo V., Doherty P.. Cloning of the first sn1-DAG lipases points to the spatial and temporal regulation of endocannabinoid signaling in the brain. *J Cell Biol*. **163**, 463-468 (2003).

17. Boland L.M., Morrill J.A., Bean B.P. omega-Conotoxin block of N-type calcium channels in frog and rat sympathetic neurons. *J Neurosci.* **14**, 5011-5027 (1994).

18. Bolshakov V.Y., Siegelbaun S.A. Hippocampal long-term depression: arachidonic acid as a potential retrograde messenger. *Neuropharmacology* **34**, 1581-1587 (1995).

19. Bonner T.I., Buckley N.J., Young A.C. and Brann M.R. Identification of a family of muscarinic acetylcholine receptor genes. *Science* **237,** 527–532(1987).

20. Bonner T.I., Modi W.S., Seuanez H.N., O'Brien S.J. Chromosomal mapping of the five human genes encoding muscarinic acetylcholine receptors. *Cytogenet Cell Genet* **58**, 1850–1851(1991).

21. Brice N.L., Dolphin A.C. Differential plasma membrane targeting of voltage-dependent calcium channel subunits expressed in a polarized epithelial cell line.*J Physiol*. **515**, 685-694 (1999).

22. Bridges D., Rice A.S., Egertova M., Elphick M.R., Winter J., Michael G.J. Localisation of cannabinoid receptor 1 in rat dorsal root ganglion using in situ hybridisation and immunohistochemistry. *Neuroscience* **119**, 803-812 (2003).

23. Brody D.L., Patil P.G., Mulle J.G., Snutch T.P., Yue D.T. Bursts of action potential waveforms relieve G-protein inhibition of recombinant P/Q-type Ca2+ channels in HEK 293 cells. *J Physiol*., **499,** 637-644 (1997).

24. Brosenitsch T.A. & Katz D.M. Physiological patterns of electrical stimulation can induce neuronal gene expression by activating N-type calcium channels. *J Neurosci.* **21**,2571-2579 (2001).

25. Brown D.A. Slow cholinergic excitation - a mechanism for increasing neuronal excitability *Trends Neurosci* **6,** 302-307(1983).

26. Brown D.A., Adams P.R. Muscarinic suppression of a novel voltage-sensitive K+ current in a vertebrate neurone. *Nature* **283**, 673-676 (1980).

27. Cahill A.L., Hurley J.H., Fox A.P. Coexpression of cloned alpha(1B), beta(2a), and alpha(2)/delta subunits produces non-inactivating calcium currents similar to those found in bovine chromaffin cells. *J Neurosci*. **20**,1685-1693 (2000).

28. Canti C., Page K.M., Stephens G.J., Dolphin A.C. Identification of residues in the N terminus of alpha1B critical for inhibition of the voltage-dependent calcium channel by Gbeta gamma. *J Neurosci.* **19**, 6855-6864 (1999).

29. Carafoli E. Calcium signaling: a tale for all seasons. *Proc Natl Acad Sci U S A*. **99,** 1115-1122.(2002).

30. Carraway R.E., Hassan S., Cochrane D.E. Regulation of neurotensin receptor function by the arachidonic acid-lipoxygenase pathway in prostate cancer PC3 cells. *Prostaglandins Leukot Essent Fatty Acids* **74,** 93-107 (2006).

31. Catterall W.A. Structure and regulation of voltage-gated Ca2+ channels. *Annu Rev Cell Dev Biol*. **16**, 521-555 (2000).

32. Caulfield M.P., Birdsall N.J.M. International union of pharmacology. XVII. classification of muscarinic acetylcholine receptors. *Pharmacol. Rev.* **50,** 279-290 (1998).

33. Chen Y.H., Li M.H., Zhang Y., He L.L., Yamada Y., Fitzmaurice A., Shen Y., Zhang H., Tong L., Yang J.. Structural basis of the alpha1-beta subunit interaction of voltage-gated Ca2+ channels. *Nature*. **429**, 675-680 (2004).

34. Chien A.J., Carr K.M., Shirokov R.E., Rios E, Hosey M.M. Identification of palmitoylation sites within the L-type calcium channel beta2a subunit and effects on channel function. *J Biol Chem.* **271**, 26465-26468 (1996).

35. Chien A.J., Gao T., Perez-Reyes E., Hosey M.M. Membrane targeting of L-type calcium channels. Role of palmitoylation in the subcellular localization of the beta2a subunit. *J Biol Chem*. **273**, 23590-23597 (1998).

36. Chorvat R.J., Zaczek R., Brown B.S. Related Ion channel modulators that enhance acetylcholine release: potential therapies for Alzheimer's disease. *Expert Opin Investig Drugs*. **7**, 499-518 (1998).

37. Constanti A, Brown DA. M-Currents in voltage-clamped mammalian sympathetic neurones. *Neurosci Lett.* **24**, 289-294 (1981).

38. Cools A.R., Boudier A.J., Rossum J.M. Dopamine receptors: selective agonists and antagonists of functionally distinct types within the feline brain. *Eur J Pharmacol.* **37**, 283-923 (1976).

39. Costa M., Barrington M., Majewski H. Evidence that M1 muscarinic receptors enhance noradrenaline release in mouse atria by activating protein kinase C.*Br J Pharmacol*. **110,** 910-916 (1993).

40. Crick, F. Astonishing Hypothesis: The Scientific Search for the Soul Charles Scribner's Sons, New York, NY (1994).

41. Czech M.P. PIP_2 and PIP_3: complex roles at the cell surface. Cell. **100**, 603-606 (2000).

42. Delmas P., Abogadie F.C., Dayrell M., Haley J.E., Milligan G., Caulfield M.P., Brown D.A., Buckley N.J. G-proteins and G-protein subunits mediating cholinergic inhibition of N-type calcium currents in sympathetic neurons. *Eur J Neurosci.* **10,** 1654-1666 (1998).

43. Delmas P., Brown D.A. Pathways modulating neural KCNQ/M (Kv7) potassium channels.*Nat Rev Neurosci.* **6,** 850-862 (2005).

44. Delmas P., Coste B., Gamper N., Shapiro M.S. Phosphoinositide lipid second messengers: new paradigms for calcium channel modulation. *Neuron*. **47**, 179-182 (2005).

45. De Waard M., Liu H., Walker D., Scott V.E., Gurnett C.A., Campbell K.P. Direct binding of G-protein beta gamma complex to voltage-dependent calcium channels. *Nature*., **385,** 446-450 (1997).

46. Dolphin A.C. Beta subunits of voltage-gated calcium channels. *J Bioenerg Biomembr*. **35**, 599-620 (2003).

47. Dolphin A.C., Scott R.H. Calcium channel currents and their inhibition by (-)-baclofen in rat sensory neurones: modulation by guanine nucleotides. *J Physiol*., **386**, 1-17 (1987).

48. Dubel S.J., Starr T.V., Hell J., Ahlijanian M.K., Enyeart J.J., Catterall W.A., Snutch T.P. Molecular cloning of the alpha-1 subunit of an omega-conotoxin-sensitive calcium channel. *Proc Natl Acad Sci U S A*.,**89,** 5058-5062 (1992).

49. Dunlap K., Fischbach G.D. Neurotransmitters decrease the calcium component of sensory neurone action potentials. *Nature*. **276,** 837-839 (1978).

50. Durell, S. R., Guy, H. R. Atomic scale structure and functional models of voltage-gated potassium channels. *Biophys. J*. **62**, 238-247 (1992).

51. Elmslie K.S., Zhou W., Jones S.W. LHRH and GTP-gamma-S modify calcium current activation in bullfrog sympathetic neurons. *Neuron* 5, 75-80 (1990).

52. Elmslie K.S. Neurotransmitter modulation of neuronal calcium channels. *J Bioenerg Biomembr.* 35, 477-489 (2003).

53. Ertel E.A., Campbell K.P., Harpold M.M., Hofmann F., Mori Y., Perez-Reyes E., Schwartz A., Snutch T.P., Tanabe T., Birnbaumer L., Tsien R.W., Catterall, W.A. Nomenclature of voltage-gated calcium channels. *Neuron.* **25**, 533-535.

54. Fatt P., Katz B. The electrical properties of crustacean muscle fibers. *J Physiol.* **120,** 171-204 (1953).

55. Feldberg W., Gaddum J.H. The chemical transmitter at synapses in a sympathetic ganglion. *J Physiol.* **81,** 305-319 (1934).

56. Felder C.C. Muscarinic acetylcholine receptors: signal transduction through multiple effectors. *FASEB J*. **9**, 619-625 (1995).

57. Ford C.P. Stemkowski P.L., Smith P.A. Possible role of phosphatidylinositol 4,5 bisphosphate in luteinizing hormone releasing hormone-mediated M-current inhibition in bullfrog sympathetic neurons. *Eur J Neurosci*. **20**, 2990-2998 (2004).

58. Fox A.P., Nowycky M.C., Tsien R.W. Kinetic and pharmacological properties distinguishing three types of calcium currents in chick sensory neurones. *J Physiol.*, **394**, 149-172 (1987).

59. Gamper N., Reznikov V., Yamada Y., Yang J., Shapiro M.S. Phosphatidylinositol 4,5-bisphosphate signals underlie receptor-specific Gq/11-mediated modulation of N-type Ca2+ channels. *J Neurosci*. 24,10980-10992 (2004).

60. Garcia D.E., Li B., Garcia-Ferreiro R.E., Hernandez-Ochoa E.O., Yan K., Gautam N., Catterall W.A., Mackie K., Hille B. G-protein beta-subunit specificity in the fast membrane-delimited inhibition of Ca2+ channels. J Neurosci. **18**, 9163-9170 (1998).

61. Gouliaev A.H., Senning A. Piracetam and other structurally related nootropics. *Brain Res Brain Res Rev.* 19,180-222 (1994).

62. Guo J., Ikeda S.R. Endocannabinoids modulate N-type calcium channels and G-protein-coupled inwardly rectifying potassium channels via CB1 cannabinoid receptors heterologously expressed in mammalian neurons. *Mol Pharmacol.* **65**, 665-674 (2004).

63. Haley J.E., Abogadie F.C., Delmas P., Dayrell M., Vallis Y., Milligan G., Caulfield M.P., Brown D.A, Buckley N.J. The subunit of Gq contributes to muscarinic inhibition of the M-type potassium current in sympathetic neurons. *J Neurosci* **18**, 4521-4531(1998).

64. Hamid J., Nelson D., Spaetgens R., Dubel S.J., Snutch T.P., Zamponi G.W. Identification of an integration center for cross-talk between protein kinase C and G protein modulation of N-type calcium channels. *J Biol Chem*. **274**, 6195-6202 (1999).

65. Herlitze S., Garcia D.E., Mackie K., Hille B., Scheuer T., Catterall W.A. Modulation of Ca2+ channels by G-protein beta gamma subunits. *Nature*. **380**, 258-262 (1996).

66. Herlitze S., Hockerman G.H., Scheuer T., Catterall W.A. Molecular determinants of inactivation and G protein modulation in the intracellular loop connecting domains I and II of the calcium channel alpha1A subunit. *Proc Natl Acad Sci USA.,* **94,** 1512-1516 (1997).

67. Hilgemann D.W., Ball R. Regulation of cardiac Na+,Ca2+ exchange and KATP potassium channels by PIP2. *Science*. **273**, 956-959 (1996).

68. Hille B. Ion channels of excitable membranes, 3rd ed., Sinauer Associates, Sunderland ,MA (2001).

69. Hille B. Modulation of ion-channel function by G-protein-coupled receptors. *Trends Neurosci*. **17**, 531-536 (1994).

70. Hirning L.D., Fox A.P., McCleskey E.W., Olivera B.M., Thayer S.A., Miller R.J., & Tsien RW. Dominant role of N-type Ca2+ channels in evoked release of norepinephrine from sympathetic neurons. *Science*. **239**, 57-61 (1988).

71. Hodgkin A. L., Huxley A F. A quantitative description of membrane current and its application to conduction and excitation in nerve. J. Physiol. (Lond.) **117,** 500–544 (1952).

72. Holz G.G., Rane S.G., Dunlap K. GTP-binding proteins mediate transmitter inhibition of voltage-dependent calcium channels. Nature. **319**, 670-672 (1986).

73. Hosey M., Benovic J.L., DebBurman S.K., Richardson R.M. Multiple mechanisms involving protein phosphorylation are linked to desensitization of muscarinic receptors. *Life Sci*. **56,** 951-955 (1995).

74. Huang K., El-Husseini A. Modulation of neuronal protein trafficking and function by palmitoylation. *Curr Opin Neurobiol*. **15**, 527-535 (2005).

75. Hulme E.C., Birdsall N.J.M., Buckley N.J. Muscarinic receptor subtypes. *Ann Rev Pharmacol Toxicol* **30**, 633–673 (1990).

76. Hurley J.H., Cahill A.L., Currie K.P., Fox A.P. The role of dynamic palmitoylation in Ca2+ channel inactivation. *Proc Natl Acad Sci U S A*. **97**, 9293-9298 (2000).

77. Ibach, B., and Haen, E. Acetylcholinesterase inhibition in Alzheimer's Disease. *Curr. Pharm. Des.* **10**, 231–251 (2004).

78. Ikeda S.R. Voltage-dependent modulation of N-type calcium channels by G-protein beta gamma subunits. *Nature*. **380**, 255-258 (1996).

79. Jaiswal J.K. Calcium - how and why? *J Biosci.* **26**,357-363 (2001).

80. Jan C.R., Titeler M., Schneider A.S. Identification of omega-conotoxin binding sites on adrenal medullary membranes: possibility of multiple calcium channels in chromaffin cells. *J Neurochem*., **54** 355-358 (1990).

81. Jones L.P., Wei S.K., Yue D.T. Mechanism of auxiliary subunit modulation of neuronal alpha1E calcium channels. *J Gen Physiol*. **112**, 125-143 (1998).

82. Kamatchi G.L., Franke R., Lynch C. 3rd, Sando J.J. Identification of sites responsible for potentiation of type 2.3 calcium currents by acetyl-beta-methylcholine. *J Biol Chem*. **279,** 4102-4109. (2004).

83. Kammermeier P.J., Ruiz-Velasco V., Ikeda S.R. A voltage-independent calcium current inhibitory pathway activated by muscarinic agonists in rat sympathetic neurons requires both Galpha q/11 and Gbeta gamma. *J Neurosci*. **20**, 5623-5629 (2000).

84. Kandel E.R. In search of memory: The emergence of a new science of mind W.W. Norton & Company. New York, New York, USA (2006).

85. Keren O, Gafni M, Sarne Y. Opioids potentiate transmitter release from SK-N-SH human neuroblastoma cells by modulating N-type calcium channels. *Brain Res.* **764**, 277-282 (1997).

86. Keren O, Gafni M, Sarne Y. Potentiation of transmitter release from NMB human neuroblastoma cells by kappa-opioids is mediated by N-type voltage-dependent calcium channels. *Brain Res*. **843**,193-198. (1999).

87. Klugbauer N., Marais E., Hofmann F. Calcium channel alpha2delta subunits: differential expression, function, and drug binding. *J Bioenerg Biomembr*. **35**, 639-647 (2003).

88. Kubo T., Fukuda K., Mikami A., Maeda A., Takahashi H., Mishina M., Haga T., Haga K., Ichiyama A., Kangawa K., Kojima M., Matsuo H. Hirose T. and Numa S. Cloning, sequencing and expression of complementary DNA encoding the muscarinic acetylcholine receptor. *Nature* **323**, 411–416(1986a).

89. Kubo T., Maeda A., Sugimoto K., Akiba I., Mikami A., Takahashi H., Haga T., Haga K., Ichiyama A., Kangawa K., Matsuo H., Hirose T. and Numa S. Primary structure of porcine cardiac muscarinic acetylcholine receptor deduced from the cDNA sequence. *FEBS Lett* **209**, 367–372 (1986b).

90. Kwatra M.M., Schwinn D.A., Schreurs J., Blank J.L., Kim C.M., Benovic J.L., Krause J.E., Caron M.G.., Lefkowitz RJ. The substance P receptor, which couples to Gq/11, is a substrate of beta-adrenergic receptor kinase 1 and 2. *J Biol Chem*. 268, 9161-9164 (1993).

91. Levey A.I., Kitt C.A., Simonds W.F., Price D.L., Brann M.R. Identification and localization of muscarinic acetylcholine receptor proteins in brain with subtype-specific antibodies. *J Neurosci*., **11,** 3218-3226 (1991).

92. Lie A.A., Blumcke I., Volsen S.G., Wiestler O.D., Elger C.E., Beck H. Distribution of voltage-dependent calcium channel beta subunits in the hippocampus of patients with temporal lobe epilepsy. *Neuroscience* **93**, 449-456 (1999).

93. Liman, E. R., Hess, P., Weaver, F., Koren, G. Voltage sensing residues in the S4 region of a mammalian K+ channel. Nature 353, 752-756(1991).

94. Lin Z., Harris C., Lipscombe D. The molecular identity of Ca channel alpha 1-subunits expressed in rat sympathetic neurons. *J Mol Neurosci*. **7**, 257-267(1996).

95. Lin Z., Haus S., Edgerton J., Lipscombe D. Identification of functionally distinct isoforms of the N-type Ca^{2+} channel in rat sympathetic ganglia and brain. *Neuron*. **18**, 153-166 (1997).

96. Liu L. Regulation of lung surfactant secretion by phospholipase A2. *J Cell Biochem.* **72,** 103-110. (1999).

97. Liu L., ZhaoR., Bai Y.,Stanish L.F., Evans J.E., Michael J. Sanderson M.J., Bonventre J.V.,Rittenhouse A.R. M_1 Muscarinic Receptors Inhibit L-type Ca^{2+} Current and M-Current by Divergent Signal Transduction Cascades. *J Neurosci*., **26,** 11588-11598 (2006).

98. Liu L., Roberts M.L., Rittenhouse A.R. Phospholipid metabolism is required for M1 muscarinic inhibition of N-type calcium current in sympathetic neurons. *Eur Biophys J*. **33**, 255-264 (2004).

99. Liu L. & Rittenhouse A.R. Arachidonic acid mediates muscarinic inhibition and enhancement of N-type Ca^{2+} current in sympathetic neurons. *Proc Natl Acad Sci U S A.* **100**, 295-300 (2003a).

100. Liu L., Rittenhouse A.R. Pharmacological discrimination between muscarinic receptor signal transduction cascades with bethanechol chloride. *Br J Pharmacol*. **138**, 1259-1270 (2003b).

101. Liu L., Barrett C.F. & Rittenhouse A.R. Arachidonic acid both inhibits and enhances whole cell calcium currents in rat sympathetic neurons. *Am J Physiol Cell Physiol.* **280**, C1293-C1305. (2001)

102. Liu L., Rittenhouse A.R.. Effects of arachidonic acid on unitary calcium currents in rat sympathetic neurons. *J Physiol*. **525**, 391-404 (2000).

103. Lopez H.S., Brown A.M. Correlation between G protein activation and reblocking kinetics of Ca2+ channel currents in rat sensory neurons. *Neuron*. **7**, 1061-1068 (1991).

104. MacKinnon R., Yellen G. Mutations Affecting TEA Blockade and Ion Permeation in Voltage-Activated K^+ Channels. *Science*. **250,** 276-279 (1990).

105. Maeno-Hikichi Y., Chang S., Matsumura K., Lai M., Lin H., Nakagawa N., Kuroda S., Zhang J.F. A PKC epsilon-ENH-channel complex specifically modulates N-type Ca2+ channels. *Nat Neurosci.* **6**, 468-475 (2003).

106. Marchetti C., Carbone E., Lux H.D. Effects of dopamine and noradrenaline on Ca channels of cultured sensory and sympathetic neurons of chick. *Pflugers Arch.* **406**, 104-111 (1986).

107. Marchetti C., Robello M. Guanosine-5'-O-(3-thiotriphosphate) modifies kinetics of voltage-dependent calcium current in chick sensory neurons. Biophys J. **56**, 1267-1272 (1989).

108. Marrion N.V., Smart T.G., Marsh S.J., Brown D.A. Muscarinic suppression of the M-current in the rat sympathetic ganglion is mediated by receptors of the M1-subtype. *Br J Pharmacol* **98**, 557-573(1989).

109. Mathie A., Bernheim L., Hille B. Inhibition of N- and L-type calcium channels by muscarinic receptor activation in rat sympathetic neurons. *Neuron***.** **8**, 907-914 (1992).

110. McCleskey E.W., Fox A.P., Feldman D.H., Cruz L.J., Olivera B.M., Tsien R.W., Yoshikami D. Omega-conotoxin: direct and persistent blockade of specific types of calcium channels in neurons but not muscle. *Proc Natl Acad Sci U S A.*, **84**, 4327-4331 (1987).

111. McEnery M.W., Snowman A.M., Seagar M.J., Copeland T.D., Takahashi M. Immunological characterization of proteins associated with the purified omega-conotoxin GVIA receptor. *Ann N Y Acad Sci*. **707**, 386-391 (1993).

112. McEnery M.W., Vance C.L., Begg C.M., Lee W.L., Choi Y., Dubel S.J. Differential expression and association of calcium channel subunits in development and disease. *J Bioenerg Biomembr.*, **30**, 409-418 (1998).

113. Melliti K., Meza U., Adams B.A. RGS2 blocks slow muscarinic inhibition of N-type Ca(2+) channels reconstituted in a human cell line. *J Physiol*., **532**, 337-347 (2001).

114. Michael G.J., Averill S., Shortland P.J., Yan Q., Priestley J.V. Axotomy results in major changes in BDNF expression by dorsal root ganglion cells: BDNF expression in large trkB and trkC cells, in pericellular baskets, and in projections to deep dorsal horn and dorsal column nuclei. *Eur J Neurosci.*, **11**, 3539-3551 (1999).

115. Noda, M., Shimizu, S., Tanabe, T., Takai, T., Kayano, T., Ikeda, T., Takahashi, H., Nakayama, H., Kanaoka, Y., Minamino, N., Kangawa K, Matsuo H., Raftery M.A., Hirose T., Inayama S., Hayashida H., Miyata T., Numa S. Primary structure of Elecfrophorus electricus sodium channel deduced from cDNA sequence. *Nature* **372**, 121-127 (1984).

116. Nowycky M.C., Fox A.P., Tsien R.W. Three types of neuronal calcium channel with different calcium agonist sensitivity. *Nature*, **316**, 440-443 (1985).

117. Olcese, R., Qin, N., Schneider, T., Neely, A., Wei, X., Stefani, E. &Birnbaumer, L. The amino terminus of a calcium channel β subunit sets rates of channel inactivation independently of the subunit's effect on activation. *Neuron*, **13**, 1433–1438 (1994).

118. Oliver D., Lien C.C., Soom M., Baukrowitz T., Jonas P., Fakler B. Functional conversion between A-type and delayed rectifier K+ channels by membrane lipids. *Science*, **304**, 265-270 (2004).

119. Opatowsky Y., Chen C.C., Campbell K.P., Hirsch J.A. Structural analysis of the voltage-dependent calcium channel beta subunit functional core and its complex with the alpha 1 interaction domain. *Neuron* **42,** 387-399 (2004).

120. Page K.M., Canti C., Stephens G.J., Berrow N.S., Dolphin A.C. Identification of the amino terminus of neuronal Ca2+ channel alpha1 subunits alpha1B and alpha1E as an essential determinant of G-protein modulation. *J Neurosci.*, **18**, 4815-4824 (1998).

121. Peralta E.G., Ashkenazi A., Winslow J.W., Smith D.H., Ramachandran J. Capon D.J. Distinct primary structures, ligand binding properties and tissue-specific expression of four human muscarinic acetylcholine receptors. *EMBO J* **6**, 3923–3929 (1987).

122. Peralta E.G., Ashkenazi A., Winslow J.W., Ramachandran J., Capon D.J. Differential regulation of PI hydrolysis and adenylyl cyclase by muscarinic receptor subtypes. *Nature* **334**, 434-437 (1988).

123. Plummer M.R., Logothetis D.E., Hess P. Elementary properties and pharmacological sensitivities of calcium channels in mammalian peripheral neurons. *Neuron*. **2**, 1453-1463 (1989).

124. Pragnell M., De Waard M., Mori Y., Tanabe T., Snutch T.P., Campbell K.P. Calcium channel beta-subunit binds to a conserved motif in the I-II cytoplasmic linker of the alpha 1-subunit. *Nature*. **368,** 67-70 (1994).

125. Qin N., Platano D., Olcese R., Stefani E., Birnbaumer L. Direct interaction of gbetagamma with a C-terminal gbetagamma-binding domain of the Ca2+ channel alpha1 subunit is responsible for channel inhibition by G protein-coupled receptors. *Proc Natl Acad Sci U S A*. **94**, 8866-8871 (1997).

126. Rittenhouse A.R. & Zigmond R.E. Role of N- and L-type calcium channels in depolarization-induced activation of tyrosine hydroxylase and release of norepinephrine by sympathetic cell bodies and nerve terminals. *J Neurobiol*. **40**, 137-148 (1999).

127. Robbins J., Marsh S.J., Brown D.A. Probing the regulation of M (Kv7) potassium channels in intact neurons with membrane-targeted peptides. *J Neurosci*. **26**, 7950-7961 (2006).

128. Roche J.P., Anantharam V., Treistman S.N. Abolition of G protein inhibition of alpha 1A and alpha 1B calcium channels by co-expression of the beta 3 subunit. *FEBS Lett.* **371**, 43-46 (1995).

129. Roche J.P., Treistman S.N. Ca^{2+} channel beta3 subunit enhances voltage-dependent relief of G-protein inhibition induced by muscarinic receptor activation and Gbetagamma. *J Neurosci.* **18**, 4883-4890 (1998).

130. Scott V.E., De Waard M., Liu H., Gurnett C.A., Venzke D.P., Lennon V.A., Campbell K.P. Beta subunit heterogeneity in N-type Ca2+ channels. J Biol Chem. 271, 3207-3212 (1996).

131. Santi C.M., Ferreira G., Yang B., Gazula V.R, Butler A., Wei A., Kaczmarek L.K., Salkoff L. Opposite regulation of Slick and Slack K+ channels by neuromodulators. J Neurosci. 26, 5059-5068 (2006).

132. Shapiro M.S., Loose M.D., Hamilton S.E., Nathanson N.M., Gomeza J., Wess J., Hille B. Assignment of muscarinic receptor subtypes mediating G-protein modulation of Ca(2+) channels by using knockout mice. *Proc Natl Acad Sci U S A.* **96**, 10899-10904 (1999).

133. Sher E., Clementi F. Omega-conotoxin-sensitive voltage-operated calcium channels in vertebrate cells. Neuroscience. **42**, 301-307 (1991).

134. Sher E., Biancardi E., Pollo A., Carbone E., Li G., Wollheim C.B., Clementi F. omega-Conotoxin-sensitive, voltage-operated Ca2+ channels in insulin-secreting cells. *Eur J Pharmacol*. **216**, 407-414 (1992).

135. Shapiro M.S., Wollmuth L.P., Hille B. Modulation of Ca^{2+} channels by PTX-sensitive G-proteins is blocked by N-ethylmaleimide in rat sympathetic neurons. J Neurosci. 14, 7109-7116 (1994).

136. Snutch TP. Targeting chronic and neuropathic pain: the N-type calcium channel comes of age. *NeuroRx.*, **2**, 662-670 (2005).

137. Song S.Y., Saito K., Noguchi K., Konishi S. Different GTP-binding proteins mediate regulation of calcium channels by acetylcholine and noradrenaline in rat sympathetic neurons. *Brain Res.* **494**, 383-386 (1989).

138. Strosznajder J., Samochocki M. Carbachol-stimulated release of arachidonic acid and eicosanoids from brain cortex synaptoneurosome lipids of adult and aged rats.Adv Exp Med Biol. 318, 251-258 (1992).

139. Suh B.C., Hille B. Related Regulation of ion channels by phosphatidylinositol 4,5-bisphosphate.Curr Opin Neurobiol. 15, 370-378 (2005).

140. Suh B.C., Hille B. Does diacylglycerol regulate KCNQ channels? *Pflugers Arch.* May 24 (2006).

141. Sutherland C.A., Amin D. Relative activities of rat and dog platelet phospholipase A2 and diglyceride lipase. Selective inhibition of diglyceride lipase by RHC 80267. *J Biol Chem*. **257**(23):14006-14010 (1982).

142. Swartz K.J. Modulation of Ca2+ channels by protein kinase C in rat central and peripheral neurons: disruption of G protein-mediated inhibition. *Neuron*. **11**, 305-320 (1993).

143. Swartz K.J., Merritt A., Bean B.P., Lovinger D.M. Protein kinase C modulates glutamate receptor inhibition of Ca2+ channels and synaptic transmission. *Nature*. **361,** 165-168 (1993).

144. Tai C., Kuzmiski J.B., MacVicar B.A. Muscarinic enhancement of R-type calcium currents in hippocampal CA1 pyramidal neurons. J Neurosci. 26, 6249-6258 (2006).

145. Takahashi T, Momiyama A. Different types of calcium channels mediate central synaptic transmission. Nature. 366, 156-158 (1993).

146. Talavera K., Staes M., Janssens A., Droogmans G., Nilius B. Mechanism of arachidonic acid modulation of the T-type Ca2+ channel alpha1G. J Gen Physiol. 124, 225-238 (2004).

147. Tanabe T., Takeshima H., Mikami A., Flockerzi V., Takahashi H., Kangawa K., Kojima M., Matsuo H., Hirose T., Numa S. Primary structure of the receptor for calcium channel blockers from skeletal muscle. *Nature*. **328**, 313-318(1987).

148. Tence M., Cordier J., Premont J., Glowinski J. Muscarinic cholinergic agonists stimulate arachidonic acid release from mouse striatal neurons in primary culture.J Pharmacol Exp Ther. 269, 646-653 (1994).

149. Toullec D., Pianetti P., Coste H., Bellevergue P., Grand-Perret T., Ajakane M., Baudet V., Boissin P., Boursier E., Loriolle F., et al. The bisindolylmaleimide GF 109203X is a potent and selective inhibitor of protein kinase C. *J Biol Chem*. **266**, 15771-15781 (1991).

150. Tsien R.W., Lipscombe D., Madison D.V., Bley K.R., Fox A.P. Multiple types of neuronal calcium channels and their selective modulation. *Trends Neurosci*., **11**, 431-438 (1988).

151. Turner T.J., Adams M.E., Dunlap K. Multiple Ca2+ channel types coexist to regulate synaptosomal neurotransmitter release. Proc Natl Acad Sci U S A. 90, 9518-9522 (1993).

152. Van Petegem F., Clark K.A., Chatelain F.C., Minor D.L. Jr. Structure of a complex between a voltage-gated calcium channel beta-subunit and an alpha-subunit domain. *Nature*. **429**, 671-675 (2004).

153. Wanke E., Ferroni A., Malgaroli A., Ambrosini A., Pozzan T., Meldolesi J. Activation of a muscarinic receptor selectively inhibits a rapidly inactivated Ca2+ current in rat sympathetic neurons. *Proc Natl Acad Sci U S A.* **84**, 4313-4317 (1987).

154. Wei J., Walton E.A., Milici A., Buccafusco J.J. m1-m5 muscarinic receptor distribution in rat CNS by RT-PCR and HPLC. *J Neurochem*. **63**, 815-821 (1994).

155. West A.E., Chen W.G., Dalva M.B., Dolmetsch R.E., Kornhauser J.M., Shaywitz A.J., Takasu M.A., Tao X., Greenberg M.E. Calcium regulation of neuronal gene expression. *Proc Natl Acad Sci U S A*. **98**,11024-11031 (2001).

156. Wheeler D.B., Randall A., Tsien R.W. Roles of N-type and Q-type Ca2+ channels in supporting hippocampal synaptic transmission. *Science*. **264,** 107-111 (1994).

157. Willars G.B., Nahorski S.R., Challiss R.A. Differential regulation of muscarinic acetylcholine receptor-sensitive polyphosphoinositide pools and consequences for signaling in human neuroblastoma cells. *J Biol Chem.* **273**, 5037-5046 (1998).

158. Williams M.E., Brust P.F., Feldman D.H., Patthi S., Simerson S., Maroufi A., McCue A.F., Velicelebi G., Ellis S.B., Harpold M.M. Structure and functional expression of an omega-conotoxin-sensitive human N-type calcium channel. *Science*., **257**, 389-395 (1992).

159. Williams J.H., Errington M.L., Lynch M.A., Bliss T.V.P. Arachidonic acid induces a long-term activity dependent enhancement of synaptic transmission in the hippocampus. *Nature* **341**, 739-742 (1989).

160. Wisgirda M.E., Dryer S.E. Functional dependence of Ca(2+)-activated K+ current on L- and N-type Ca2+ channels: differences between chicken sympathetic and parasympathetic neurons suggest different regulatory mechanisms. *Proc Natl Acad Sci U S A*. **91**, 2858-2862 (1994).

161. Witcher D.R., De Waard M., Sakamoto J., Franzini-Armstrong C., Pragnell M., Kahl S.D., Campbell K.P. Subunit identification and reconstitution of the N-type Ca2+ channel complex purified from brain. *Science*. **261**, 486-489 (1993).

162. Woolf N.J. The critical role of cholinergic basal forebrain neurons in morphological change and memory encoding: a hypothesis. *Neurobiol Learn Mem.* **66**, 258-266 (1996).

163. Wu L., Bauer C.S., Zhen X.G., Xie C., Yang J. Dual regulation of voltage-gated calcium channels by PtdIns(4,5)P2. *Nature*. **419**, 947-52 (2002).

164. Yang J., Tsien R.W. Enhancement of N- and L-type calcium channel currents by protein kinase C in frog sympathetic neurons. *Neuron*. **10**, 127-136 (1993).

165. Yoshii M., Watabe S., Murashima Y.L., Nukada T., Shiotani T. Cellular mechanism of action of cognitive enhancers: effects of nefiracetam on neuronal Ca2+ channels. *Alzheimer Dis Assoc Disord*.14 S95-S102 (2000).

166. Yoshii M., Furukawa T., Ogihara Y., Watabe S., Shiotani T., Ishikawa Y., Nishimura M., Nukada T. Negative regulation of opioid receptor-G protein-Ca2+ channel pathway by the nootropic nefiracetam. *Ann N Y Acad Sci.* 1025, 389-397 (2004).

167. Zamponi G.W., Bourinet E., Nelson D., Nargeot J., Snutch T.P. Crosstalk between G proteins and protein kinase C mediated by the calcium channel alpha1 subunit. *Nature*. **385**, 442-446 (1997).

168. Zhang H., Craciun L.C., Mirshahi T., Rohacs T., Lopes C.M., Jin T., Logothetis D.E. PIP(2) activates KCNQ channels, and its hydrolysis underlies receptor-mediated inhibition of M currents. *Neuron*. **37,** 963-975 (2003).

169. Zhang J.F., Ellinor P.T, Aldrich R.W., Tsien R.W. Multiple structural elements in voltage-dependent Ca2+ channels support their inhibition by G proteins. *Neuron*. **17**, 991-1003 (1996).

170. Zhu Y., Ikeda S.R. Modulation of Ca(2+)-channel currents by protein kinase C in adult rat sympathetic neurons. *J Neurophysiol.* **72**, 1549-1560 (1994).